UNIVERSITE BIOLOGIE BRETAGNE SANTE LOIRE

UNIVERSITÉ DE NANTES

The University of Nottingham

THESE DE DOCTORAT DE

L'UNIVERSITE DE NANTES
COMUE UNIVERSITE BRETAGNE LOIRE
UNIVERSITY OF NOTTINGHAM

ECOLE DOCTORALE N° 605
Biologie Santé
Spécialité : Biologie des organismes

Par
Lara FIGUEIREDO

3D biomimetic matrices to design *in vitro* stem cell niches

Thèse présentée et soutenue à Nantes, le 17 septembre 2018
Unité de recherche : INSERM UMRS 1229 RMeS et
Regenerative Medicine and Cellular Therapies Group, University of Nottingham
Thèse N° : (8)

Rapporteurs avant soutenance :
Hervé PETITE Directeur du Laboratoire INSERM UMR7052 Université Paris VII
Raphaël DEVILLARD PU-PH, Université de Bordeaux

Composition du Jury :

Président:	Erwan NICOL	Maitre de Conférences, Institut des Molécules et Matériaux du Mans
Examinateurs:	Hervé PETITE	Directeur du Laboratoire INSERM UMR7052 Université Paris VII
	Raphaël DEVILLARD	PU-PH, Université de Bordeaux
	Felicity ROSE	Associate Professor and Reader, University of Nottingham
	Erwan NICOL	Maitre de Conférences, Institut des Molécules et Matériaux du Mans
Dir. de thèse:	Pierre WEISS	Professeur des universités, Praticien Hospitalier, Université de Nantes, REGOS INSERM U 1229 RMES
Co-dir. de thèse:	Jing YANG	Assistant Professor, University of Nottingham
	Gildas RETHORÉ	Assistant Hospital Universitaire, Université de Nantes

Invitée
Catherine le Visage Directeur adjoint Unité Inserm U1229, Université de Nantes

Acknowledgments

These wonderful and trying years as a PhD student were only made possible by the funding provided by European Commission, Education, Audiovisual and Culture Executive Agency (EACEA) which supported the NanoFar programme, an Erasmus Mundus Joint Doctorate in nanomedicine and pharmaceutical innovation. I would like to thank Dr. Frank Boury, coordinator of the programme, and all NanoFar representatives for giving us, Nanofar students, such a wonderful opportunity of a European based PhD programme shared with students from all over the world, which to me was very enriching.

I would like to thank my supervisor Dr. Pierre Weiss for welcoming me at the Laboratoire d'Ingénierie OstéoArticulaire et Dentaire (LIOAD) – Université de Nantes, and for all the advices and patience. I would also like to thank Dr. Catherine le Visage, for the constructive criticism and good advices.

I would like to thank Dr. Jing Yang, my supervisor at the University of Nottingham, for welcoming me, for all the fruitful discussions and support. I also would like to thank Dr. Kevin Shakesheff for accepting me as a PhD student and inviting me to the Regenerative Medicine and Cellular Therapies Group.

I would like to thank Dr. Thibaud Corandin, Dr. Gérald Thouand, Dr. Cameron Alexander and Dr. Gildas Rethore for being part of my thesis comity, providing me with interesting discussion and following the evolution of my work over the years.

I would like to thank Dr. Hervé Petite, Head of the CNRS/INSERM Biology Biomecanics service at the Université Paris VII, Dr. Raphaël Devillard maître de conférence at the Université de Bordeaux, Dr. Erwan Nicol, maître de conference at the Institut des Molécules et Matériaux du Mans and Dr. Felicity Rose, Associate Professor and Reader in Tissue Engineering, at the University of Nottingham, for accepting being part of the jury assessing this thesis.

I would also like to thank all the colleagues working at the LIOAD. My special thanks to Richard Pace, for all the help with the calculations regarding oxygen diffusion and for writing the paper with me. A big thank you to Iva Guberović and Pauline Chichiriccò for their important friendship and support.

I would like to thank my labmates at the CBS, University of Nottingham, especially Pritesh, Elisabetta, Laura, Lalitha, Hosam, Jamie and Meena for their kindness and all the help. I would also like to thank Pritesh for proofreading my thesis.

A big thank you to my Nanofar friends and fellows, especially Ana Cadete, Ivana, Aishwarya and Emma for being such an inspiration.

Thank you to Dr. Lídia Gonçalves for always believing in me, giving me strength to pursue this PhD and always caring.

To the friends and family that always supported me; I recognize that without them none of this would be possible. My parents, my brother and my sister Susana thank you for never letting me give up. My friends Diana, Karina, Ana, Marisa, prima Giuly, Joana, Goreti and Daniela for being part of this amazing journey that made us take separate ways but that never separated us.

Por tudo isto e muito mais, um grande obrigado a todos!

Contents

List of Abbreviations

2D two dimensions

3D three dimensions

CT computed tomography

ECM extracellular matrix

EHS Engelbreth–Holm–Swarm

ESC embryonic stem cells

FDA Food and Drug Administration

GAG glycosaminoglycan

GelMA Gelatin methacrylate

HA Hyaluronic acid

iPSC induced pluripotent stem cells

MSC mesenchymal stem cells

PEG polietilenoglicol

PCL Poly(caprolactone)

PLGA poly(lactic-co-glycolic acid)

RGD Arginylglycylaspartic acid

RM regenerative medicine

Si-HPMC silated- hydroxypropylmethylcellulose

TCP tri-calcium phosphate

VEGF vascular endothelial growth factor

bFGF basic fibroblast growth factor

Extended abstract in French/ Résumé

Bien que la médecine régénératrice remonte à plus d'un demi-siècle, avec la première transplantation réussie d'organes humains, elle a repris son souffle au cours de la dernière décennie grâce aux évolutions technologiques et à l'amélioration des connaissances en biologie cellulaire. L'ingénierie tissulaire (IT) est apparue au début des années 1990 comme un concept, associant des cellules, parfois même celles d'un patient, avec des polymères biocompatibles dans le but de créer des tissus biologiques à visée régénérative. La distinction entre l'ingénierie tissulaire (TE pour tissue engineering en anglais) et la médecine régénératrice (RM pour regenerative medicine en anglais) n'est pas simple et parfois les deux termes sont utilisés de façon interchangeable. Néanmoins, l'ingénierie tissulaire est plus souvent associée aux principes de conception et d'échafaudage utilisés pour créer des implants tissulaires et est de fait considérée comme faisant partie de la médecine régénératrice. La médecine régénératrice comprend également un axe qui met l'accent sur la formation tissulaire endogène, liée à la capacité de réparation intrinsèque de la plupart des organes humains.

L'ingénierie tissulaire est un domaine interdisciplinaire en évolution rapide qui réunit la science des matériaux, le génie biomédical et la biologie cellulaire, dans le but de reconstruire les tissus vivants en cas de blessure ou de perte. Pour cette raison, elle a le potentiel d'avoir un impact médical important, en élargissant l'approvisionnement en tissus pour les thérapies de transplantation.

L'échafaudage est une pièce maîtresse dans l'ingénierie tissulaire, car il vise à imiter la matrice extracellulaire (Extracellular Matrix, ECM) qui se trouve dans les tissus naturels. Cet échaffaudage peut constituer un agent de remplissage de l'espace (rôle conducteur), un système bioactif de délivrance de molécules (rôle inducteur) et un système de délivrance (ensemencement cellulaire). La matrice extracellulaire est composée d'une vaste gamme de biomolécules comprenant du collagène et de l'élastine (protéines structurales), de la fibronectine et de la vitronectine (protéines adhésives) et divers glycosaminoglycanes (GAG). Ces biomolécules fonctionnent pour maintenir la stabilité tissulaire, car la matrice extracellulaire fonctionne comme un support physique pour les cellules tout en jouant un rôle régulateur sur le comportement des cellules.

Plusieurs découvertes ont propulsé des avancées majeures dans l'ingénierie tissulaire telles que le développement constant de nouveaux biomatériaux comme tissus biomimétiques et l'augmentation des connaissances sur la biologie humaine et l'immunologie. En outre, la disponibilité des cellules d'intérêt, a considérablement augmenté depuis que des cellules souches méesnchymateuses (MSC) ont été identifiées dans divers tissus adultes et que des cellules différenciées peuvent être reprogrammées en des cellules souches pluripotentes (iPS). Une autre caractéristique importante de l'ingénierie tissulaire a été l'attribution d'un rôle plus important aux signaux physiques dirigeant la différenciation des cellules souches, depuis la découverte de la modulation de la différenciation des cellules souches par la rigidité du substrat. Les progrès des techniques de formation de nano et micromotifs ont permis une distribution précise des biomolécules et des biomatériaux sur un microenvironnement tridimensionnel, imitant les gradients cellulaires et biomoléculaires ainsi que la rigidité de la matrice extracellulaire naturelle.

Néanmoins, une contrainte majeure dans la réalisation de constructions plus importantes a été le manque de moyens pour transporter l'oxygène vers les cellules et pour éliminer les déchets produits par celles-ci. La construction de structures complexes avec un système vasculaire intégré, avec une haute résolution spatiale, est maintenant une réalité qui ouvre la porte à la fabrication de tissus et d'organes plus complexes et de taille plus importante.

Typiquement, trois types de biomatériaux sont utilisés dans la fabrication d'échafaudages pour l'ingénierie tissulaire : céramiques, polymères synthétiques et polymères naturels,. Ces biomatériaux peuvent être utilisés seuls ou en combinaison pour former des composites afin de potentialiser une ou plusieurs caractéristiques de chacun.

Les cellules souches diffèrent des autres cellules selon deux caractéristiques principales. Les cellules souches sont capables de se renouveler en tant que cellules non spécialisées par division cellulaire et sont capables de se différencier en une vaste diversité de cellules dans certaines conditions physiologiques ou expérimentales. En dépit de la même information génétique, in vivo, les cellules souches reçoivent différents signaux intrinsèques et extrinsèques de leur environnement local qui les conduisent vers différents chemins de différenciation.

Des cellules souches peuvent être isolées pendant la phase de développement embryonnaire du blastocyste (cellules souches embryonnaires), dans des tissus adultes (cellules souches adultes) en encore obtenues à partir de cellules adultes différenciées (cellules souches pluripotentes induites (iPS).

En raison de leur capacité à s'auto-renouveler et à se différencier en différents types cellulaires d'un tissu ou d'un organe particulier, les cellules souches sont au cœur de l'ingénierie tissulaire. Cependant, des défis subsistent, tels que la façon de contrôler la différenciation cellulaire dans les échafaudages et la difficulté de maintenir une de greffe fonctionnelle après implantation dans un tissu. Une autre préoccupation concerne la façon dont les cellules souches sont cultivées en laboratoire, car l'environnement aura un impact sur leur différenciation. Comme l'environnement de culture se démarque de l'environnement in vivo, les signaux biochimiques et mécaniques de la niche des cellules souches sont absents et de nombreuses caractéristiques des cellules souches sont perdues. La présence d'un biomatériau permet de guider la différenciation des cellules souches, voire même de contrôler leur devenir.

Le concept de niche de cellules souches a d'abord été suggéré par Schofield qui le définissait comme un site anatomique, où les cellules pouvaient s'auto-renouveler avec des conditions qui inhibent la différenciation et limitent le nombre de

cellules, favorisant l'homéostasie des niches. Bien que la présence de la niche des cellules souches ait été initialement supposée circonscrite aux sites anatomiques régulant l'activité des cellules souches hématopoïétiques, elle a ensuite été identifiée dans de nombreux tissus dont la moelle osseuse, l'apex du testicule, le bulbe du follicule pileux. Les différentes niches partagent une nature complexe qui comprend des cellules voisines hétérologues, une matrice extracellulaire de support et des facteurs solubles de signalisation tels que les cytokines et les facteurs de croissance. Les signaux physiques comme la contrainte de cisaillement, la raideur et la topographie, ainsi que les signaux environnementaux tels que l'hypoxie et l'inflammation, guident le devenir des cellules souches. Ces signaux permettent aux cellules de rester quiescentes, de devenir actives, de se différencier, de migrer ou de participer à la régénération. La capacité de la niche à s'auto-réguler empêche l'épuisement du pool de cellules souches et, au bon moment, déclenche la prolifération des cellules souches de sorte que la régénération tissulaire puisse se produire. Il a également été démontré que la perturbation de l'homéostasie de la niche est liée à des maladies telles que la leucémie, les gliomes, la maladie de Crohn et le cancer épithélial de la peau. Il est généralement admis que le microenvironnement de la niche produit des stimuli biophysiques et biochimiques intégrés complexes qui agissent sur le devenir des cellules souches. L'effet des signaux biochimiques sur la différenciation des cellules souches a été le premier à être étudié et caractérisé. Cependant, après un travail historique d'Engler et collaborateurs sur l'impact de l'élasticité de la matrice, les attentions se sont tournées vers l'importance des signaux biophysiques. Les progrès de la science des matériaux combinés à la microfabrication et à la microfluidique ont permis d'étudier systématiquement des signaux biophysiques complexes dans des microstructures adaptées. Les composants de la matrice extracellulaire (MEC) représentent une grande partie du pouvoir instructif de niche avec des facteurs de croissance solubles liés à celle-ci. Les proportions de composition matricielle fluctuent d'un tissu à l'autre. Dans la matrice osseuse, par exemple, le collagène de type I représente jusqu'à 90% de la matrice extracellulaire et est essentiel pour maintenir le phénotype des ostéoblastes, alors que le collagène de type I induit la dédifférenciation des chondrocytes in vitro. La MEC peut influencer sélectivement l'adhésion cellulaire et

par conséquent la morphologie et le devenir des cellules. D'autre part, la MEC fournit des signaux biochimiques aux cellules, en partie en séquestrant des biomacromolécules, telles que des facteurs de croissance, influençant le niveau d'accessibilité des cellules à ces macromolécules et en créant des gradients de cytokines. Les protéoglycanes peuvent se lier aux facteurs de croissance en devenant des co-récepteurs de faible affinité ou des diffuseurs de signaux qui influencent les communications cellule-cellule. La composition moléculaire de la MEC va influencer la présence ou l'absence de récepteurs intégrines permettant l'existence d'adhérences focales. Le moyen le plus courant pour la MEC d'exercer une influence directe sur les cellules est à travers l'intégrine. La communication médiée par l'intégrine a été identifiée comme le récepteur clé pour l'ancrage de l'adhésion des cellules souches. Ces récepteurs transmembranaires hétérodimériques permettent la connexion entre le cytosquelette cellulaire et le microenvironnement extracellulaire, appelés adhérences focales, transmettant des signaux qui peuvent conduire à la migration cellulaire, la prolifération et même la survie cellulaire. Les ligands pour les intégrines comprennent la fibronectine, la vitronectine, le collagène et la laminine.

La diffusion de l'oxygène et des nutriments constitue également une préoccupation majeure dans l'ingénierie tissulaire et les échafaudages de grande dimension. Les composites d'hydrogel sont souhaitables dans l'ingénierie tissulaire pour maintenir la haute teneur en eau fournie par l'hydrogel tout en améliorant ses propriétés mécaniques avec d'autres matériaux biocompatibles et biodégradables.

Le travail décrit dans le chapitre 2 a permis d'établir que la diffusion de l'oxygène n'est pas altérée par le renforcement de l'hydrogel Si-HPMC par l’incorporation de laponites. Ces découvertes sont importantes en particulier pour les travaux futurs sur la mimétisation du cartilage puisque les constructions décrites ont des propriétés mécaniques similaires. Afin de caractériser la diffusion de l'oxygène dans des biomatériaux qui pourraient être utilisés comme support de niches de cellules souches, nous avons étudié l'effet de l'augmentation de la concentration de polymère de Si-HPMC sur la diffusion de l'oxygène et la viabilité cellulaire . Bien que les hydrogels Si-HPMC soient principalement constitués d'eau [14] [108], ce qui pourrait favoriser la diffusion des solutés, il a été mis en évidence que des

concentrations élevées de polymères entravent la diffusion de l'oxygène. La diffusion du glucose à travers l'hydrogel polysaccharidique était directement corrélée à la distance moyenne des nœuds du réseau polymérique, mais on ne peut pas en dire autant de l'oxygène. Le chapitre 3 décrit les propriétés de diffusion de l'oxygène du Si-HPMC, et la mise en jeu de ses propriétés dans le design d'une niche spécifique. Par exemple, si l'on essaie d'encourager l'angiogenèse locale par sécrétion de VEGF, un pourcentage plus élevé de Si-HPMC pourrait être utilisé pour limiter la diffusion de l'oxygène natif. D'autre part, si l'on souhaite implanter un hydrogel de Si-HPMC in vivo, la dimension maximale de matériau injecté peut être déterminée avant que l'anoxie ne soit atteinte.

L'ensemencement de fortes densités cellulaires a entraîné une déplétion en oxygène de la construction in vitro et semble être lié à des répercussions concomitantes sur la viabilité cellulaire. Bien qu'une faible tension d'oxygène puisse être souhaitable pour la réplication de la niche des cellules souches, l'extinction complète de l'oxygène dans une construction in vivo a été associée à une viabilité cellulaire compromise. Nous avons émis l'hypothèse que la présence de cellules pourrait agir comme une barrière à l'oxygène de diffusion avec une faible diffusivité de l'oxygène à travers les cellules.

Les résultats du chapitre 3 suggèrent que pour atteindre une densité cellulaire plus élevée, il faut aborder le problème de la diffusion de l'oxygène. Une plus grande capacité de diffusion de l'oxygène dans les premières étapes de l'implantation pourrait être obtenue dans des hydrogels moins concentrés, mais cela signifierait sacrifier les propriétés mécaniques de la construction. Sachant que les cellules in vivo se trouvent généralement à moins de 100 µm d'un capillaire, la prévascularisation ou l'ajout d'un transporteur d'oxygène pourrait être la solution pour des hydrogels plus concentrés

La constitution des canaux devrait faciliter la diffusion de l'oxygène et des nutriments dans les constructions épaisses (chapitre 4). Des constructions perfusables ont été imprimées avec un hydrogel de Si-HPMC. Etant auto-durcissant, l'hydrogel Si-HPMC ne nécessite pas de réticulation par exposition aux UV, ce qui élimine les restrictions de taille imposées par la faible profondeur de perméation

dans les tissus de ce type de rayonnement. L'hydrogel Si-HPMC offre également des propriétés mécaniques ajustables par variation de la concentration de polymère comme indiqué au chapitre 3. Alors que nous avions déterminé qu'une densité cellulaire de 8M / mL dans une construction épaisse (10 mm de haut) conduisait à la mort cellulaire et l'épuisement complet de l'oxygène dans le centre de la construction, la perfusion de microcanaux dans cette même construction épaisse et à la même desinté de 8M / mL permet une viabilité de 80% des cellules après 14 jours de culture.

À notre connaissance, ceux sont les premières données représentant les niveaux d'oxygène dans les constructions avec différents types d'oxygénations. Les niveaux d'oxygène n'ont en effet pas été influencés par la présence de microcanaux en l'absence de perfusion, mettant en évidence l'importance d'une connexion avec le système vasculaire de l'hôte lors d'une greffe in vivo. Les deux constructions sans perfusion ont des niveaux d'oxygène similaires même lorsque la construction interne est traversée par des microcanaux. Cela signifie que la perfusion est nécessaire pour le maintien des niveaux d'oxygène dans la construction ensemencée avec des cellules et que la simple diffusion d'oxygène dans les milieux n'est pas suffisante pour compenser la consommation d'oxygène par les cellules.

Les trois principaux objectifs de cette thèse ont été atteints dans trois chapitres correspondants. Dans le chapitre 2, il a démontré que l'ajout de laponite XLG aux hydrogels Si-HPMC augmente les propriétés mécaniques sans interférer avec la diffusion de l'O2 et la viabilité cellulaire. La capacité d'auto-assemblage des laponites permet la formation d'un réseau hybride interpénétré qui améliore la rigidité de l'hydrogel. Cet hydrogel composite à gélification plus rapide devrait être évalué chez le gros animal afin d'évaluer la préservation du matériel à l'intérieur d'un défaut cartilagineux ainsi que la pertinence clinique de ce composite.

Dans le chapitre 3, nous avons démontré que les hydrogels de Si-HPMC, malgré leur contenu de 95% d'eau, ont fortement restreint les propriétés de diffusion des molécules. La diffusion du glucose à travers l'hydrogel de polysaccharide était directement corrélée à la distance moyenne des nœuds du réseau polymère. Nous avons émis l'hypothèse que la diffusion de l'oxygène était le facteur limitant de la

viabilité cellulaire dans les hydrogels de Si-HPMC. La concentration en oxygène à l'intérieur des hydrogels cellulaires était plus dépendante de la densité cellulaire que de la concentration en polymère. Les hydrogels à faible concentration de polymère présentent une viabilité cellulaire élevée, mais leur propriétés mécaniques sont faibles. D'autre part, une densité cellulaire élevée a entraîné une déficience fatale en nutriments. Dans l'ensemble, ces expériences nous ont fourni des informations utiles pour le développement de futurs microenvironnements cellulaires basés sur des hydrogels de Si-HPMC ou des hydrogels de polysaccharides similaires. De plus, cette méthode peut facilement être étendue à l'analyse de la distribution de nutriments et de l'échange gazeux dans une variété d'hydrogels pour des applications en médecine régénérative.

Le chapitre 4 a été consacré à la quantification de l'impact sur la diffusion de l'oxygène et la viabilité cellulaire après la création d'un réseau de microcanaux à l'intérieur des constructions grâce à la technique de bioprinting. Des constructions cellulaires avec des réseaux de micro-canaux interconnectés 3D intégrés ont été imprimées avec succès en utilisant un hydrogel Si-HPMC chargé de cellules stromales de moelle osseuse et de la gélatine sacrificielle qui peut être facilement éliminée à 37℃. Les concentrations d'oxygène à différentes positions ont été mesurées dans les constructions chargées de cellules avec et sans canaux perfusables. Dans ce chapitre, il a été montré que la perfusion est la clé pour maintenir une concentration élevée en oxygène dans les constructions. Sans perfusion, la concentration en oxygène dans les constructions canalisées était similaire à celle des constructions solides. Lorsque la perfusion a été interrompue, l'oxygène a chuté de 6% en moins de 20 minutes et récupéré 17% en 14 minutes après l'activation de la perfusion. La quantification de la teneur en oxygène dans les constructions perfusables bioprintées peut aider à donner un aperçu de la conception des canaux et à expliquer les réponses cellulaires.

Chapter 1 - Introduction

1.1. Regenerative medicine and tissue engineering

Although the origin of regenerative medicine (RM) can be traced back to more than half a century ago, to when the first successful human organ transplantation took place, it has in the last decade caught a new breath due to technology evolution and improved cell knowledge.

Tissue engineering emerged as concept in the early 1990s, joining patient's own tissue-forming cells and biocompatible polymers with the purpose of creating regenerating biological tissues [1].

It is not a trivial task to make the distinction between tissue engineering (TE) and RM and sometimes both terms are used interchangeably [2]. Nonetheless, TE is more often associated with the principles of design and scaffolding used to create tissue implants and viewed as a subfield of RM. The capacity of repair most human organs possess upon injury is the principle behind RM, the emphasis being on the endogenous tissue formation that may or may not be secondary to a starting material.

TE is a rapidly evolving interdisciplinary field that joins together materials science, biomedical engineering and cellular biology, in a quest to reconstruct living tissues upon injury or loss. For this reason TE has the potential to have a large impact in clinical implantations, expanding tissue supply for transplantation therapies.

The **scaffold** is a centrepiece in TE, since it aims to mimic the extracellular matrix (ECM) that is found in natural tissue. The ECM is composed of a vast array of biomolecules including collagen and elastin (structural proteins), fibronectin and vitronectin (adhesive proteins) and various glycosaminoglycans (GAGs). These biomolecules function to maintain tissue stability, as the ECM functions as physical support for the cells while playing a regulatory role on cell behaviour.

One of the most common approaches in TE is the cell seeding approach, loading stem cells into scaffolds *in vitro* and implanting the scaffold-cell construct after incubation, to ensure cell attachment. Otherwise, the construct can be used as a space filling agent (conductive) or as bioactive molecule delivery system (inductive) as shown in Figure 1.

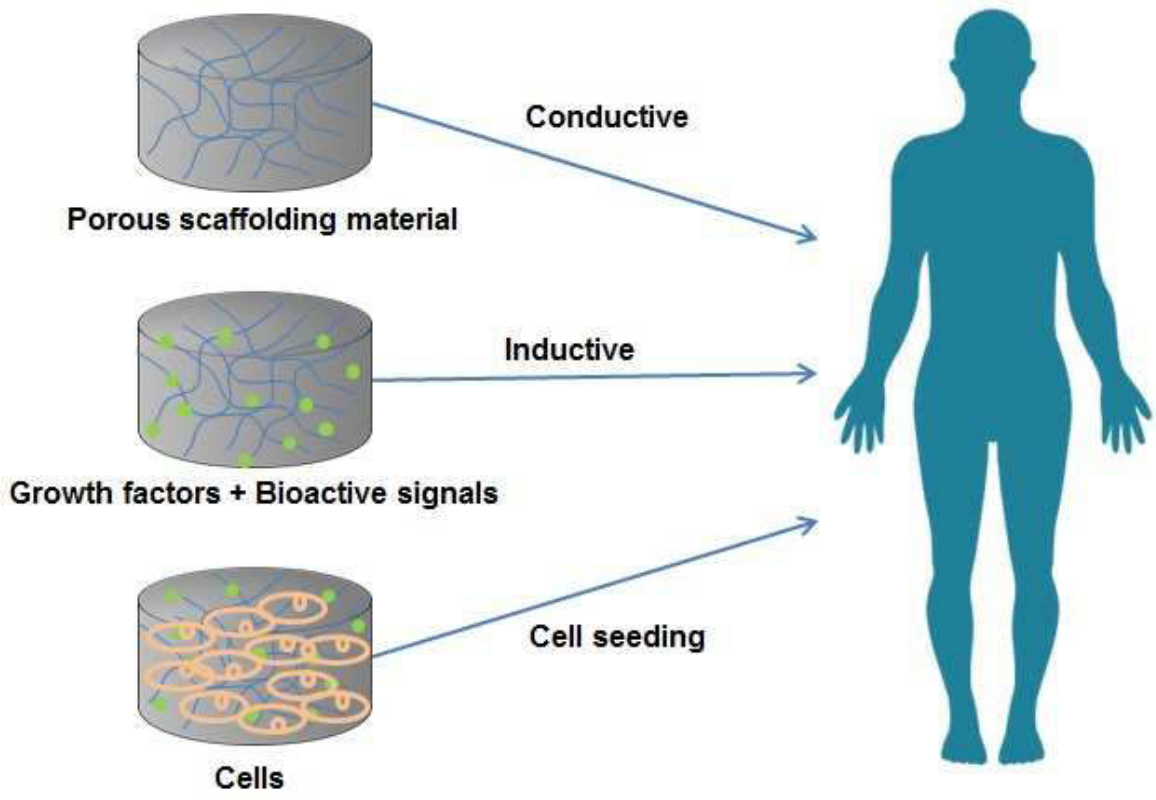

Figure 1 – Scaffolding strategies - Conductive: a biodegradable scaffold is implanted at the site of injury providing mechanical support while new tissue is forming. Inductive: before implantation the scaffold is loaded with bioactive signals to attract and induce cells through tissue formation. Cell seeding: cells are seeded *ex vivo* into the scaffold and tissue is grown prior to implantation. Adapted from [3].

The **scaffold** and its critical characteristics have been largely defined as follows:

- Must be biodegradable, being degraded by the organism and replaced by *de novo* synthetized extracellular matrix (ECM);
- Must not induce acute or chronic immune responses;
- Should allow mass transport of nutrients and metabolic waste;
- Must allow cell attachment, proliferation and differentiation;
- Must provide a 3D template that guides tissue growth.

Constant development of new biomaterials as biomimetic tissues and increasing knowledge about human biology and immunology, have propelled major

advancements in tissue engineering. Furthermore, a well-known limitation, cell availability, was bypassed with the realization that MSCs can be found in various adult tissues and that differentiated cells can be reprogrammed to acquire stem cells pluripotency (iPSCs). Another important mark, in tissue engineering, was the attribution of a more important role to the physical cues directing stem cell differentiation, since the discovery of the modulation of stem cell differentiation through substrate stiffness. Advances in micropatterning techniques allowed the precise distribution of biomolecules and biomaterials on a three-dimensional cell microenvironment, mimicking cell and biomolecules gradients as well as biomaterials stiffness.

Nonetheless, a major constraint in achieving larger constructs has been the lack of means to transport oxygen and waste produced by the cells. The construction of complex structures with an integrated vasculature, with high spatial resolution, is now a reality that opens the door for more complex and larger engineered tissues and organs.

.

1.1.1. Biomaterials and scaffolds

Typically, three individual groups of biomaterials, ceramics, synthetic polymers and natural polymers, are used in the fabrication of scaffolds for tissue engineering. These biomaterials can be used alone or as composites, in order to potentiate certain characteristics of each material.

1.1.1.1. Natural biopolymers

Materials derived from natural sources such as plants or animals help the maintenance of the natural tissue phenotype and function. Natural materials used as stem cell culture scaffolds include proteins (collagen, gelatin, matrigel) and polysaccharides (chitosan, cellulose, alginate hyaluronic acid). These biomolecules

possess bioactive motifs and cell-binding domains, necessary for communication between the cell and the ECM while also having the ability to enhance stem cell adhesion, expansion and differentiation. Another interesting feature of natural materials is their biodegradability, which enables the replacement of the degraded scaffold by the newly produced ECM by the host's cells.

However, due to their biological nature, natural polymers present biological variability which hampers the production of homogeneous and reproducible scaffolds. Moreover, these kind of material possess poor mechanical properties, limiting their application in load-bearing scaffolds and their clinical use might be restricted by the risk of immune rejection.

Collagen is the main component of the ECM and it is vastly used in 3D cell cultures due to its biocompatibility, biodegradability, diminished immunogenicity and mechanical strength. Collagen is a structural protein with a characteristic fibrillar structure, which is important in the extracellular scaffolding, maintaining the biological and structural integrity of the ECM.

Extensive research has been done on electrospinning pure collagen scaffolds with results showing this technique to be suitable to support cell growth [4]. Electrospun collagen fibers were able to recapitulate the structural and biological properties of the natural collagen ECM.

Despite the excellent results at the biological level, pure collagen scaffolds present poor mechanical proprieties, weak structural stability and rapid degradation. Intermolecular cross-linking of collagen through physical or chemical methods has become a common process to improve mechanical proprieties to scaffolds. Physical methods are advantageous in the sense that will not introduce potential toxic residuals, however the cross linking yield is quite reduced. Amongst various chemical reagents, such as glutaraldehyde and formaldehyde, genipin has gained momentum as a naturally occurring cross-linking reagent [5].

Hyaluronic acid (HA) is a glycosaminoglycan that can be found in the ECM and has an important role in lubrication, cell differentiation and cell growth. Due to the short residence time and poor mechanical strength in aqueous environment, HA modification is quite pervasive. HA hydrogel formation by crosslinking is the most common practise [6].

Chemical modification process of esterification has been used to produce HA-derived biopolymers, like HYAFF®. These HA-derived biopolymers have controllable degradation rates and have been applied in orthobiologic, dermal and surgical interventions [3].

HA has also been paired with natural and synthetic polymers to improve biomechanical proprieties. Recently a dual-cross-linking hyaluronic acid system was used as printable hydrogel ink, producing stable constructs that could be functionalized with RGD peptide to support cell adhesion [7].

Alginate, an anionic polymer, has been widely used as drug delivery system and as cell encapsulation agent, due to its low toxicity, and gained particular attention in bone tissue engineering due to its biocompatibility and gel forming properties.

As a composite, alginate has been used to improve mechanical proprieties of other biomaterials such as chitosan, producing biodegradable porous scaffolds, putatively due to the formation of a complex structure of chitosan and alginate. Osteoblasts attached to the chitosan–alginate scaffold, proliferated and deposited calcified matrix, showing a high degree of tissue compatibility in vivo [8].

Other alginate composites for bone tissue engineering include alginate-polymer (PLGA and PEG), alginate-protein (collagen and gelatin), alginate-ceramic and alginate-bioglass, which have shown enhanced biochemical significance in terms of porosity, mechanical strength, cell adhesion, biocompatibility, cell proliferation, increased mineralization and osteogenic differentiation [9].

Chitosan is a linear polysaccharide of β-(1→4) linked d-glucosamine and N-acetyl-d-glucosamine residues derived from chitin. Chitosan is structurally similar to

glycosaminoglycans (GAGs) and is degradable by human proteases, mainly lysozyme.

Chitosan can form “physical” hydrogels based on the reversible interactions of non-covalent nature that can occur between polymer chains, after chitosan amino groups neutralization, inhibiting the repulsion between chitosan chains.

Chitosan has been used for 3D scaffolds, as gels and sponges and in 2D scaffolds, as films for artificial skin and wound healing applications [10].

Electrospinning of chitosan alone can be problematical due to the repulsive forces between charged species within the polymer backbone, that arise at the application of an electric field. It is thus common to add another polymer that helps the electrospinning of the chitosan and ameliorates the mechanical properties, biocompatibility, and the antibacterial behaviour of the resulting fibres.

Gelatin is a natural biopolymer that can be derived by partial acid or alkaline hydrolysis of animal collagen from skin, bones and tendons.

For long term biomedical application, gelatin must be crosslinked to improve both water-resistant ability and thermo mechanical performance of the resulting scaffolds. Gelatin composites of natural or synthetic polymers, exhibit attractive physicochemical, biomechanical, and biocompatibility properties.

Gelatin methacrylate (**GelMA**) is a photocrosslinkable, cell-responsive hydrogel which has been widely for tissue engineering applications [11]. GelMA proprieties are tunable for different tissue engineering (TE) applications through modification of the polymer concentration, methacrylation degree, or UV light intensity.

Cellulose is a polysaccharide consisting of a linear chain β(1 → 4) linked d-glucose units. It is the most abundant biopolymer on Earth and can be found in plant cell walls and produced by certain bacteria.

Cellulose scaffolds have been considered for tissue engineering, however, as a hydrophilic material with low non-specific protein adsorption, matrix ligands addition to these scaffolds is necessary, in order to enable cell attachment to their surfaces. Modifications of cellulose have rendered biocompatible and enhanced mechanical properties for tissue engineering applications.

Cellulose ether derivative hydrogels were developed by the addition of silanol Si-OH groups along the polysaccharide polymer chain. The siloxane bonds creates a polymer network with crosslinked hydrophilic polysaccharide called a silated-hydroxypropylmethylcellulose (**Si-HPMC**) hydrogel [12]. Hydrogels made of Si-HPMC have been used in cartilage [13] bone [14] and have demonstrated to be biocompatible.

Matrigel is a gelatinous protein mixture secreted by Engelbreth–Holm–Swarm (EHS) mouse sarcoma cells, and it is particularly interesting because it contains collagen, laminin, entactin, and important growth factors that mimic the ECM.

Matrigel is highly biocompatibile and has been used widely as cell-culture substrate and as scaffolds for tissue vascularization and angiogenesis [15].

1.1.1.2. Ceramics

Ceramics such as hydroxyapatite and tri-calcium phosphate (TCP) have been mainly used in tissue engineering for bone regeneration applications. Due to their high mechanical stiffness, low elasticity, biocompatibility and chemical similarity to the mineral part of the bone, the use of ceramics scaffolds has been widespread. Furthermore, ceramics are known to enhance osteoblast differentiation and proliferation. The use of ceramics in dental and orthopaedic applications is quite common, being used to fill bone defects and to coat metallic implants.

1.1.1.3. Clay nanoparticles

Clays are considered of great potential for regenerative medicine for their biocompatibility (at higher doses than most nanomaterials), nontoxicity and relevance to osteogenic cell function. Some studies have shown that clay nanoparticles can positively affect cellular adhesion, proliferation and differentiation [16]. On the other hand clays have been used to enhance mechanical or rheological properties of hydrogels and scaffolds [17]. Re-enforcement of hydrogels with laponites is appealing since these silicates grant mechanical proprieties similar to those exhibited by cartilage tissue.

1.1.1.4. Synthetic polymers

Scaffolds for tissue engineering applications derived from synthetic materials may offer advantages over natural biomaterials, such as reproducibility and better control over mechanical properties and degradation rates. The production of porous scaffolds from these polyesters has been achieved through solvent casting or particular leaching method, which is a major advantage for diffusion characteristics of the scaffolds.

Nonetheless, synthetic biomaterials have a major disadvantage as they often lack sites for cell adhesion and may need to be modified to introduce cell attachment cues, such as matrix ligands, for adhesion. Usually these approaches will mean complex chemistries, or expensive crosslinking reagents. Some of these polymers lack biocompatibility and may trigger inflammatory response when implanted or upon degradation *in vivo.*

Common synthetic polymers used for tissue engineering research include poly(lactic-co-glycolic acid) (PLGA), and Poly(caprolactone) (PCL).

PLGA is a polyester copolymer of lactic and glycolic acids, biocompatible and biodegradable. PLGA possesses tuneable mechanical properties turning it into an appealing biomaterial for various applications ranging from bone grafts [18] to tissue/ organ printing [19]. Furthermore, PLGA has been approved for clinical use in humans

by the U.S. Food and Drug Administration (FDA). However, *in vivo*, PLGA degrades into acidic metabolites that can affect the local pH of the ECM, which can lead to inflammation and immune responses.

PCL is another FDA approved biodegradable polymer, biocompatible and that safely breaks down in the body. Compared to PLGA, PCL has better mechanical strength and is less brittle, and the blending of the polymers is common [20]. However, PLGA is linked with better cell adhesion and proliferation than PCL due to its hydrophilic character.

As a thermoplastic polymer, PCL is quite used in extrusion based 3D printing, to construct patient-specific scaffolds. PCL has been used to guide the internal architecture of the scaffold after a patient computed tomography (CT) scan [21]. PCL has been used as kidney vascular corrosion casts in the fabrication of biomimetic vascular scaffolds [22].

1.1.2. Stem cells

Stem cells differ from other cells in two main characteristics; stem cells are capable of renewing themselves as unspecialized cells through cell division and are able to differentiate into a vast diversity of cells under certain physiologic or experimental conditions. Despite possessing the same genetic information, *in vivo* stem cells receive different types of intrinsic and extrinsic cues from the local environment, that drive them into different differentiation paths [23][24]. *In vivo,* stem cells can serve as a repair system dividing without limit to replenish cells that have disappeared.

Stem cells can be found in embryos formed during the blastocyst phase of embryological development (embryonic stem cells) and in adult tissue (adult stem

cells) or adult differentiated cells (e.g. skin) can be induced pluripotent stem cells (iPSC) as represented in Figure 2.

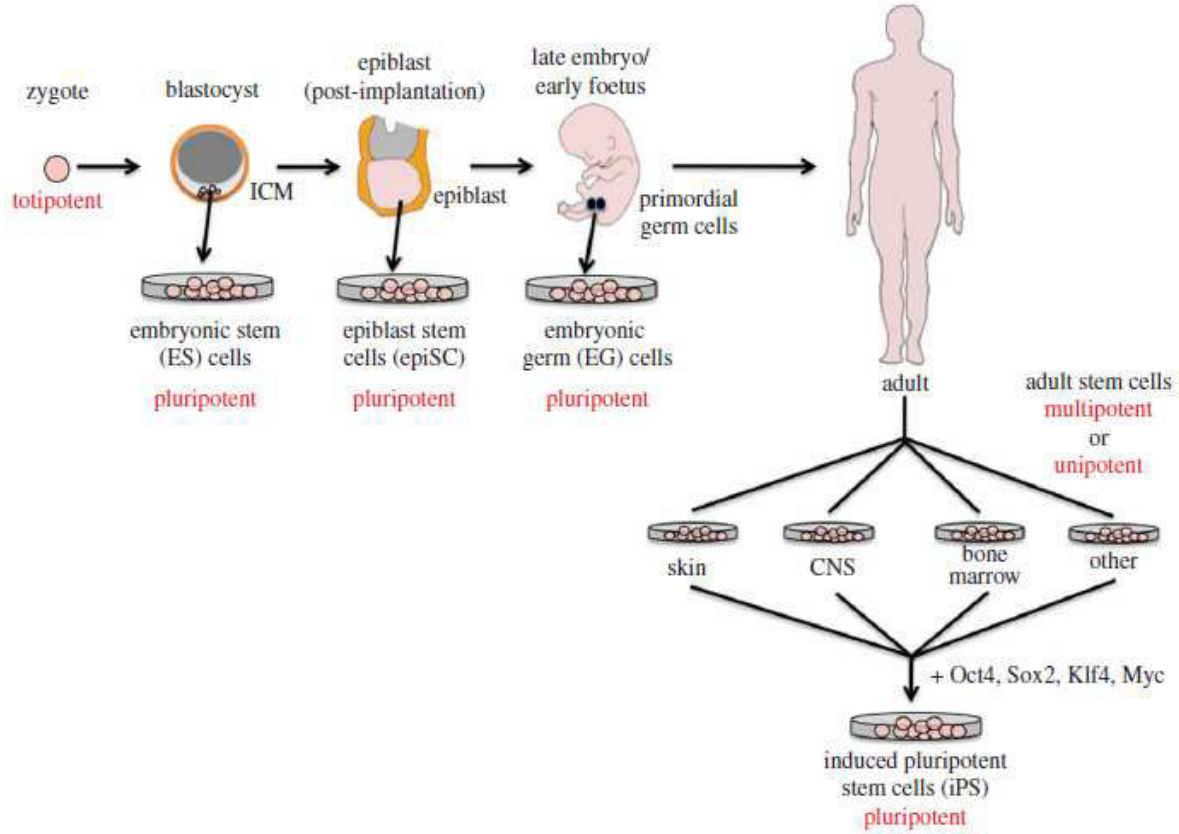

Figure 2- Types of stem cells. ESC and iPSC are described as pluripotent as they can form all the cell types of the adult organism. MSCs are multipotent stem cells because they have the ability to form all the differentiated cell types of a given tissue. In some cases, a tissue contains only one differentiated lineage and the stem cells that maintain the lineage are described as unipotent. Adapted from [25].

Because embryonic stem cells (ESC) must be obtained from an embryo in early development, the use of ECSs raises ethical questions that the utilization of adult stem cells, either mesenchymal stem cells (MSCs) or induced pluripotent stem cells (iPSCs), does not. For this reason, it is easily understandable that MSCs and iPSCs have been the preferred choice for tissue engineering development and these are the stem cells that will be the focus of this brief introduction.

MSCs are able to differentiate into mesenchymal lineages, including osteoblasts, adipocytes, and chondroblasts. MSCs can be isolated from a variety of sources in the human body such as bone marrow, adipose tissue, and the heart. Furthermore, as they are culture-dish adherent, they can be expanded in culture while maintaining their multipotency. MSCs have been used in preclinical models for tissue engineering of bone, cartilage, muscle, marrow stroma, tendon, fat, and other connective tissues.

Since the discovery of iPSC by Shinya Yamanaka in 2006, the knowledge on reprogramming somatic cells has advanced considerably. Initially a combination of four transcription factors was used and delivered to somatic cells through a retrovirus. Nowadays, there are a vast number of techniques and protocols that allow for the productions of iPSC [25]. iPSCs have become a feasible source of cells for tissue engineering applications, since they can be derived from patients generating patient-specific stem cells. However, since cell reprogramming is a fairly new technology, there are some aspects that raise concern. iPSC production remains a low efficiency process and the use of viral vectors raises the risks of chromosomal instability and oncogenic transformation.

1.1.2.1. Stem cell based therapies

Stem cell based therapies involve the transplantation of human cells into patients and have been practiced with success for over 50 years, most notably through the transplantation of bone marrow in hematological cancers such as leukemia [26]. Stem cell therapy potential is mammoth, and organ regeneration is one of the applications that have been vastly explored.

Stem cell injections have been used to repair defective tissues like cartilage and heart [27]. Injection of MSCs is a promising treatment for cellular therapy since MSCs home in to the site of inflammation when injected intravenously [28]. However, when the purpose of MSC injection is to regenerate a large defect area, like

segmental bones and articular cartilage defects, MSCs need to be delivered in a protected manner.

Owing to their ability to self-renew and differentiate into different cell types of a particular tissue or organ, stem cells are at the heart of tissue engineering. However, challenges remain, on how to control cell differentiation in the scaffolds and present functional engraftments of implanted tissues. Another concern is related with how stem cells are cultured in laboratory, because the environment will have an impact in stem cell differentiation. As the culture environment draws apart from the *in vivo* environment, the stem cell niche, biochemical and mechanical cues are lost and so are many of the stem cell characteristics. Biomaterials are thought to protect and guide stem cell differentiation and have been proven to control stem cell fate [29].

1.2. Introduction to the stem cell niche

The concept of stem cell niche was first hypothesised by Schofield [30] that defined it as an anatomical site, where cells could self-renew with conditions that inhibit differentiation and limit the cell number, promoting the niche homeostasis. Although the presence of the stem cell niche was initially hypothesized to be circumscribed to anatomical sites regulating the hematopoietic stem cell activity, it has since been identified in numerous tissues including the bone marrow, the apex of the testis and the bulge of the hair follicle [31].

The different niches share a complex nature that includes heterologous neighbouring cells, a supporting ECM and signalling soluble factors such as cytokines and growth factors. Physical cues like shear stress, stiffness and topography, as well as environmental signals such as hypoxia and inflammation, will provide cues guiding stem cell fate. These cues will direct cell to remain quiescent, become active, differentiate, migrate, or participate in regeneration [32]. The regulatory capability ensures that the niche does not exhaust the stem cell pool and, at the right moment, triggers stem cell proliferation so that tissue regeneration can occur.

The perturbation of the homeostasis of the niche has equally been proven to be related with such diseases as leukemia, gliomas, Crohn disease, and epithelial skin cancer [33].

1.2.1. Why bioengineer the stem cell niche?

A successful replication of the stem cell niche is expected to have impact in various aspects of modern biological and biomedical research. Such structure would

provide means for the study of stem cell behaviour, *in vitro* expansion of stem cells and support for the therapeutic potential of stem cells.

Stem cell culture in a 3D environment *in vitro* allows for the investigation of the stem cell niche, and downstream applications such as the creation of tissue engineered constructs and drug screening platforms[34].

Mimicking the niche can be used as a tool to control stem cell fate in contrast to the non- hierarchically organized cultures, leading to cell renewal or cell differentiation [35]. The reconstitution of the niche *in vitro* can be engineered to identify contributions of different cues in the regulation of stem cell fate, as for example spatial gradients [36]. More and more high throughput approaches have been used to screen different cues in a combinatorial and more efficient way [37].

The replication of the niche could also be convenient for the creation of models to be used in toxicity studies and function as disease models. Furthermore, a functioning model can evolve to a have clinical benefit from the delivery and protection of stem cells, to injured tissues, to actual organs that can be recreated *in vitro* and latter transplanted into patients [38].

1.2.2. Bioengineering the niche

The complete engineered niche has to encompass, besides stem cells, the many complexities of the *in vivo* inspiration such as signalling molecules, cell-cell interactions, cell-ECM interactions, 3D mechanical forces and physicochemical cues, such as oxygen, metabolites, and hormones. The most significant part of extrinsic cues arriving to the niche come from the ECM, characterized by specific biochemical, mechanical and biophysical properties [39]. Biophysical cues include matrix elasticity, surface topography and rigidity. Surface modification can also be tuned to instruct biochemical and biophysical cues.

A common feature of the stem cell niche in different tissue types is this dynamic microenvironment that changes in time and space, in response to a myriad of physical and chemical cues. The complexity of everything niche concerned makes

the *in vitro* recreation a complex task that is progressing every day. Over the years, soluble factors have been widely recognized as impacting stem cell fate, and have been transferred to *in vitro* culture. More recent is the interest in biophysical proprieties, inherent to biomaterials, which have been identified as an important signal. It has been shown that cells will respond to material stiffness, elasticity and viscosity. In this way, attention has been drawn to the replication of the niche through mechanical proprieties, as studies of the impact of physical proprieties in stem cell fate abound nowadays. Nonetheless, biophysical cues alone suffer from less sustainability, and their role is not yet entirely scrutinized [40]. The conciliation of both biochemical and biophysical factors would potentiate the success of an *in vitro* stem cell niche.

There are several approaches to a 3D culture of stem cells, including scaffold-free sheroids or aggregates that unfortunately lack in the possibility of control over the ECM properties, or even the cell culture in decellularized ECM from native tissues, that will present batch-to batch variability. However, hydrogels, a biomaterial that is constituted of hydrated polymer networks, have been widely used as scaffolds for stem cells. Hydrogels are standardized biomaterial with a water content similar to the ECMs, similar range of elasticity, tunable mechanical proprieties. Hydrogels can also be engineered to present patterns of adhesion, growth factors and mechanical gradients, degradation rates and geometry.

1.2.3. Challenges of in vitro design

Current 3D models feature materials ranging from decellularized ECM to synthetic biomaterials. Complex matrices such as Matrigel or decellularized ECM represent a variable product (batch-to-batch), however the employment of these matrices could be the means to provide important cues for the cells. On the other hand, synthetic polymers can be easily controlled but usually lack cell adhesion sites.

While the response of stem cells to extrinsic factors is still not yet completely characterized, it is also known that cells can exhibit a range of responses to signals

arising from the niche. For this reason, when trying to replicate the stem cell niche *in vitro*, it is a challenge to choose which cues should be included. In order to move forward, there is a need for a better understanding of the role of each niche component, and each should be studied both isolated and in an integrated fashion. The cell may sense, not independently, complex physical cues such as cell shape, microtopography, or force application, but rather, these cues may differentially impact signalling pathways. Although a large amount of characterization has been done in this field, the mechanisms and the extent to which a cell distinguishes these signals as distinct information are yet to be fully understood [41].

Collecting the necessary number of cells for tissue engineering purposes is a challenge, since availability is reduced and stem cell fate *in vitro* is still hard to control. Amongst stem cell types, MSCs have become an interesting source for tissue regeneration as they can be found in various adult tissues. How to create cell microenvironments, close to the *in vivo* scenario, that will facilitate the survival of the implanted cells and influence cell fate as well, is the major challenge. For this purpose there is the need to better understand the niche-mediated stem cell regulation.

1.3. Microenvironmental cues directing stem cell fate

It is generally accepted that the niche microenvironment produces complex integrated biophysical and biochemical stimuli that act on stem cell fate. Biochemical cue effect, on stem cell differentiation, was the first to be studied and characterized. However, after landmark work by Engler et al [29] on the impact of matrix elasticity, attentions turned to the importance of biophysical cues. Progress in material science combined with microfabrication and microfluidics allowed the systematic study of complex biophysical cues in tailored microstructures [42].

Virtually every cell in the in the human body is exposed to the ECM and the signals that have origin at the matrix level. The ECM components represent a large part of the niche instructive power along with ECM-bound and soluble growth factors [43].

Matrix composition proportions fluctuate from tissue to tissue. In bone matrix, for example, collagen type I adds up to 90% and is essential to maintain osteoblast phenotype, whereas type I collagen induces dedifferentiation of chondrocytes *in vitro*. ECM can selectively influence cell adhesion and consequently their morphology and fate [44].

On the other hand, ECM provides biochemical cues to cells, partly by sequestering biomacromolecules, such as growth factors, influencing the level of accessibility of cells to these macromolecules and creating cytokine gradients. Proteoglycans can bind to growth factors turning into low affinity co-receptors or signal presenters which influences cell-cell communications. The molecular composition of the ECM will influence the presence or absence of integrin receptors, enabling the existence of focal adhesions [45].

The most described way for the ECM to exert direct influence over cells is through cell receptor and integrin mediation. Integrin mediated communication has

been identified as the key receptor for stem cell adhesion anchorage and homing. These heterodimeric transmembrane receptors allow the connection between cellular cytoskeleton and the extracellular microenvironment, named focal adhesions, transmitting cues that can lead to cell migration, proliferation and cell survival. Ligands for integrins include fibronectin, vitronectin, collagen and laminin.

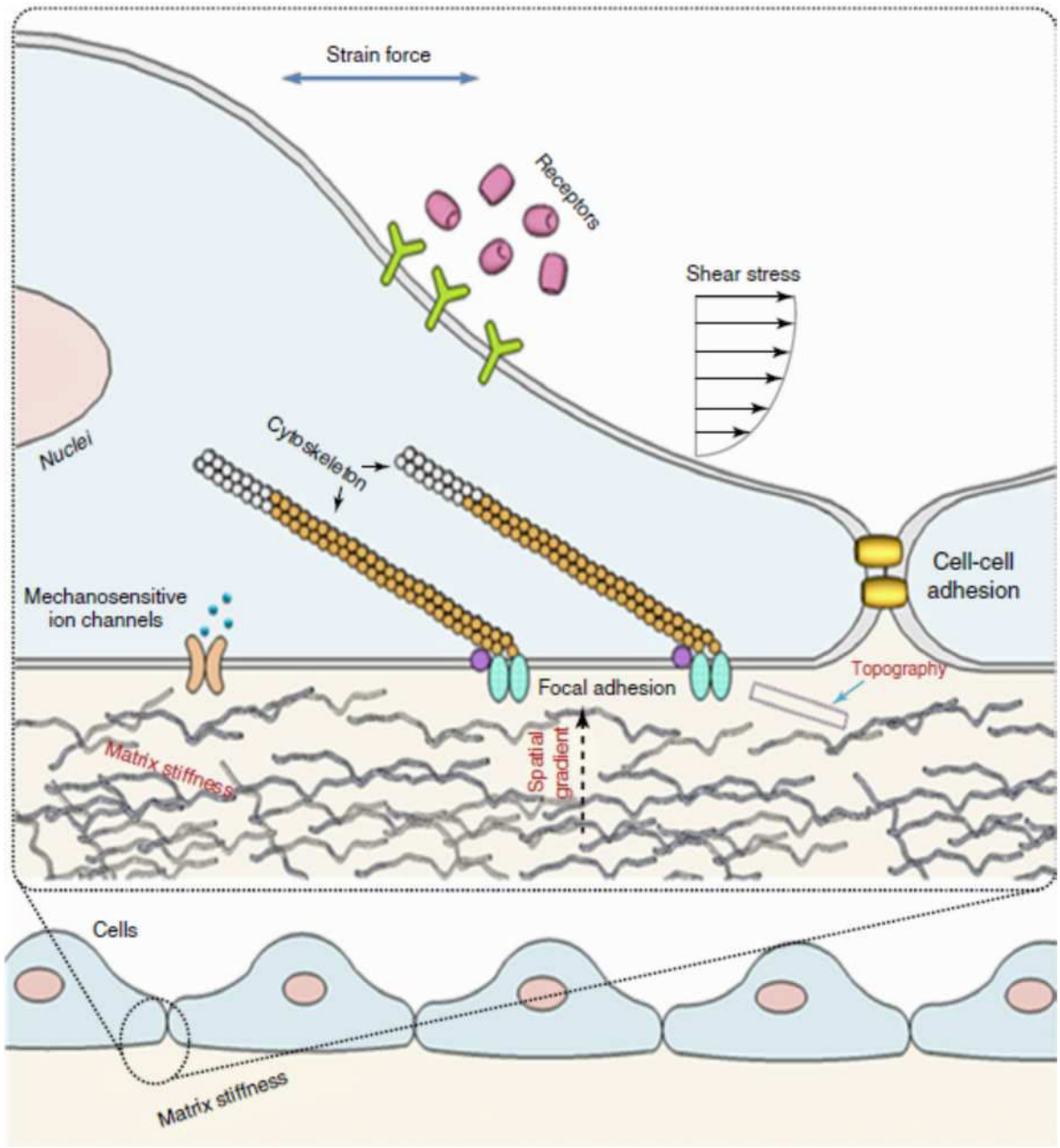

Figure 3 – Native physical microenvironment and mechanosensors of stem cells. The stem cells in vivo are subjected to a broad variety of physical cues, including matrix stiffness, mechanical forces (e.g. strain force and shear stress) and topography, mostly in a spatiotemporally dynamic manner (spatial gradients). Adapted from [27].

Tension cues from the ECM trigger a conformational change, giving place to a variety mechanochemical signals to the cell via intracellular transduction [46]. The communication between cells and ECM is bidirectional, since cells will also remodel the surrounding environment through the expression of enzymes such as metalloproteinases and lysyloxidases.

In vivo studies of integrin and ECM genes knock out have proven the importance of these interactions in maintaining tissue morphogenesis and homeostasis [45]. Other nonintegrin receptor families have been identified in mediated adhesion including selectins, cadherins, immunoglobulins.

Given the importance of the ECM role on stem cell fate, engineering the matrix is a central issue to the success of the *in vitro* stem cell niche. Biophysical cues including matrix stiffness, dimensionality mechanical forces, topography and permeability will be herein further discussed.

1.3.1. Matrix stiffness

Tissue stiffness along the body is not homogenous, as it is perceptible when comparing native tissues like soft brain tissue and leg bone. In 2006, the impact of matrix stiffness on cell fate was first demonstrated. When cultured on top of hydrogels close to brain stiffness (*0.1–1 kPa),* MSC presented a neurogenic phenotype, whereas when cultured on stiffer hydrogels, closer to the bone stiffness, (25–40 kPa), cells presented an osteogenic phenotype as can be seen in Figure 4 [29].

Furthermore, substrate stiffness was shown to affect cell survival and proliferation. Muscle stem cells, when grown on a Petri dish, lost their pluripotency and stopped proliferating, whereas when grown on softer hydrogel substrates, similar to muscle stiffness, cells kept their *stemness* [47].

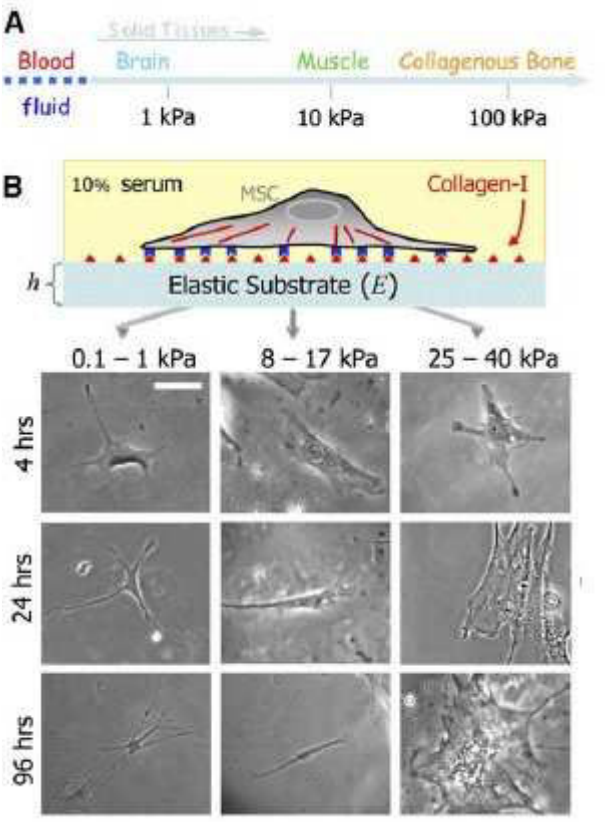

Figure 4 - (A) Solid tissues exhibit a range of stiffness, as measured by the elastic modulus, E. (B) Naive MSCs are initially small and round but develop increasingly branched, spindle, or polygonal shapes when grown on matrices respectively in the range typical of ~E_{brain} (0.1–1 kPa), ~E_{muscle} (8– 17 kPa), or stiff crosslinked-collagen matrices (25–40 kPa). Adapted from [29].

To further investigate the effects of matrix stiffness and stiffness variation, MSCs were cultured in mechanical heterogeneous hydrogels with a stiffness gradient. Cells were found to migrate towards increasing stiffness [48].

The dimensionality plays an important role in cell phenotype and the effect of substrate stiffness in 3D has been increasingly studied, showing that cell do behave differently. The morphology of MSCs remains rounded during differentiation when encapsulated alginate hydrogels independently of matrix stiffness [49]. Contrary to the observed in 2D, MSC in 3D did not migrate in stiffness gradients [50]. If from one side stiffer matrices favour osteogenic differentiation in 2D, in 3D osteogenesis is favoured at an intermediate stiffness.

While softer matrices favoured cell proliferation in three dimensions, it also provided a permissive environment for MSC osteogenic differentiation, even in the absence of RGD ligands [51]. These results support the theory that these compliant matrices allow for the surrounding of the MSC by self-synthesized ECM, creating a new biochemical and mechanical microenvironment that in turn controls MSC behaviour. In fact, stem cell differentiation has been shown to be regulated by the viscoelasticity of the hydrogel. Viscoelastic matrices accommodate the reorganization of the matrix and through cycles of strain and stress relaxation lead to ligand clustering and cell spreading [52].

1.3.2. Dimensionality

Despite cells natural microenvironment being in three dimensions, the current body of knowledge of many biological processes was largely gathered from experiments in two dimensions. In 2D culture cells are polarized, having a side attached to the substrate and a free side in contact with media. In this context, there is a polarization of the integrins biding and mechanotransduction affecting intracellular signalling. Biophysical cues that would be delivered by the 3D ECM structure are absent and cell-cell interactions are reduced if not completely absent. Moreover, cells are exposed to a homogenous concentration of nutrients and growth factors contrasting the dynamic spatial gradients that exist *in vivo*. The importance dimensionality has over stem cell fate has been shown by comparing cell cultures in different dimensions.

Biomaterials can be chemically modified to incorporate cell adhesion RGD and other biomolecules in 3D in order modulate stem cell fate [42]. Culturing cells in 3D has been proven to influence the cell phenotype versus 2D, through diffusion of soluble signals and differences in polarity [53]. When cells were cultured in a 3D environment, chondrocyte differentiation was promoted whereas in a collagen substrate in 2D, it was not [54]. 3D embryoid bodies of embryonic stem cells favour chondrogenesis when compared to 2D culture [55].

However technical limitations in imaging and real time monitoring arise when studying 3D complex cultures interactions. There is a need for technology that benefits from the engineering techniques developed in recent years. The added dimension *in vitro* allows for the inclusion of biochemical cues that exist *in vivo,* through the recreation of growth factors gradients, while providing the structural and mechanical cues, cell-matrix interaction, and diffusive transport of soluble molecules [54]. The addition of these parameters allows the study of cell adhesion, mechanical proprieties over cell fate, effect of diffusion rates of biomolecules and creation of local gradients of oxygen and nutrients.

It is clear that dimensionality is essential in order to maintain cellular phenotype and function as part of a developed physiological relevant structure. The

three dimensions also allow for a dynamic between a differentiating cell and its matrix, as an opportunity to change its surroundings [56].

1.3.3. Mechanical forces

Cells ability to change and be influenced by their surroundings via transduction of forces has been proven to alter stem cell fate [57]. The mechanical forces that can be exerted at the cellular level can be divided in the internal and external components, as cells produce and are exposed to forces. Mechanical forces are known to influence stem cell fate from the embryogenesis to adulthood. Internal forces arise from within cells, namely from the cellular actomyosin cytoskeleton and the external component is the group of forces exerted on the cell that can be modulated *in vitro* [27]. External forces can influence cells directly through mechanotransduction. This process happens as a transformation of a mechanical signal perceived by mechanosensitive ion channels and focal adhesion. Dominant external forces are shear stress and tensile forces, originated by physiological events like blood flow and muscular movement respectively. Stem cells have been shown to respond to such mechanical stimulation *in vivo* as early in development as the embryonic phase. During gastrulation, the spheres of cells organized in 3 layers experience several types of forces [58]. Mechanical stimulation has been used to induce MSC differentiation in conjunction with substrate guidance without biochemical signals [59]. MSCs seeded in type I collagen exposed to tensile strain showed increased expression of osteogenic markers and downregulation of chondrogenic and adipogenic markers [60].

Tensile forces can be applied on stem cells *in vitro* via stretching of cell embedded substrates or magnetic beads. Mechanical stimulation can be used both to study *in vivo* behaviour and to differentiate cells pre-implantation.

1.3.4. Topography

In vivo, ECM presents different micro and nano topographies such as groves and ridges that ultimately affect stem cell growth and differentiation. Stem cell fate has been shown to be influenced by surface nanotopography size, shape and orientation. By altering dimensions of nanotubular-shaped titanium oxide it was possible to augment stem cell adhesion or differentiation into osteoblasts without biochemical cues [61]. When nerve cells were seeded in aligned 3D nanofibrous core-sheath scaffolds, these cells were found to grow orientated with the scaffold. *In vivo* results showed that the scaffold worked to support axonal regeneration [62]. The organization of the fibers constituting the ECM can affect cell membrane curvature which has an impact at the organizational level of membrane receptors [63]. Alignment phenomena, also known as contact guidance, occurs as topographical structures of nano and microgrooves guide cell alignment and migration toward the grooves [64]. Again focal adhesions play a major part in the orientation of the cells, being that actin filaments that originate from that point will be orientated the same way and consequently orientate the cell along the direction of the fiber [65].

Different patterning cues determines the locations of stem cells, differentiated cells and proliferating cells [66]. Micropatterned islands were created with specific shapes to observe cell behaviour at single-cell level. By changing the shape of the islands from elongated to circular, the differentiation ability of epidermal stem cells was increased [67].

The advent of new technologies made possible the construction of sophisticated microstructures and the generation of active biophysical signals that can be used to direct stem cell fate.

1.3.5. Oxygen tension / gradient

The highest oxygen concentration in the human body, a partial pressure (pO_2) of 95mm Hg, can be found in arterial blood, in normal physiological conditions [68].

However cells that are more distant from capillaries will depend on the diffusion of oxygen and a concentration gradient will be formed. In some cases, whole tissues like the renal medulla, can function at low oxygen concentrations. Oxygen has been identified as a critical component of the niche [69] but studies on the subject are still scarce. Stem cells are commonly located in the proximity of blood vessels, suggesting an intervention of the niche vasculature over the niche regulation [70]. The engineering of the niche should thus take into account that oxygen should be reaching the stem cell since it is as important factor in stem cell renewal.

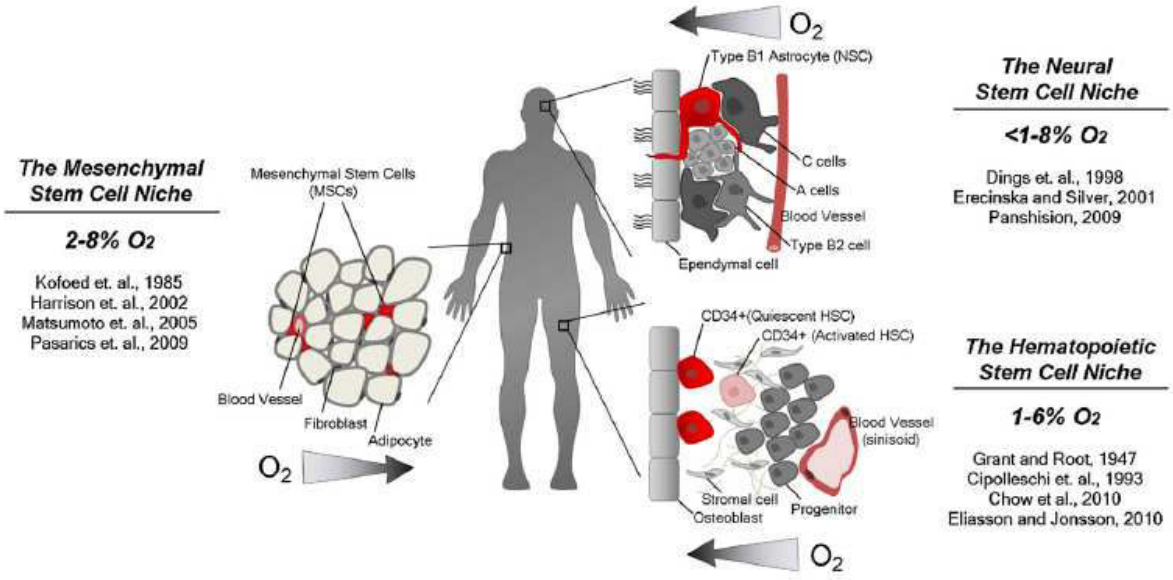

Figure 5- Current available data for the hematopoietic, mesenchymal, and neural stem cells in their designated niches: the bone marrow, adipose tissue, and the subventricular zone (SVZ), respectively. Red cells represent HSCs, MSCs, and NSCs. Adapted from [71].

In vitro, while low oxygen concentration can be closer to physiological conditions for certain cells than normoxic levels, exceedingly low oxygen levels will most certainly lead to cell death. Whilst in 2D, cell cultures have been subject to hyperoxia, in 3D oxygen gradients are formed and constructs with large dimensions end up with a hypoxic core [72], which limits the tissue engineers to non-celllularized, thin or pre-vascularized constructs [68]. Very thin or avascular tissues such as the

trachea, nasal alar lobule cartilage, are easier to engineer since oxygen diffusion does not pose a problem [73].

On the other hand, hypoxic conditions have been show to promote vascular degeneration and can be necessary to control stem cell differentiation. There is a need for a compromise in order to limit oxygen concentration within a range that would best suit the purposes of the designed construct. Depending on the size of the scaffold, host mediated angiogenesis can be considered too slow since vascular ingrowth can take up to 2 weeks in a 3 mm scaffold [73]. Other strategies to overcome hypoxia in tissue engineering include pre-vascularized scaffolds and oxygen carriers.

Oxygen carriers such as haemoglobin and PFC can be used for improving the oxygen transport within aqueous solutions. Haemoglobin has to be modified to prevent immunogenic reactions and the breakdown of haemoglobin outside of the red blood cell. However modified haemoglobin has been used with moderate success since it provokes vasoconstriction as a side effect.

Microfabrication technologies facilitate the engineering of branched microfluidic channels within biocompatible materials. Techniques like bioprinting allow the construction of cell laden vascularized multi-material and cell types that exceed 1cm in thickness [74].

1.4. Bioengineering strategies to mimic the stem cell niche

Despite the enormous potential that self-renewal and differentiation of stem cells represent for regenerative medicine, a lot is still dependent on the ability to direct stem cell fate. Cell-based therapies are a promising clinical approach but the long term survival and functional engraftment of the transplanted cells challenge still remains. Delivery of unprotected cells often results in poor engraftment rates. The site of delivery is usually damaged which means adverse conditions to the stabilization of the engraftment. Biomaterials can be used to protect the cells from aggression at the site of injection and improve cell survival after engraftment.

Natural biopolymers often offer poor mechanical proprieties and are poorly defined, while synthetic materials often lack sites for cell adhesion. In order to achieve more control over artificial scaffolds, novel technologies for 3D scaffold fabrication, like micropatterning, and 3D printing have been under the spotlight.

The combination of stem cell potential with biomaterials and microfabrication technologies is promising in recapitulating the complex biochemical and structural aspects of the niche. A scaffold can also be used to support the load left by a large defect, allowing the reconstruction and the means for a long term function of the construct that mature at the site. In this segment we discuss how biomaterials can be used and some of the trending techniques used in biomimicking stem cell niches.

1.4.1. Biofunctional materials for engineering the niche

Hydrogels have been extensively studied as mimetic platforms of the stem cell niche. These materials possess ECM characteristics such as high levels of hydration 95-99% and tunable physicochemical proprieties that can influence stem cell fate as

described previously. Mass transport characteristics should allow the diffusion of external stimuli although this will depend on polymer concentration and individual characteristics of each hydrogel. Cell culture in hydrogels implies the inclusion of a third dimension, contrasting with the classic tissue culture flask, since it permits the introduction of gradients and spatial and temporal complexity. An interesting advantage of hydrogels is that they can be polymerized in the presence of cells, ensuring a uniform distribution throughout the three-dimensional network. MSCs grown in biomimetic pullulan-collagen hydrogels showed enhanced secretion of angiogenic factors compared to standard culture conditions [75]. Furthermore, this type of materials can be functionalized with the necessary bioactive signals such as integrin receptors, mimicking the natural presentation of niche proteins. Complexity may be built with a bottom up approach adding desired features to a simple backbone material [76]. Hydrogels containing substrates for proteases naturally secreted by cells allows for cells to degrade and remodel their microenvironment [77]. This feature allows for the matrix breakdown at a pace regulated by the cells, accommodating cell migration and proliferation.

Material microarrays have been useful to investigate cell response under various different conditions since many specific niche components have not been well characterized yet. A 3D microarray platform allowed for the characterization of more than 1000 variations of synthetic polyethyleneglycol (PEG) hydrogels with varying mechanical properties, sensitivity to matrix metalloproteinase degradation, cell-cell and cell-ECM interaction [78].

In *in vivo* applications hydrogels have been used to protect transplanted cells and to promote tissue regeneration, releasing soluble cues or recruiting endogenous cells. Controlled released of hepatocyte growth factor from hydrogels showed efficacy in recruiting bone marrow MSC populations while allowing cell infiltration and proliferation yielding what could be called of synergetic regeneration system [78].

1.4.2. Micro/Nanopatterning substrates

Virtually all the cells *in vivo* are surrounded by topographical signals as is the case with nanofibers in the basement membrane, nanocrystals in the form of hydroxyapatite in the bone microstucture and nanopores from capillaries. The replication of such cues is thus desirable and necessary for the mimicking the stem cell niche.

Recent progresses in micro and nanofabrication allowed the composition of complex structures with patterns, shape and dimensions defined to the nanometre. Techniques like nanobioprinting, photolithography and soft lithography can be used to accomplish different levels of detail in structured microenvironments that stimulate cell growth and guide tissue regeneration. The most prevalent method to achieve microscale patterning in a topographical surface is soft lithography, where a substrate, generally plastic or gold-coated glass is stamped usually with a pattern in a PDMS stamp, which leaves an ink design that will selectively bind to the exposed substrate to create ECM islands.

Micropatterning can indeed control cell morphology through the shape of the substrate for single cells or microgrooved patterning to elongate cell shape. These techniques can be applied to the printing of a growth factor array in order to scan the effect of each factor in stem cell fate. Complex shapes of micropatterned islands will guide mesenchymal stem cell differentiation [79]. Furthermore, the micropattern topography can be combined with soluble factors in order to mimic the niche environment[80]. In stem cell niche research aligned micropatterns have been employed as a topographical cue for neuronal differentiation [81].

Although micropatterning is most commonly employed in studying the impact of surface topography in a two dimension scenario, in combination with 3D printing, 3D micropatterning can be used to generate microtissues that mimic the 3D native architecture. 3D Micropatterning has the potential to provide high throughput microtissues with the topographical characteristics of the native tissues, which will be important to study the impact of each 3D topography in stem cell fate[82].

1.4.3. 3D bioprinting

From the concept of stereolithography rose the 3D bioprinting approach, envisioning tissue engineering purposes, which started as a sequential addition of layers. These layers can contain cells, extracellular matrix, other relevant materials or a combination of all the above. This is one of the most promising techniques in tissue engineering, which can occur as a two-step biofabrication process, seeding cells onto a printed 3D scaffold, or in a one-step process, where the cells are encapsulated in a hydrogel and then printed[83].

In research labs microextrusion systems are dominant, although there are other technologies options like inkjet and laser assisted bioprinters [84] as represented in Figure 6.

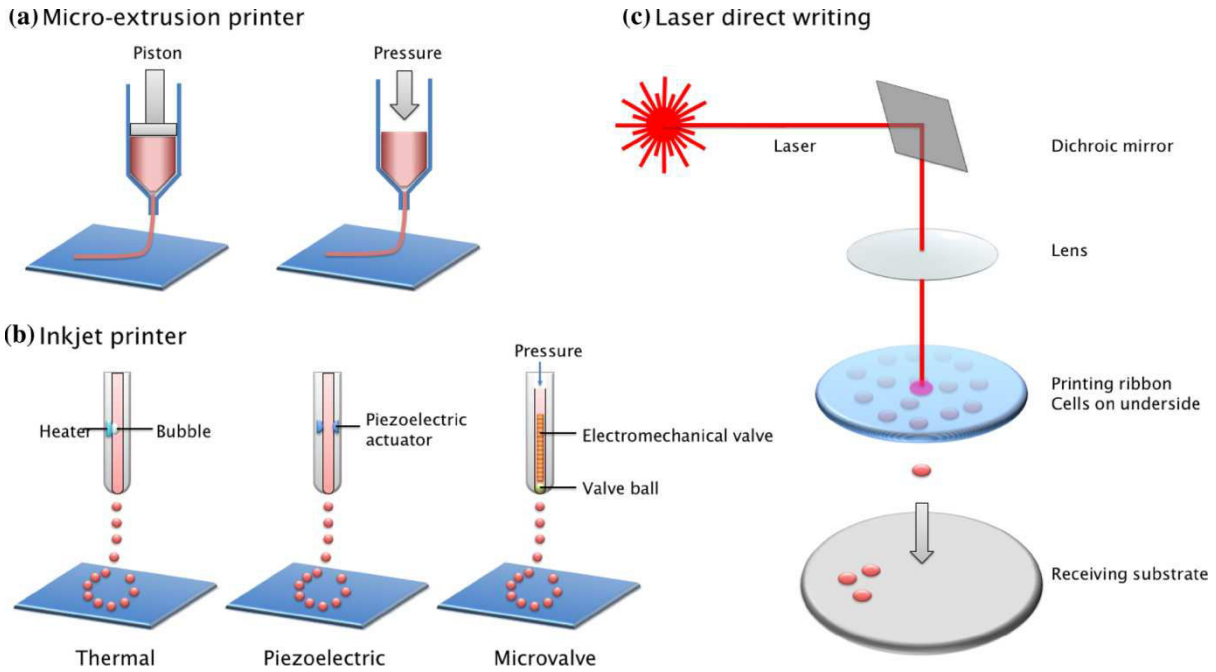

Figure 6 - Printing mechanisms of major cell printing techniques. (a) Micro-extrusion based cell printer uses computer con-trolled piston or pneumatic pressure to extrude the materials out of a syringe needle. (b) Inkjet printer uses several mechanisms (thermal bubble, piezoelectric or electromechanical valve) to create droplets out of liquid solution. (c) Laser direct writing uses the energy of the focused laser beam to generate localized heat to form liquid droplet. Adapted from [11].

Different materials, mainly hydrogels, have now been 3D printed without the need for photopolymerization and it has been done while supporting encapsulated cells. The so called bioinks can be propelled out of the nozzle head and deposit layer-by-layer, cells, biomaterials, or both simultaneously, with great resolution.

This technology together with hydrogel engineering can be used to construct complex structures, and ultimately achieve the formation of functional tissue in vitro. This technique allows for the bioprinting of several constructs ranging from 3D artificial niches to large scale tissue models [42]. Recent studies combine 3D bioprinting with micropattering in order to provide microvascularization to the construct [86]. Microvascularization becomes a big issue as the size of the construct enlarges.

3D bioprinting can be used to reproduce functional tissue units, known as 'organs-on-a-chip', multi-channel 3-D microfluidic cell culture chips, connected to a microfluidic network. This microfluidic devices can be used as high-throughput screenings for drug discovery, toxicology or as *in vitro* models of diseases [38].

Thesis objectives

The broader scope of this PhD project is to deepen the knowledge and provide suitable strategies for diffusion related problems in stem cells biomimetic niches. The successful replication of the stem cell niche is expected to make an impact in various aspects of modern biological and biomedical research. However, the complexity of the niche and regulating cues makes this a herculean task. Enhancing the mechanical properties of the scaffolds may jeopardize diffusion inside the constructs. Oxygen, nutrient and waste diffusion will influence cues arriving to the stem cells and it constitutes a greater problem in large dimensions scaffolds.

The three main objectives of the present work are to:

- Study the impact on oxygen diffusion and cell viability in stem cell seeded constructs after mechanical reinforcement of a biomaterial (hydrogel) with a laponite clay, considered to be of great potential for regenerative medicine;
- Study the impact on oxygen and nutrient diffusion and cell viability in stem cell seeded constructs after hydrogel mechanical reinforcement through polymer concentration;

- Quantify the impact on oxygen diffusion and cell viability, after the creation of a microchannel network inside stem cell constructs through a bioprinting technique.

This thesis is one of the outcomes of NanoFar, an Erasmus Mundus Joint Doctorate in nanomedicine and pharmaceutical innovation funded by the European Commission, Education, Audiovisual and Culture Executive Agency (EACEA).

This project was developed as a collaboration between Laboratoire d'Ingénierie OstéoArticulaire et Dentaire (LIOAD) – Université de Nantes, home partner institution, and Tissue Engineering and Drug Delivery Division, Nottingham University, host partner institution.

Chapter 2 - Oxygen diffusion and cell viability on a reinforced hydrogel with laponite

Introduction

Hydrogels are considered a good candidate to act as a substitute of the ECM, since these polymeric materials can provide a highly hydrate 3D structure for cell support. More specifically, hydrogels are a natural choice to mimic the stem cell niche.

A major constraint, on the use of hydrogels as scaffolds, is the weakness of their mechanical proprieties, which, depending on the characteristic of the target tissue, may render hydrogels a less suitable choice. Mechanical property coherence with the defect area characteristics is not only important for the support of the mechanical load, when the objective of the scaffold+cells is to be implanted, but has also been proven fundamental in guiding stem cells fate through biomechanical cues [29].

For these reasons, hydrogel reinforcement is expected to improve hydrogel performance as an ECM mimic. Hydrogel reinforcement can be achieved through increased stiffness, which may be achieved by increasing hydrogel polymer concentration or crosslinking density, or through the formation of composites. In

composites, the mechanical properties of hydrogels are not the focus, allowing to relax the crosslinking density, which is advantageous for cell migration and tissue formation.

Clays have been used to enhance mechanical or rheological properties of hydrogels and scaffolds [17]. Clays are considered of great potential for regenerative medicine for their biocompatibility, at higher doses than most nanomaterials, nontoxicity and relevance to osteogenic cell function. Some studies have shown that clay nanoparticles can positively affect cellular adhesion, proliferation and differentiation [16]. On the other hand, hydrogel re-enforcement with laponites is interesting, since these silicates grant mechanical proprieties similar to those exhibited by cartilage tissue.

Laponite clays (XLG) are disk-like nanoparticles, that are negatively charged on one side and positively charged on the opposite side, resulting in interesting and controlled gelling properties. However, one major concern with the use of laponites for hydrogel reinforcement is the impact that it could have on oxygen diffusion. In fact, XLG, a silicate nanoclay has been described as an oxygen barrier [87].

How laponite reinforcement would affects oxygen transport, which is essential for cell survival and proliferation, is a relevant issue. Oxygen tension was monitored on 2% Si-HPMC hydrogels and 2% Si-HPMC+1% XLG composites subject to de-oxygenation and re-oxygenation cycles. A study on O_2 diffusion in hydrogels reinforced with laponites was published as part of a broader paper describing the effects of an interpenetrating network, such as laponites, on the mechanical properties of the Si-HPMC hydrogel, its cytocompatibility and the ability of chondrogenic cells to produce extracellular matrix components. These findings were published in Acta Biomaterialia and can be found on the next pages of this thesis under the title:

Article 1 - Laponite nanoparticle-associated silated hydroxypropylmethyl cellulose as an injectable reinforced interpenetrating network hydrogel for cartilage tissue engineering

Acta Biomaterialia 65 (2018) 112–122

Contents lists available at ScienceDirect

Acta Biomaterialia

journal homepage: www.elsevier.com/locate/actabiomat

Full length article

Laponite nanoparticle-associated silated hydroxypropylmethyl cellulose as an injectable reinforced interpenetrating network hydrogel for cartilage tissue engineering

Cécile Boyer [a,b,1], Lara Figueiredo [a,b,1], Richard Pace [a,b], Julie Lesoeur [a,b,d], Thierry Rouillon [a,b], Catherine Le Visage [a,b], Jean-François Tassin [e], Pierre Weiss [a,b,c,*], Jerome Guicheux [a,b,c,2], Gildas Rethore [a,b,c,2]

[a] Inserm, UMR 1229, RMeS, Regenerative Medicine and Skeleton, Université de Nantes, ONIRIS, Nantes F-44042, France
[b] Université de Nantes, UFR Odontologie, Nantes F-44042, France
[c] CHU Nantes, PHU4 OTONN, Nantes F-44042, France
[d] SC3M, SFR Santé F. Bonamy, FED 4203, UMS Inserm 016, CNRS 3556, Nantes F-44042, France
[e] CNRS UMR6283, Institut des Molécules et Matériaux du Mans (IMMM), Université du Maine, Le Mans F-72000, France

ARTICLE INFO

Article history:
Received 17 August 2017
Received in revised form 20 October 2017
Accepted 7 November 2017
Available online 8 November 2017

Keywords:
Hydrogel
Cartilage
Biomaterial
Tissue Engineering

ABSTRACT

Articular cartilage is a connective tissue which does not spontaneously heal. To address this issue, biomaterial-assisted cell therapy has been researched with promising advances. The lack of strong mechanical properties is still a concern despite significant progress in three-dimensional scaffolds. This article's objective was to develop a composite hydrogel using a small amount of nano-reinforcement clay known as laponites. These laponites were capable of self-setting within the gel structure of the silated hydroxypropylmethyl cellulose (Si-HPMC) hydrogel. Laponites (XLG) were mixed with Si-HPMC to prepare composite hydrogels leading to the development of a hybrid interpenetrating network. This interpenetrating network increases the mechanical properties of the hydrogel. The *in vitro* investigations showed no side effects from the XLG regarding cytocompatibility or oxygen diffusion within the composite after cross-linking. The ability of the hybrid scaffold containing the composite hydrogel and chondrogenic cells to form a cartilaginous tissue *in vivo* was investigated during a 6-week implantation in subcutaneous pockets of nude mice. Histological analysis of the composite constructs revealed the formation of a cartilage-like tissue with an extracellular matrix containing glycosaminoglycans and collagens. Overall, this new hybrid construct demonstrates an interpenetrating network which enhances the hydrogel mechanical properties without interfering with its cytocompatibility, oxygen diffusion, or the ability of chondrogenic cells to self-organize in the cluster and produce extracellular matrix components. This composite hydrogel may be of relevance for the treatment of cartilage defects in a large animal model of articular cartilage defects.

Statement of Significance

Articular cartilage is a tissue that fails to heal spontaneously. To address this clinically relevant issue, biomaterial-assisted cell therapy is considered promising but often lacks adequate mechanical properties. Our objective was to develop a composite hydrogel using a small amount of nano reinforcement (laponite) capable of gelling within polysaccharide based self-crosslinking hydrogel. This new hybrid construct demonstrates an interpenetrating network (IPN) which enhances the hydrogel mechanical properties without interfering with its cytocompatibility, O_2 diffusion and the ability of chondrogenic cells to self-organize in cluster and produce extracellular matrix components. This composite hydrogel may be of relevance for the treatment of cartilage defects and will now be considered in a large animal model of articular cartilage defects.

1. Introduction

Articular cartilage (AC) is frequently damaged due to trauma or degenerative diseases. The incidence of joint diseases is constantly

* Corresponding author at: Inserm, UMR 1229, RMeS, Regenerative Medicine and Skeleton, Université de Nantes, ONIRIS, Nantes F-44042, France.
E-mail address: pierre.weiss@univ-nantes.fr (P. Weiss).
[1] Co-first authors.
[2] Co-last authors.

https://doi.org/10.1016/j.actbio.2017.11.027
1742-7061/

increasing due to a rising life expectancy of the general population leading to a global public health issue. The AC tissue is mainly composed of a unique cell type (chondrocyte) embedded within an abundant extracellular matrix (ECM). Cartilaginous ECM is composed of proteoglycans (mainly aggrecans) and collagens (mainly type II, IX and XI). Additionally, AC tissue is aneural and avascular. These characteristics prevent AC from having intrinsic regenerative properties after injuries leading to an inescapable degeneration of the tissue that culminates in osteoarthritis. Therefore, repairing lost or injured cartilage represents a challenge for both clinical and scientific perspectives [1,2].

Several strategies have been developed including tissue engineering which consists in the association of cells (e.g. adipose stromal cells (hASC) and human nasal chondrocytes (hNC)) with biomaterials [3]. Biomaterials, and more specifically hydrogels, have been widely studied over the past years [4]. In the last few years, the authors of this body of work have developed a self-setting hydrogel consisting of silanized hydroxypropylmethyl cellulose (Si-HPMC). This Si-HPMC hydrogel has already been demonstrated to be a convenient matrix for the three dimensional (3D) culture of hASC and hNC [5–7]. Hydrogels are of particular interest in biotechnology, tissue engineering, and drug delivery applications due to their hydrophilic character, porous structure, high water content and often biocompatible nature [8–10]. Despite their many advantages, the stiffness of hydrogels is often two orders of magnitude lower than cartilage's (100–1000 kPa) [11]. This lack of mechanical properties usually limits their application to space-filling scaffolds used for the delivery of bioactive molecules and cells [12,13].

Throughout the literature, several strategies have been developed to tune the mechanical properties of hydrogels, e.g. polymerization rate, polymer concentration as well as particles, carbon nanotubes or fibers embedding. To reach higher stiffness, these strategies usually require high polymer or particle concentrations. Among all these strategies, we decided to use reinforcements capable of crosslinking and forming an interpenetrated network (IPN) with Si-HPMC to increase the mechanical properties without interfering with the oxygen diffusion or cell viability.

Silicate nanoclays have shown great abilities of self-assembly with polymers and hydrogel formation. Indeed, in recent years, there has been much interest in using various clay nanoparticles to modify the properties of polymeric hydrogels and obtain organic/inorganic hybrid hydrogels with enhanced storage modulus [14]. In particular, the laponite clays (XLG), which are disk-like nanoparticles with a diameter of 25 nm and a thickness of about 1 nm, have been utilized in previous studies along with polymers such as poly(lactide)-poly(ethylene oxide)-poly(lactide) triblock copolymers [15], poly(N-isopropylacrylamide) [16], poly(N-vinyl-2-pyrrolidone-co-acrylic acid) [17], poly(ethylene oxide) [18,19], or sodium humate and polyacrylamide to form nanocomposite hydrogels with enhanced mechanical properties. The faces of XLG are negatively charged while their slices are positively charged. These properties allow them to form a hydrogel with controlled gelling properties [20,21] resembling a "house of cards" structure. Controlling the gelling properties has numerous advantages, such as *in situ* gelling which allows for the delivery of cells and bioactive molecules to the tissue defects in a minimally invasive manner.

Within this context, our objective was to use a minimal amount of XLG nano-reinforcements to form an IPN with Si-HPMC to increase the mechanical properties without modifying the interactions and behaviors of our hydrogel in biological environments (cell survival, proliferation, and diffusion).

In this study, we synthesized cellularized composite hydrogels and evaluated their physicochemical properties such as viscosity, gel point, storage modulus and oxygen diffusion. Then, we characterized their *in vitro* cytocompatibility. Based on these preliminary results, the ability of selected composite hydrogels to support the *in vivo* chondrogenic activity of chondrocytes in subcutaneous pockets of nude mice was ultimately assessed.

2. Materials and methods

2.1. Materials

Silanized hydroxypropylmethyl cellulose (Si-HPMC) and the acidic buffer solution (ABS) at pH 3.2 were prepared in our laboratories according to previously published protocols [22,23].

2.2. Hydrogel formulation

Si-HPMC hydrogels were prepared according to the already published protocol [22,23]. Si-HPMC polymer was dissolved in 0.2 M NaOH aqueous solution (30.9 mg ml^{-1}, pH 12.5); then two dialyses with molecular weight cut off at 6–8 kDa were performed in 0.09 M NaOH aqueous solution. The dialyses eliminate the non-grafted 3-glycidoxypropyltrimethoxysilane, used for siloxane grafting onto the HPMC. The hydrogel precursor solution was then obtained by mixing 1 vol of the above Si-HPMC basic solution contained in one luer-lock syringe, with 0.5 vol of ABS in another luer-lock syringe, by interconnection of both syringes; the final pH is 7.4. To prepare a nanocomposite hydrogel, we used two different protocols (Fig. 1A). In protocol A, we dispersed the desired amount of XLG into the ABS. Then we mixed 1 vol of 3 % wt Si-HPMC basic solution with 0.5 vol of ABS containing XLG. In protocol B, we dispersed the desired amount of XLG into distilled water. Then we mixed 1 vol of 4 % wt Si-HPMC basic solution with 0.5 vol of ABS and with 0.5 vol of XLG solution. The XLG amount inside each hydrogel is given as weight percentages of XLG concerning the mass of pure Si-HPMC hydrogel (without XLG). It varied between 0 and 5 % wt/v with protocol A and between 0 and 1% with protocol B. More than 1% of XLG yielded too quickly of a gelation time when using protocol B.

2.3. Rheology and mechanical properties

2.3.1. Gel point and storage modulus measurements

The gel points were measured on HAAKE RheoStress RS300 rheometer (Thermo Scientific) using cone geometry (1°/60 mm). Liquid hydrogel precursor solutions were injected on the plate immediately after mixing and the measurements started 1–2 min later.

Storage (G') modulus was monitored as a function of time under oscillation frequency sweep (from 1 to 22 Hz) at constant temperature (23 °C). The gel point was determined when tan $\delta = G''/G'$ became independent from frequency. Each sample was measured in triplicate.

2.3.2. Dynamic mechanical analysis (DMA)

A volume of 2 mL of the Si-HPMC/ XLG liquid mixtures was injected into each well of 12-well plastic plates for cell culture which served as molds. We prepared hydrogel specimens of each XLG concentration (n = 3). To ensure the complete gelification, the samples were kept enclosed under a humid atmosphere at room temperature for 2 weeks. The 2-week old hydrogels were taken out of molds, and their diameters and heights were measured with a caliper. The DMA study in uniaxial unconfined mode was performed using BOSE ElectroForce® 3100 Test Instrument equipped with the WinTest® digital control system. The sinusoidal oscillations started at 5% deformation of the sample's height, and the oscillation amplitude reached 10% of the height. We then

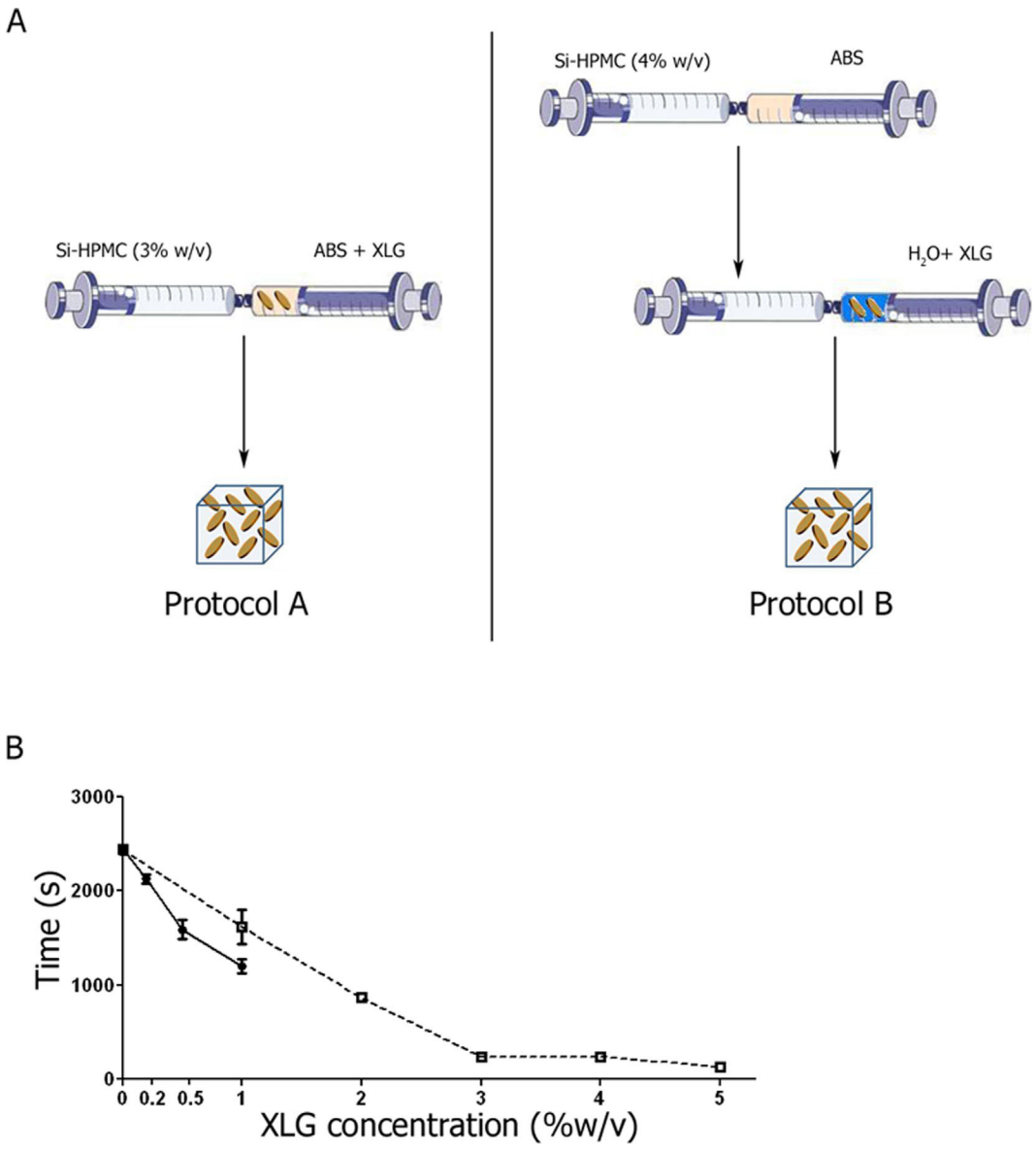

Fig. 1. Preparation protocols and rheological characterization (gel point) of Si-HPMC hydrogels as a function of of XLG concentration. (A) Schematic overview of Protocols A and B (ABS: acidic buffer solution). (B) Gel point of Si-HPMC hydrogels mixed with increasing concentrations of XLG was measured with a RS300 rheometer. Constructs were prepared with either protocol A (dashed line) or protocol B (solid line), as described in materials and methods section.

determined the real part E′ of the complex compressive modulus for each nanocomposite hydrogel at a frequency of 1 Hz.

2.4. Oxygen tension measurements

2.4.1. Oxygen measurements

Core oxygen (O_2) partial pressures in the 3D constructs were monitored with a needle type O_2 microsensor (PreSens, Germany). The optic fiber coated on a 140 μm flat-broken tip with sensitive PSt1 microsensor material (PreSens, Germany) is protected within a standard hollow needle. The sensor allows real-time O_2 measurements, without O_2 consumption, through dynamic fluorescence quenching, with data reported to an oxy-4 transmitter (PreSens, Germany). Since O_2 diffusion is a temperature dependent phenomenon, all measurements were performed at 37 °C.

For determination of O_2 content kinetics in acellular hydrogels (protocol B, Fig. 1A), samples prepared at atmospheric conditions were moved into a SCI-live Hypoxia Workstation (Ruskinn, Pencoed, UK), at 37 °C and 5% CO_2 with O_2 levels set at 0.1%. Deoxygenation of the hydrogel samples (with the tip of the O_2 microsensors positioned in the center of the construct) was followed until equilibrium was reached, after which re-oxygenation was monitored in a 5% CO_2, 37 °C humidified incubator in normoxic conditions (20%).

2.5. Scanning electron microscopy (SEM)

For the SEM experiments, samples of Si-HMPC hydrogel containing laponites were embedded in an acrylic resin obtained by polymerization of a mixture of Glycol Methacrylate (GMA) and n-Butyl Methacrylate (BMA) monomers. Samples were gently dehydrated by soaking them in gradually concentrated baths of GMA monomer with water until to finish by several baths in 100% of GMA. They were then impregnated overnight at 4 °C in a mixture of (GMA/BMA) monomers with catalyst peroxide compound before to be transferred in gelatin capsules and to be cured

during several days from 37 °C to 60 °C. After polymerization, blocks of samples embedded in resin were lapped and polished using a grinder-polisher (MetaServ2000, BUEHLER) and then coated with a thin layer of amorphous carbon using a vacuum evaporator (JEE-4B, JEOL) before SEM observations. The SEM observations of embedded samples were performed using a scanning electron microscope (LEO 1450VP, ZEISS) operating at 9 kV or 15 kV and pictures were recorded from the back-scattered electron detector (BSE). A sample of Si-HMPC hydrogel containing laponites was also observed by SEM in its hydrated state using a WETSEM® sealed capsule having SiN windows (QX-102, QuantomixTM). SEM observations of the wet sample were performed at 20 kV, and pictures were recorded from the BSE mode.

2.6. Cell viability

2.6.1. Adipose stromal cell culture

To determine the viability of cells when cultured in the presence of our hydrogels, human adipose stromal cells (hASC) were used. ASC were obtained from human patients undergoing liposuction and who had given written consent (Agence de BioMedecine n ° PFS08-018, legislation code L.1211-3 to L.1211-9). hASC were isolated by collagenase digestion of lipoaspirates. Briefly, and as previously described [24], lipoaspirates were washed extensively with HBSS to remove debris, treated with collagenase and centrifuged at 250*g* for 5 min. hASC were cultured in a 5% CO_2 incubator at 37 °C in Dulbecco's modified Eagle's medium (DMEM) with Glutamax (Life Technologies, France) supplemented with 10% fetal bovine serum (FBS) and 1% penicillin/streptomycin.

2.6.2. Cell viability in 2D

hASC viability was evaluated by methyl tetrazolium salt (MTS) assay (Promega, USA). Two different experiments were performed, (1) evaluation of hASC viability cultured in direct contact with increasing concentrations of XLG and (2) evaluation of hASC cell viability cultured in contact with Si-HPMC hydrogel containing increasing concentrations of XLG (protocol B, Fig. 1A). hASC were seeded onto culture plates and were allowed to attach to 48-well plates at a final density of 10,000 cells per cm^2. After 24 h, the culture medium was removed, and either XLG or Si-HPMC containing XLG was added onto the cell layer. For the culture in direct contact, 200 μL of culture medium containing 0.001, 0.01, 0.1 or 1% XLG (% w/v) were added to each well and refreshed every two days. For the culture in contact with hydrogel, 250 μL of Si-HPMC hydrogel containing 0%, 0.2%, 0.5% or 1% XLG were added per well. After 1 h of gelation at 37 °C, 200 μL of culture medium was added to each well and refreshed every two days. As a positive control for both experiments, hASC were cultured in the presence of actinomycin-D (5 μg/mL), a well-known inducer of cell death. Finally, MTS assay was performed at day 0, 1, 2, 3 and 6. The MTS assay is based on the reduction of MTS tetrazolium compound by viable cells that generates a colored formazan product soluble in the culture medium. The colored product was measured by the optical density reading at 490 nm (Victor^{3}V 1420 Multilabel Counter). Each condition was tested in quadruplicate.

2.6.3. Cell viability in 3D

3D cell viability was evaluated by Live/Dead Cell Viability assay (ThermoFisher Scientific, MA, USA) with hASC mixed into hydrogels (protocol B, Fig. 1A) at a final density of $1x10^6$ cells per mL of Si-HPMC. Si-HPMC hydrogels containing 0%, 0.2%, 0.5% or 1% XLG were molded and allowed to gelate in wells of a 48-well plate at 37 °C for 1 h. After gelation, 200 μL of culture medium were added to each well and refreshed every two days. As a positive control, hASC were cultured in 3D into Si-HPMC hydrogel in the presence of actinomycin-D (5 μg/mL). At day 0, 2 and 6, a Live/Dead Cell Viability assay was performed according to the manufacturer's instructions. A green fluorescence can be observed due to the calcein AM indicating the intracellular esterase activity. And a red fluorescence can be observed due to the ethidium homodimer-1 indicating the loss of plasmic membrane integrity. Living cells were stained green and dead cells were stained red. Red and green fluorescence were observed with a confocal microscope (Nikon D-eclipse C1 (Ar/Kr)). Each condition was tested in quadruplicate.

2.7. In vivo experiment

We embarked on *in vivo* experiments based on the subcutaneous implantation of well-known chondrogenic cells, namely human nasal chondrocytes (hNC), in conjunction with Si-HPMC/1% XLG hydrogel to investigate whether our hybrid biomaterial was able to support chondrogenesis (protocol B, Fig. 1A). The hNC were obtained from human patients undergoing rhinoplasty and who had given written consent (Agence de BioMedecine n° PFS08-018, legislation code L.1211-3 to L.1211-9). The hNC were isolated by enzymatic digestion of nasal cartilage as described previously [25]. Briefly, nasal cartilage was cut into small slices and digested at 37 °C with 0.05% hyaluronidase in HBSS for 10 min, then with 0.2% trypsin for 15 min and finally with 0.2% type II collagenase for 30 min. Finally, slices were digested overnight at 37 °C in 0.03% collagenase in DMEM. The suspended hNC were cultured in DMEM with Glutamax supplemented with 10% FCS, 1% penicillin/streptomycin. hNC were expanded at 37 °C in a humidified atmosphere of 5% CO_2 and culture medium was changed every 2–3 days.

Seven-week-old swiss nude female mice were used for the *in vivo* study (Charles River Laboratory, France). All animals were treated in accordance with the Medical Animal Care Guidelines of the University of Nantes (APAFIS#3082-2015120811802781 6v2). Si-HPMC hydrogels both with and without 1% XLG were mixed with hNC at 1, 2 and 5×10^6 cells/mL as described previously [25]. 250 μL of each cellularized hydrogel were injected subcutaneously in the back along each side of nude mice. The implantations were performed under general anesthesia using isoflurane gas (Halothane, Baxter, Switzerland) and under aseptic conditions. After six weeks, mice were euthanized, and hydrogels were individually explanted. Each explant was fixed in formaldehyde solution for subsequent histological analyses.

2.8. Histological analyses

All explants were fixed in 4% paraformaldehyde solution and embedded in paraffin. Embedded samples were sectioned (5 μm thick). After that paraffin sections were de-paraffinized using toluene, rehydrated through a graded series of ethanol and rinsed in distilled water. Tissue sections were stained with hematoxylin-eosin-safran (HES), alcian blue (AB) and Masson's Trichrome (MT) as described elsewhere [25,26]. Sections were finally visualized using a light microscope (Zeiss Axioplan 2, Göttingen, Germany).

2.9. Image analyses

After histological staining, slides were scanned, and images were analyzed by ImageJ software. Three squares (250 μm × 250 μm) were randomly defined on each image. Nodules of hNC were counted and their areas measured.

2.10. Statistical analysis

Results are expressed as mean ± SEM of triplicate determinations. Comparative studies of means were performed by using

Kruskal-Wallis test followed by a post hoc test (Dunn's Multiple Comparison Test) with statistical significance at $p < 0.05$.

3. Results

3.1. Rheology, mechanical properties, and microscope analysis

Our objective was to use nanoparticles to reinforce our hydrogel made of Si-HPMC polymer. First, the rheology investigation showed that the gel point, the time needed to reach the sol-gel transition of our hydrogels, decreases when the concentration of XLG increases (Fig. 1B). Moreover, the protocol (A or B) used for the formulation of the composite hydrogels seems to not influence the gel point, reaching in both cases 1500 s at 1% wt/v of laponites.

As depicted in Fig. 2, adding XLG within Si-HPMC induces an increase in the mechanical properties when compared to Si-HPMC hydrogel alone. The storage moduli of the Si-HPMC/XLG hybrid constructs were tested using shear stress and DMA compression experiments (G' and E' respectively). Regardless of the technique used, the results obtained showed the same behavior with an increase in the storage moduli when the quantity of added XLG increases. The E' modulus of Si-HPMC hydrogel is approximately 5 kPa. Upon increasing the XLG amount, an increase of E' was observed. The increase of XLG amount in hydrogel allowed the modulus to reach a 4-fold increase for 5% XLG mixed with protocol A and a 3-fold increase for only 1% of XLG mixed with protocol B. It is worth noting that it was not possible to prepare XLG loaded at a concentration higher than 1% with protocol B. The gel point was reached almost instantly when using more than 1% XLG making the mixing process impossible.

Following the mechanical investigations, microscopic observations were performed to deeply investigate the structural differences of the composite hydrogels depending on the protocol used. When XLG are dispersed in ABS before mixing with Si-HPMC, XLG remained in aggregates (Fig. 3A, D), while when XLG are dispersed in water before mixing with Si-HPMC, they formed

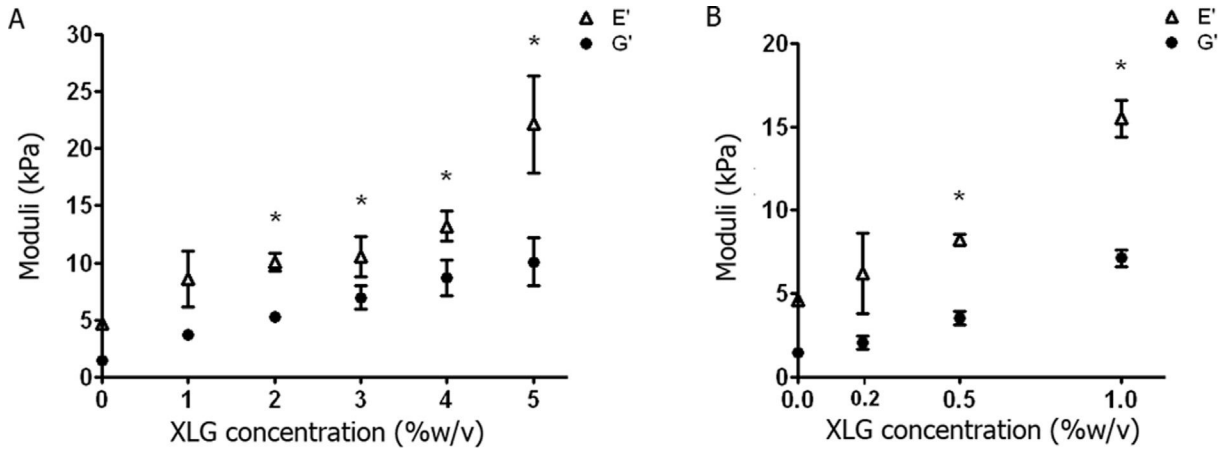

Fig. 2. Viscoelastic moduli G′ and E′ of Si-HPMC hydrogels containing increasing concentrations of XLG. The G′ modulus (dot) was measured with MARS rheometer while the E' modulus (triangle) was measured with DMA. Si-HPMC hydrogels mixed with increasing concentrations of XLG as indicated were tested. Hybrid constructs were prepared following 2 different protocols, protocol A (A) or B (B) as described in materials and methods. $^{*}p < 0.05$ compared to the 0% XLG condition.

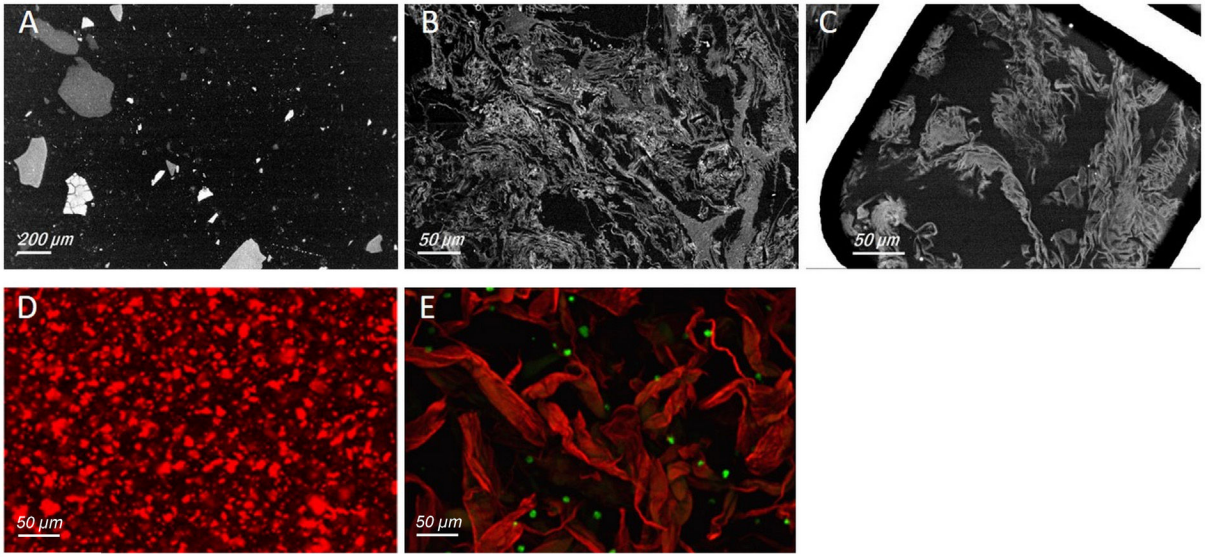

Fig. 3. Composite hydrogel ultrastructure. Microscopic analysis of Si-HPMC/XLG hydrogel prepared with protocol A. electronic (A: SEM) images showing the Si-HPMC/laponites structure and Confocal (D) image of Si-HPMC/XLG hydrogel stained in red. Microscopic analysis of Si-HPMC/XLG hydrogel prepared with protocol B: electronic (B: SEM, C: SEM in hydrated state using a WETSEM® sealed capsule) images showing the Si-HPMC/XLG structure and Confocal (E) image of hASC cells seeded within Si-HPMC/XLG hydrogel after Live&Dead® labelling: living cells were labelled with Calcein AM (green) and XLG with Ethidium homodimer-1 (red).

their network interpenetrated with Si-HPMC network (Fig. 3B, C, E). The dual network was observed under a confocal microscope with the formation of wave shape structures. Moreover, the use of WETSEM® sealed cap, allowed us to observe under SEM our composite hydrogel in its hydrated form, confirming the formation of an interpenetrating network.

3.2. Cellular viability in 2D and 3D

Our objective was then to evaluate the cytocompatibility of our scaffolds (i) in a 2D culture where the hydrogel is placed above the cell layer, and (ii) in a 3D culture where cells are cultured into our hydrogels.

XLG was found to alter MTS activity from 0.001% when hASC were cultured in direct contact with the XLG (Fig. 4A). However, regardless of XLG concentration, we failed to detect any alteration of MTS activity when cells were cultured in 3D within Si-HPMC/XLG (Fig. 4B).

To confirm these data, a double staining kit was then used for simultaneous staining of living and dead cells in 3D culture. Living cells are stained in green by calcein AM and dead cells in red by ethidium homodimer-1. Confocal analysis was performed on day 0, 2 and 6. Fig. 5 shows the 3D reconstructions of hybrid hydrogels associated with hASC. Cells cultured in 3D in the presence of actinomycin-D were used as a control of cell death. Confocal observations of Si-HPMC/XLG constructs showed the presence of green, living cells when hASC were cultured in 3D in this hybrid construct. The interpenetrated network can concomitantly be observed as XLG and ethidium homodimer-1 link together (due to electrostatic interactions) resulting in a red color of the XLG wave structures within the hydrogel.

3.3. Oxygen tension

Since XLG nanoparticles have been described as oxygen barrier [27,28], the O_2 diffusion was evaluated within Si-HPMC hydrogel

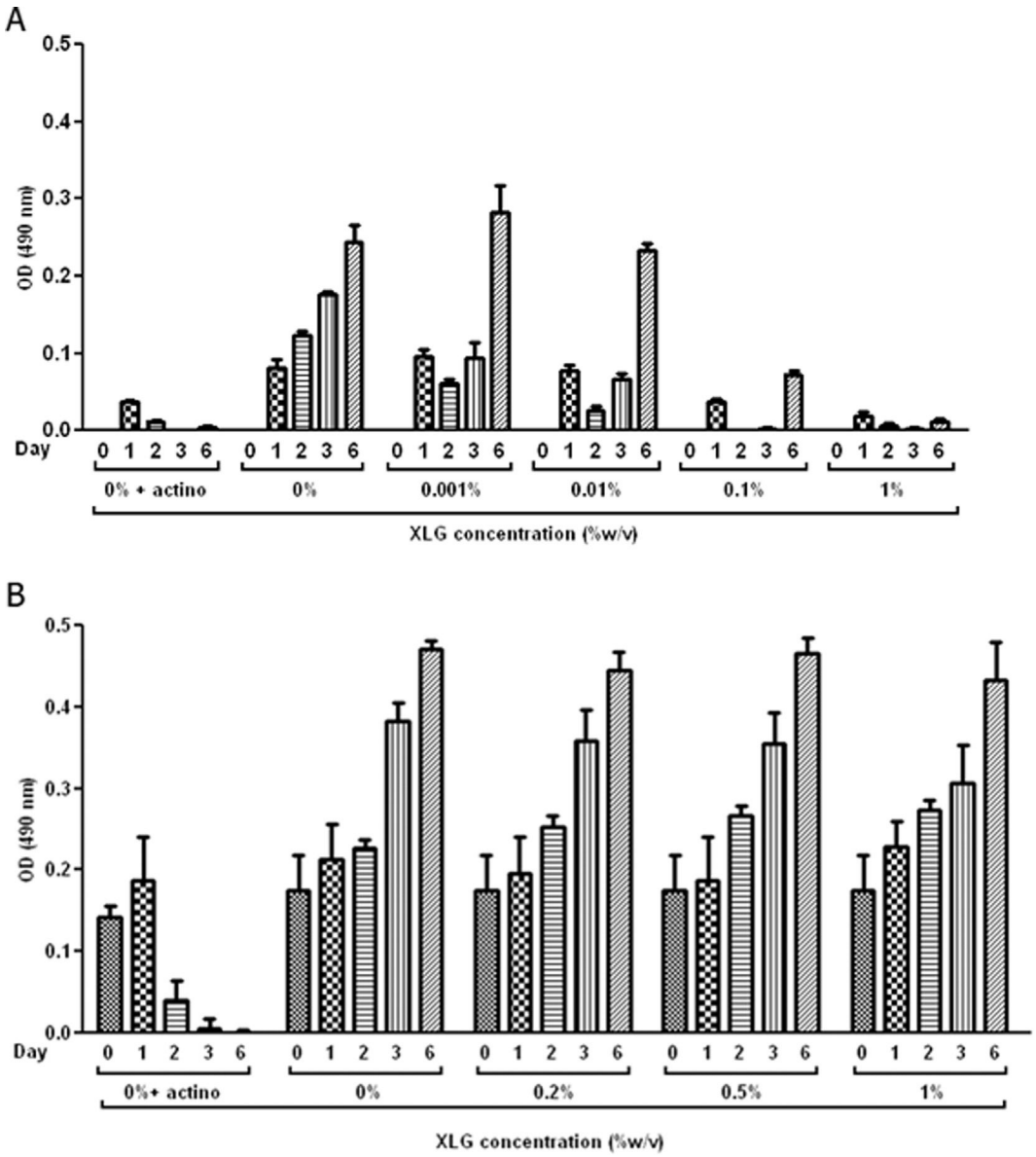

Fig. 4. MTS activity of hASC cultured in 2D. (A) hASC viability was evaluated in 2D after adding 0–1% XLG as indicated on top of the cell layer (10,000 cells/cm^2). (B) hASC viability was evaluated in 2D after molding Si-HPMC hydrogels with 0 to 1% XLG as indicated on top of the cell layer (10,000 cells/cm^2). As described in materials and methods, a MTS assay was performed at day 0, 1, 2, 3 and 6. Negative control (actino) was obtained by growing hASC in the presence of actinomycin D (5 μg/mL).

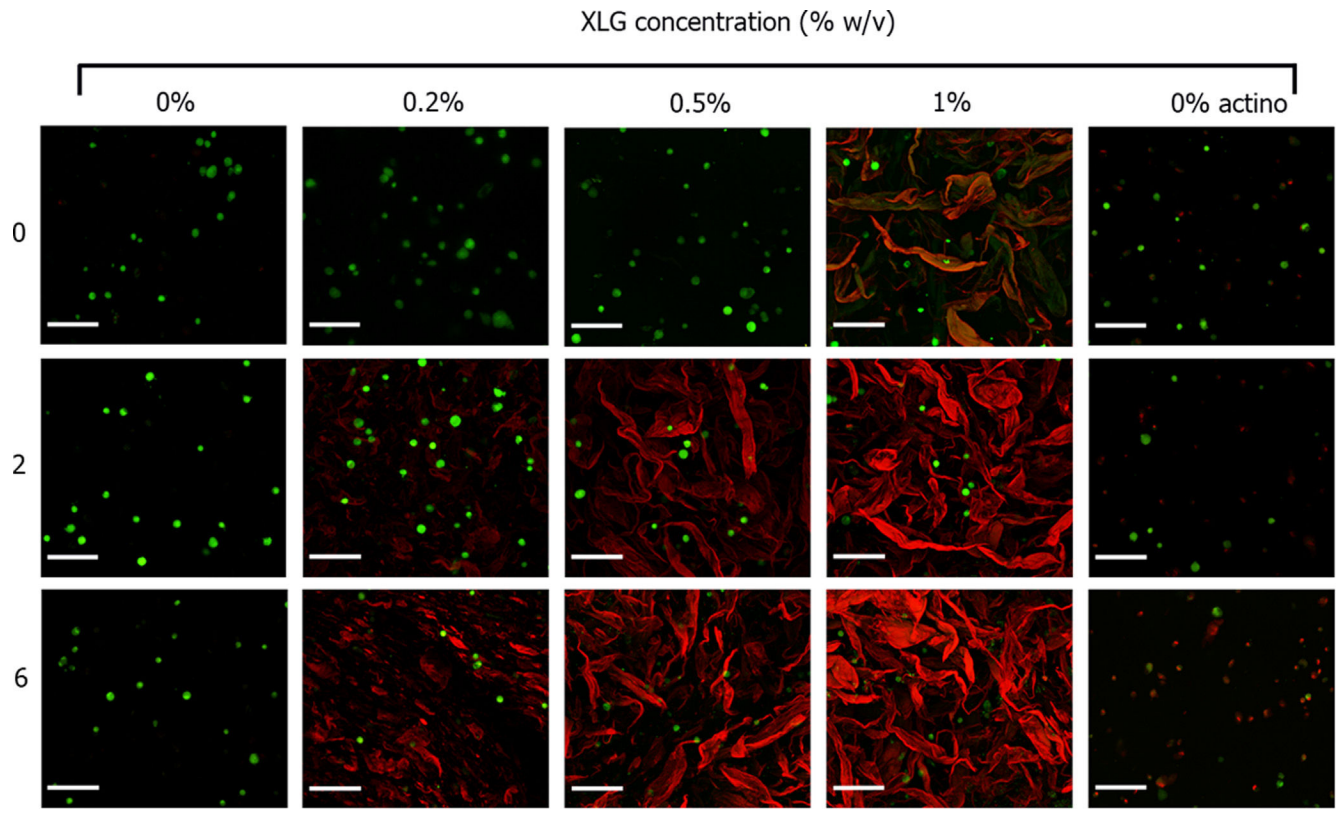

Fig. 5. 3D viability of hASC cultured into Si-HPMC hydrogel containing increasing concentrations of XLG. Human ASC viability was evaluated in 3D after molding Si-HPMC hydrogels containing increasing concentrations of XLG (0–1%) and mixed with 1 x 10^6 hASC at day 0 (0), 2 (2) and 6 (6) by Live/Dead Cell Viability assay. Living cells were stained by Calcein AM in green and dead cells were stained in red by ethidium homodimer-1. Negative control was obtained by adding actinomycin D (5 μg/mL) in the culture medium. XLG nanoparticules were also stained in red due to the electrostatic interaction with ethidium homodimer-1. Scale bar: 100 μm.

containing 1% XLG. O_2 diffusion has been monitored with and without XLG. No significant differences are observed between Si-HPMC and Si-HPMC/1% XLG constructs, both of which reached O_2 levels of around 17% at equilibrium. Acellular Si-HMPC hydrogels were prepared in atmospheric conditions and were then transferred to a controlled anoxic environment (0.1% O_2). Their de-oxygenation profile, represented as the first part of the curve in Fig. 6, shows no obvious differences between Si-HPMC and Si-HPMC/1%XLG constructs, with a slow decrease in their O_2 content. For both hydrogels, equilibrium (i.e. O_2 content of 0.1%) was reached after 60 h of incubation in anoxic conditions. The second part of the curve represents the re-oxygenation profile of hydrogels when they were transferred back to a normoxic environment (O_2 content of 20%). From this point, re-oxygenation profiles for both groups are once again superimposed, suggesting that 1% XLG addition to Si-HMPC hydrogel has no obvious effect on O_2 diffusion *per se*.

3.4. In vivo experiments

To determine whether 1% XLG-enriched Si-HPMC hydrogel may support *in vivo* chondrogenesis, we finally studied the subcutaneous implantation of robust chondrogenic cells (hNC) in combination with our biomaterial in a method described previously [7,25]. After harvest, isolation, and culture, hNC (1 to 5 × 10^6 cells/mL) were mixed with Si-HPMC or Si-HPMC/1% XLG hydrogels and injected in nude mice subcutis for 6 weeks.

As expected, samples containing Si-HPMC or Si-HPMC/1% XLG without hNC show neither cells nor coloration in the graft. Fig. 7 shows that hNC associated with Si-HPMC and Si-HPMC/1%XLG hydrogels are organized in nodules revealed in HES, AB and MT stainings. HES staining also indicated the presence of mature chondrocytes within lacunae surrounded by a basophilic matrix. Cells in the nodules secreted GAGs revealed in blue with AB staining, and collagens evidenced in green with MT staining. When 1% XLG was added to Si-HPMC, a lower amount of hNC nodules was observed into the explants. However, cells retain their ability to

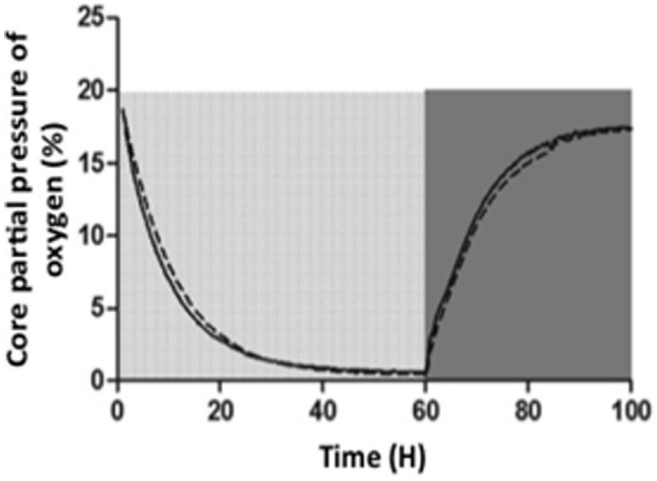

Fig. 6. Oxygen diffusion. De-oxygenation and re-oxygenation profiles of acellular Si-HPMC hydrogels (with (dashed line) or without (filled line) XLG) prepared in atmospheric conditions then transferred to hypoxic conditions (, 0.1% O_2) until equilibrium was reached, then transferred to normoxic conditions for re-oxygenation (, 20% O_2). Results are presented as core partial pressure values measured in the center of the construct (mean value ± SEM, n = 4).

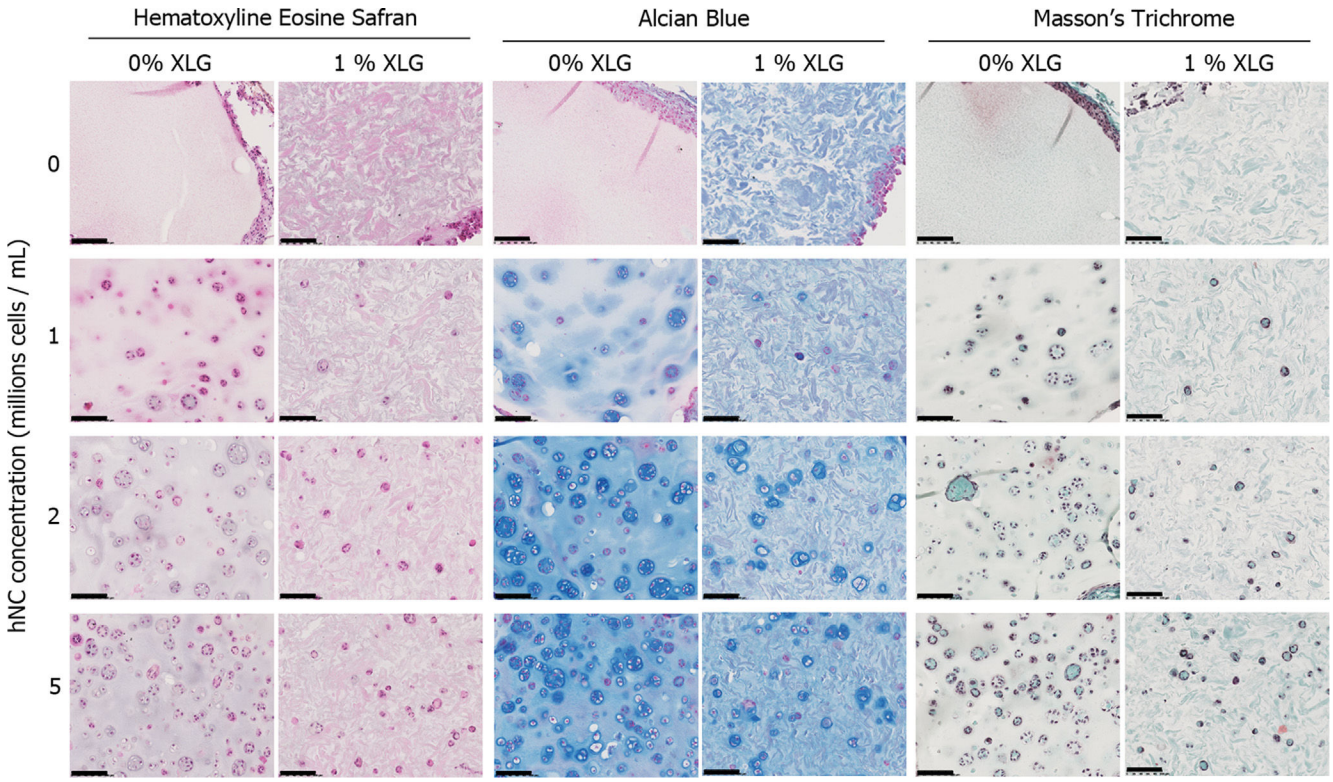

Fig. 7. Histological analysis of cartilaginous tissue formation after subcutaneous implantation of hNC with Si-HPMC/XLG hydrogels. 250 μL of Si-HPMC (0% XLG) or Si-HPMC/1% XLG (1% XLG) hydrogels mixed with hNC (cell density varying from 0 to 5 millions cells/mL of Si-HPMC) were implanted in subcutaneous pocket in nude mice. Both hydrogels without hNC were used as negative control (0). After 6 weeks, explanted samples were histologically prepared for Hematoxyline Eosine Safran, Alcian Blue and Masson's Trichrome staning. Scale bar: 100 μm.

self-organize in nodule and secret extracellular matrix components. It is worth noting that the number of nodules increases when more hNC are added during the mixing process. These results indicate that Si-HPMC/1% XLG support the formation of a cartilaginous tissue in nude mice subcutis when implanted with hNC.

Despite a significant reduction in a number of nodules and total area (Fig. 8A and B), nodules analysis shows that the area per nodule was not significantly affected by the presence of XLG.

4. Discussion

After injuries, articular cartilage shows limited repair properties leading to a progressive degeneration of the tissue that dramatically exposes the onset of osteoarthritis. Therefore, developing new regenerative therapy appears essential. Toward that goal, tissue engineering strategies, associating cells and biomaterials, have been developed. The development of biomaterials for mini-invasive surgery requires the matching of several parameters from physico-chemistry (e.g. rheology, self-hardening) to biology (e.g. cytocompatibility, biocompatibility, and biofunctionality). The physicochemical characterizations first consisted of determining the potential use of our hydrogel (Si-HPMC/XLG) in terms of handling such as the need to be injectable. The viscosity showed that there was no difficulty in injecting the solution and the gel point represents the working time during which the clinician can manipulate, mix the different components and inject the solution before it hardens. Then, mechanical investigations were performed to determine whether the composite hydrogels can withstand the mechanical stress of the implantation site. Fig. 2 showed that regardless of the protocol, the viscoelasticity of the hydrogel increases with the XLG concentration. The protocol with XLG first suspended in pure water showed a stronger reinforcement of the hydrogel reaching up to 15 kPa with 1% wt/v of XLG. This increase could help the biomaterial to last longer under the mechanical stress in the implanted site compared to Si-HPMC alone. The relative stability of the hydrogel is of particular relevance in tissue engineering strategies notably in articular cartilage regenerative medicine because it allows cells to produce a functional extracellular matrix conferring some mechanical properties comparable to that of native/healthy tissue to the newly formed tissue. This property is important for tissue engineering strategies to allow time for the encapsulated cells to secrete extracellular matrix for tissue renewal.

When particles are used to reinforce hydrogels, a large amount has to be added in order to get an increase of the modulus, such as 50% for calcium phosphate [29]. Lower amount of particles can be used in some cases such as silicate nanofibers where an increase of the storage modulus is obtained with only 5% of incorporation [30]. This property relies on the ability of the particle to covalently link to the polymer network. Moreover, Formica et al. showed that their PCL (polycaprolactone) fiber reinforced alginate scaffolds were able to stand longer subcutaneously and to produce large amount of cartilage specific ECM (extra cellular matrix) compared to their alginate scaffold alone [31–33].

Microscopic observations of the hydrogel prepared according to both mixing protocols showed drastic differences in the architectural structures. When XLG were suspended in the acid buffer, the composite hydrogels were composed of XLG aggregates within the Si-HPMC hydrogel. On the other hand, when XLG were in suspension in pure water, they formed wave-shaped structures leading to an interpenetrating network. Additionally, to further characterize the microenvironment for cell embedding, O_2 tension measurements have shown no significant influence of XLG on O_2

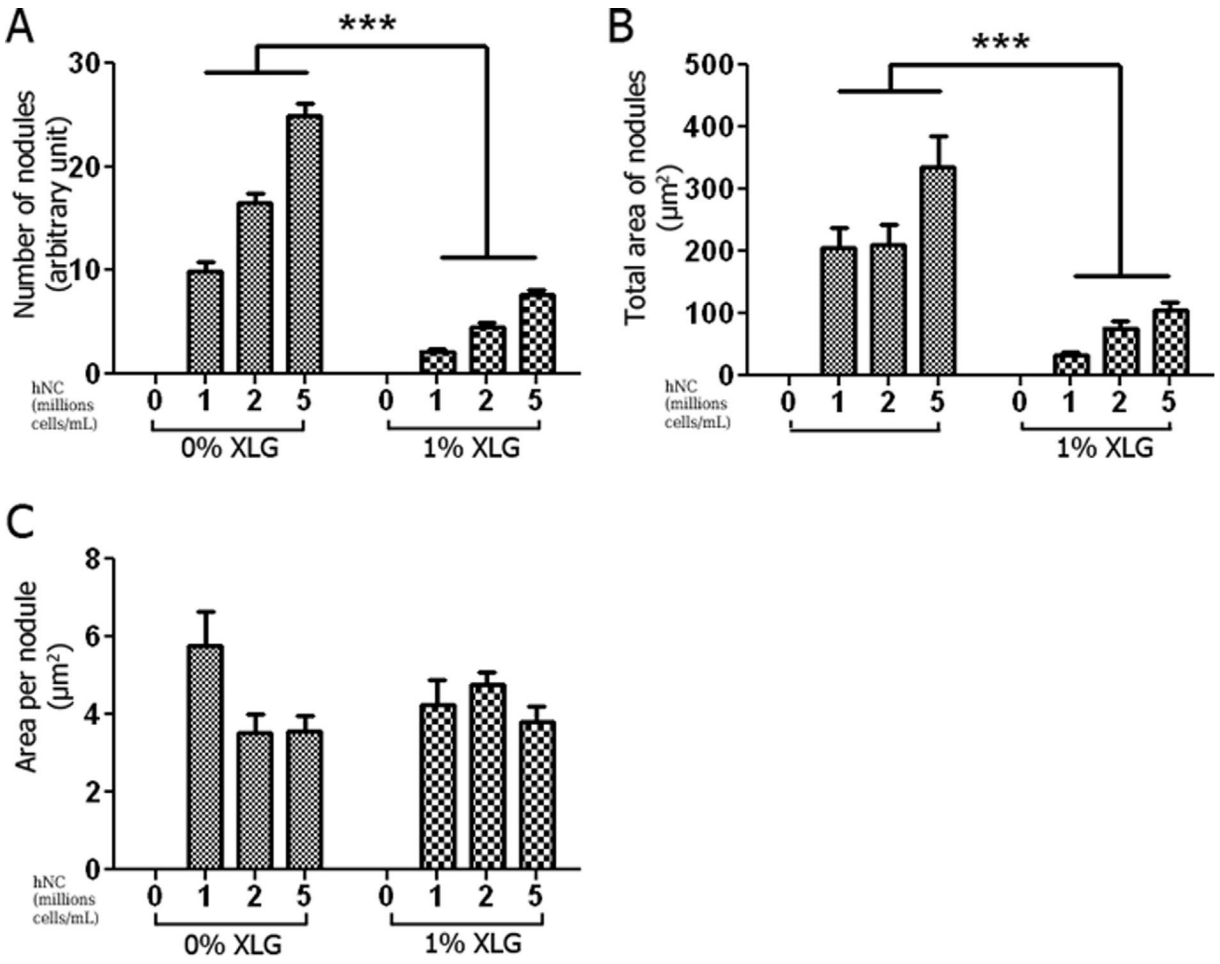

Fig. 8. Nodules analysis after histological staining. 250 µL of Si-HPMC (0% XLG) or Si-HPMC/1% XLG (1% XLG) hydrogels mixed with hNC (cell density varying from 0 to 5 millions cells/mL of Si-HPMC) were implanted in subcutaneous pocket in nude mice. After 6 weeks, explanted samples were histologically prepared for Hematoxyline Eosine Safran, Alcian Blue and Masson's Trichrome staning. Number of hNC nodules (A), total area of hNC nodules (B) and area per hNC nodule (C) have been determined by image analysis with ImageJ software. $^{*}p < 0.001$ compared to the 0% XLG condition.

tension and diffusion without cells. Put together, the ability of XLG to self-assemble and form double network leads to the increase in the mechanical properties of the final constructs without interfering with O_2 diffusion.

Based on the ability of XLG to form a double interpenetrating network, thereby increasing the mechanical properties, the XLG composite hydrogel was further investigated. MTS assay showed no modification of the mitochondrial activity up to 1% wt/v (10 mg/mL) of XLG in 2D. Live&Dead staining was then performed to confirm this result in 3D cell growth. Throughout the literature, the cytotoxicity of XLG has been studied for two main formulations (e.g. XLG suspensions and hydrogels). Indeed, Janer et al. investigated the toxicity of pristine and functionalized nanoclays [34]. They have demonstrated that the toxicity is mainly increased because of the presence of organic groups at the surface of XLG. However, XLG have been shown to be non-toxic only up to 10 µg/L (10^{-6}% wt/v). From 10 µg/L and onwards, the toxicity increased according to the concentration. In the meantime, few groups have been working on the development of silicate hydrogels. Ebato et al. have developed a nanocomposite hydrogel for 2D cell culture and they showed no toxicity of their structure [35]. Moreover, Orefo et al. prepared nanoclay-gel for cell encapsulation. They demonstrated the feasibility of their strategy, showing a very good viability in 3D and the ability to host the chondrogenic differentiation of human bone marrow stromal cells. In our strategy, XLG formed a gel and were mixed with Si-HPMC hydrogel. Altogether, these data suggest that cells can be grown within our composite hydrogel.

The ideal biomaterial for cartilage tissue engineering should not only allow for the maintenance of the chondrocyte differentiation but should also enable their transplantation via a mini-invasive surgical protocol *in vivo*. Consequently, to decipher whether Si-HPMC/XLG hydrogels could represent this ideal scaffold, we investigated its ability to support the transplantation of chondrogenic cells and the formation of cartilage tissue *in vivo*. To address this issue, we focused our attention on the use of cells exhibiting a reliable and robust chondrogenic potential such as hNC [36]. Interestingly, after six weeks *in vivo*, hNC were positively stained after respectively Alcian Blue and Masson Trichrome histology staining confirming that the entrapped hNC could still produce an extracellular matrix containing GAG and collagen. Also, a decrease in the number of clusters is shown when XLG is added to the construct. However, when the entrapped cell number increases, histology staining demonstrated that the number of the cluster also increased in the meantime. More importantly, the mean area per cluster remains unchanged independently of the initial amount of cells and the presence of XLG.

Consequently, the decrease in cells and cluster number could be due to an initial toxicity during the mixing process (1200 s before gel points (Fig. 1)) inducing cell death at the early time. Indeed, investigations on cells incubated with XLG suspension have shown 2D toxicity from 10 µg/L and onwards with drastic XLG internal-

ization inside the cells (data not shown). Before the gel point, XLG are free to move and could make contact with cells leading to their incorporation in the cytosol. After gel point, surviving cells may be able to multiply and form clusters. Regardless of the presence of XLG, the same behavior is observed such as an increase in the number of clusters when the concentration of the entrapped cells increases. To mitigate the initial cell death, the cell concentration has to be increased when XLG are mixed with Si-HPMC hydrogel. No significant difference has been shown between Si-HPMC associated with 1×10^6 hNC and Si-HPMC/XLG associated with 5×10^6 hNC. These results are in agreement with the literature as Janer et al. showed the internalization of nanoclays inside the cells [34]. Indeed, nanoclays induced apoptosis and were found in cytoplasmic vesicles of exposed cells. In the meantime, several groups have been working on the development of clay-based hydrogels and showed that cells remain viable in either 2D and 3D [20,35,37].

Altogether, our results demonstrate that when XLG are prepared as a suspension, they can be internalized and show some toxicity from 10 μg/L. However, when they are formulated as a gel, XLG increased the mechanical properties of the final construct while cells appear to remain viable in 2D and 3D (in the gelified form). The initial decrease of the cell density observed with Si-HPMC/XLG composite hydrogels could be overcome by decreasing the gel point or by increasing (5-fold) the number of cells used. This study validated the IPN hybrid hydrogel for cartilage tissue engineering in a nude mouse animal model. The larger animal model will then be used for the biocompatibility investigations of the products.

5. Conclusion

In conclusion, it has been demonstrated that adding XLG within Si-HPMC hydrogels increases the mechanical properties without interfering with the O_2 diffusion and cell viability after gelification. Therefore, the development of faster gelling composite hydrogel has to be evaluated. This could lead to an increase in the cell survival and the number of clusters. Their self-assembling capacity induces the formation of a hybrid interpenetrated network that enhances the stiffness of the hydrogel. The use of Si-HPMC/XLG hydrogels combined with chondrocytes in subcutis of nude mice has shown their potential use for cartilage tissue engineering. Investigation in the large animal model will have to be performed too thoroughly evaluate the preservation of the material inside a cartilage defect as well as the clinical relevance of our strategy.

Acknowledgements

We would like to thank, Pr. O. Malard (ENT surgery department, university hospital of Nantes, France), for providing human nasal cartilage and Dr F. Lejeune (Brétéché clinic, Nantes, France) for providing lipoaspirates. This research was supported by the regional program BIOREGOS (Pays de la Loire, France), by the Agence Nationale de la Recherche in the framework ANR-11-BSV5-0022 (HYCAR) and by FUI Marbiotech. LF was the recipient of a Nanofar Erasmus Mundus Doctorate fellowship.

References

[1] E.A. Makris, A.H. Gomoll, K.N. Malizos, J.C. Hu, K.A. Athanasiou, Repair and tissue engineering techniques for articular cartilage, Nat. Rev. Rheumatol. 11 (1) (2015) 21–34.
[2] C. Vinatier, C. Merceron, J. Guicheux, Osteoarthritis: from pathogenic mechanisms and recent clinical developments to novel prospective therapeutic options, Drug Discov. Today 21 (12) (2016) 1932–1937.
[3] J. Ringe, G.R. Burmester, M. Sittinger, Regenerative medicine in rheumatic disease-progress in tissue engineering, Nat. Rev. Rheumatol. 8 (8) (2012) 493–498.
[4] A.K. Gaharwar, C.P. Rivera, C.J. Wu, G. Schmidt, Transparent, elastomeric and tough hydrogels from poly(ethylene glycol) and silicate nanoparticles, Acta Biomater. 7 (12) (2011) 4139–4148.
[5] C. Merceron, C. Vinatier, J. Clouet, S. Colliec-Jouault, P. Weiss, J. Guicheux, Adipose-derived mesenchymal stem cells and biomaterials for cartilage tissue engineering, Joint Bone Spine 75 (6) (2008) 672–674.
[6] C. Merceron, S. Portron, M. Masson, B.H. Fellah, O. Gauthier, J. Lesoeur, Y. Cherel, P. Weiss, J. Guicheux, C. Vinatier, Cartilage tissue engineering: from hydrogel to mesenchymal stem cells, Biomed. Mater. Eng. 20 (3) (2010) 159–166.
[7] C. Vinatier, O. Gauthier, A. Fatimi, C. Merceron, M. Masson, A. Moreau, F. Moreau, B. Fellah, P. Weiss, J. Guicheux, An injectable cellulose-based hydrogel for the transfer of autologous nasal chondrocytes in articular cartilage defects, Biotechnol. Bioeng. 102 (4) (2009) 1259–1267.
[8] A.S. Hoffman, Hydrogels for biomedical applications, Adv. Drug Deliv. Rev. 54 (1) (2002) 3–12.
[9] K.Y. Lee, D.J. Mooney, Hydrogels for tissue engineering, Chem. Rev. 101 (7) (2001) 1869–1880.
[10] J.L. West, J.A. Hubbell, Photopolymerized hydrogel materials for drug delivery applications, React. Polym. 25 (2–3) (1995) 139–147.
[11] I. Levental, P.C. Georges, P.A. Janmey, Soft biological materials and their impact on cell function, Soft Matter 3 (3) (2007) 299–306.
[12] J.L. Drury, D.J. Mooney, Hydrogels for tissue engineering: scaffold design variables and applications, Biomaterials 24 (24) (2003) 4337–4351.
[13] J. Kopecek, Hydrogel biomaterials: a smart future?, Biomaterials 28 (34) (2007) 5185–5192
[14] F. Song, L.M. Zhang, J.F. Shi, N.N. Li, Viscoelastic and fractal characteristics of a supramolecular hydrogel hybridized with clay nanoparticles, Colloids Surf. BBiointerfaces 81 (2) (2010) 486–491.
[15] S.K. Agrawal, N. Sanabria-Delong, G.N. Tew, S.R. Bhatia, Nanoparticle-reinforced associative network hydrogels, Langmuir 24 (22) (2008) 13148–13154.
[16] K. Haraguchi, H.-J. Li, Mechanical properties and structure of polymer–clay nanocomposite gels with high clay content, Macromolecules 39 (5) (2006) 1898–1905.
[17] L.-M. Zhang, Y.-J. Zhou, Y. Wang, Novel hydrogel composite for the removal of water-soluble cationic dye, J. Chem. Technol. Biotechnol. 81 (5) (2006) 799–804.
[18] G. Schmidt, A.I. Nakatani, P.D. Butler, A. Karim, C.C. Han, Shear orientation of viscoelastic polymer–clay solutions probed by flow birefringence and SANS, Macromolecules 33 (20) (2000) 7219–7222.
[19] G. Schmidt, A.I. Nakatani, C.C. Han, Rheology and flow-birefringence from viscoelastic polymer-clay solutions, Rheologica Acta 41 (1–2) (2002) 45–54.
[20] J.I. Dawson, J.M. Kanczler, X.B. Yang, G.S. Attard, R.O. Oreffo, Clay gels for the delivery of regenerative microenvironments, Adv. Mater. 23 (29) (2011) 3304–3308.
[21] L.Z. Zhao, C.H. Zhou, J. Wang, D.S. Tong, W.H. Yu, H. Wang, Recent advances in clay mineral-containing nanocomposite hydrogels, Soft Matter 11 (48) (2015) 9229–9246.
[22] X. Bourges, P. Weiss, A. Coudreuse, G. Daculsi, G. Legeay, General properties of silated hydroxyethylcellulose for potential biomedical applications, Biopolymers 63 (4) (2002) 232–238.
[23] X. Bourges, P. Weiss, G. Daculsi, G. Legeay, Synthesis and general properties of silated-hydroxypropyl methylcellulose in prospect of biomedical use, Adv. Colloid Interface Sci. 99 (3) (2002) 215–228.
[24] S. Portron, C. Merceron, O. Gauthier, J. Lesoeur, S. Sourice, M. Masson, B.H. Fellah, O. Geffroy, E. Lallemand, P. Weiss, J. Guicheux, C. Vinatier, Effects of in vitro low oxygen tension preconditioning of adipose stromal cells on their in vivo chondrogenic potential: application in cartilage tissue repair, PLoS One 8 (4) (2013) e62368.
[25] C. Vinatier, D. Magne, A. Moreau, O. Gauthier, O. Malard, C. Vignes-Colombeix, G. Daculsi, P. Weiss, J. Guicheux, Engineering cartilage with human nasal chondrocytes and a silanized hydroxypropyl methylcellulose hydrogel, J. Biomed. Mater. Res. A 80 (1) (2007) 66–74.
[26] C. Merceron, S. Portron, M. Masson, J. Lesoeur, B.H. Fellah, O. Gauthier, O. Geffroy, P. Weiss, J. Guicheux, C. Vinatier, The effect of two- and three-dimensional cell culture on the chondrogenic potential of human adipose-derived mesenchymal stem cells after subcutaneous transplantation with an injectable hydrogel, Cell Transplant. 20 (10) (2011) 1575–1588.
[27] U. Tritschler, I. Zlotnikov, P. Fratzl, H. Schlaad, S. Gruner, H. Colfen, Gas barrier properties of bio-inspired Laponite-LC polymer hybrid films, Bioinspir. Biomim. 11 (3) (2016) 035005.
[28] J. Yoo, S.B. Lee, C.K. Lee, S.W. Hwang, C. Kim, T. Fujigaya, N. Nakashima, J.K. Shim, Graphene oxide and laponite composite films with high oxygen-barrier properties, Nanoscale 6 (18) (2014) 10824–10830.
[29] X. Bourges, M. Schmitt, Y. Amouriq, G. Daculsi, G. Legeay, P. Weiss, Interaction between hydroxypropyl methylcellulose and biphasic calcium phosphate after steam sterilisation: capillary gas chromatography studies, J. Biomater. Sci. Polym. Ed. 12 (6) (2001) 573–579.
[30] N. Buchtova, G. Rethore, C. Boyer, J. Guicheux, F. Rambaud, K. Valle, P. Belleville, C. Sanchez, O. Chauvet, P. Weiss, J. Le Bideau, Nanocomposite hydrogels for cartilage tissue engineering: mesoporous silica nanofibers interlinked with siloxane derived polysaccharide, J. Mater. Sci. – Mater. Med. 24 (8) (2013) 1875–1884.
[31] O. Bas, E.M. De-Juan-Pardo, C. Meinert, D. D'Angella, J.G. Baldwin, L.J. Bray, R.M. Wellard, S. Kollmannsberger, E. Rank, C. Werner, T.J. Klein, I. Catelas, D.W.

Hutmacher, Biofabricated soft network composites for cartilage tissue engineering, Biofabrication 9 (2) (2017) 025014.
[32] R.M. Domingues, M. Silva, P. Gershovich, S. Betta, P. Babo, S.G. Caridade, J.F. Mano, A. Motta, R.L. Reis, M.E. Gomes, Development of injectable hyaluronic acid/cellulose nanocrystals bionanocomposite hydrogels for tissue engineering applications, Bioconjugate Chem. 26 (8) (2015) 1571–1581.
[33] F.A. Formica, E. Ozturk, S.C. Hess, W.J. Stark, K. Maniura-Weber, M. Rottmar, M. Zenobi-Wong, A Bioinspired Ultraporous Nanofiber-Hydrogel Mimic of the Cartilage Extracellular Matrix, Adv. Healthcare Mater. 5 (24) (2016) 3129–3138.
[34] G. Janer, E. Fernandez-Rosas, E. Mas del Molino, D. Gonzalez-Galvez, G. Vilar, C. Lopez-Iglesias, V. Ermini, S. Vazquez-Campos, In vitro toxicity of functionalised nanoclays is mainly driven by the presence of organic modifiers, Nanotoxicology 8 (3) (2014) 279–294.
[35] K. Haraguchi, T. Takehisa, M. Ebato, Control of cell cultivation and cell sheet detachment on the surface of polymer/clay nanocomposite hydrogels, Biomacromolecules 7 (11) (2006) 3267–3275.
[36] M. Barandun, L.D. Iselin, F. Santini, M. Pansini, C. Scotti, D. Baumhoer, O. Bieri, U. Studler, D. Wirz, M. Haug, M. Jakob, D.J. Schaefer, I. Martin, A. Barbero, Generation and characterization of osteochondral grafts with human nasal chondrocytes, J. Orthop. Res. 33 (8) (2015) 1111–1119.
[37] B.P. Nair, M. Sindhu, P.D. Nair, Polycaprolactone-laponite composite scaffold releasing strontium ranelate for bone tissue engineering applications, Colloids Surf. B Biointerfaces 143 (2016) 423–430.

Discussion and conclusions

Oxygen diffusion can be a major concern for tissue engineering and large dimension scaffolds. Hydrogel composites are desirable in tissue engineering to maintain the high water content provided by the hydrogel, while enhancing its mechanical properties with other biocompatible and biodegradable materials.

The work described in this paper allowed to establish that the oxygen diffusion is not impaired by the reinforcement of Si-HPMC hydrogel with laponites. These findings are important especially for future work being done on mimicking cartilage, since the described constructs had similar mechanical properties.

How increasing polymer concentration of Si-HPMC would affect oxygen diffusion and cell viability was the next chosen subject of this thesis, in an effort to characterize diffusion in biomaterials, with different mechanical properties, to be used as stem cell niches.

Chapter 3 - Impact on oxygen and glucose diffusion and cell viability in stem cell seeded constructs after hydrogel mechanical reinforcement through polymer concentration

Introduction

Hydrogels have been widely used in tissue engineering due to close similarities with ECM, general biocompatibility and adaptable degradability [1][88] [89]. The survival of cells in a 3D environment such as a hydrogel scaffold is dependent on the nutrient, oxygen and waste transport.

Transport in biomimetic matrices is mainly a function of diffusion, both in *in vitro* static culture conditions and in *in vivo* implants where vascular invasion has not yet taken place. Simple diffusion will eventually lead to the formation of gradients and deficiency of nutrients and oxygen, especially in core of the construct [72][68]. The low solubility of oxygen in culture media and the high consumption of oxygen by the cells may cause low oxygen availability in the centre of constructs, as oxygen has been shown to be a limiting nutrient [90]. Despite glucose higher solubility in

water, consumption by the cells in a 3D environment and diffusion in the material will also affect the availability. It has been shown, in 3D culture of MSCs, that glucose deprivation is a limiting factor in construct maturation [91]. The importance of glucose in 2D has also been previously shown, where it protected MSCs exposed to hypoxic conditions [92].

MSC are appealing for tissue engineering for being easily accessible and the potential to differentiate in different lineages. MSC have been shown to be sensitive to oxygen and glucose content in 3D culture [91] and cell viability in the centre of the constructs diminished when compared to the periphery, evidencing a relationship between a lack of nutrients and stem cell survival.

Understanding glucose and oxygen diffusion in the hydrogel scaffolds is therefore of upmost importance, since it influences cell metabolism and it will have an impact on stem cell fate [71][93]. Establishing diffusion coefficients of key nutrients, such as glucose and oxygen, can give us important information on the potential of a given material to be used as a stem cell niche. Despite the significance, not a lot of studies can be found concerning glucose diffusion in hydrogels.[94] [95][96] Oxygen permeability has been studied in different hydrogels using a diffusion cell [72][97] or actually implanting an oxygen sensor in the construct [98] using steady state approximations.

Silated-hydroxypropylmethylcellulose (Si-HPMC), has been previously described as a self-setting by cross-linking via pH modification [99]. This biomaterial is injectable and could provide an appropriate microenvironment for cell survival and differentiation [100]. The glucose and oxygen permeability parameters of this hydrogel have yet to be quantified.

Oxygen and glucose diffusion are important key elements when designing stem cell niches of larger dimensions. On the other hand, the reinforcement of the hydrogel, a method to achieve enhanced mechanical properties, can take a toll on the very same diffusion properties.

In this chapter, the aim was to determine glucose and oxygen diffusion coefficients for Si-HPMC and describe a method to study the diffusion coefficient under transient oxygen diffusion. The impact of hydrogel reinforcement with

increasing polymer concentration was evaluated in both glucose and oxygen diffusion. MSCs were subsequently seeded in the different hydrogels and the impact of cell density was also evaluated. In both studies, cells viability was also assessed. The results provide useful insights on oxygen and nutrient transport in hydrogels and can be useful in the development of cellular microenvironments based on Si-HPMC or similar polysaccharide hydrogels. These findings were published in Journal of Tissue Engineering and Regenerative Medicine and can be found at http://rdcu.be/KhQz and on the next pages of this thesis under the title:

Article 2 - Assessing glucose and oxygen diffusion in hydrogels for the rational design of 3D stem cell scaffolds in regenerative medicine

.

Received: 30 May 2017 | Revised: 17 January 2018 | Accepted: 17 February 2018

DOI: 10.1002/term.2656

RESEARCH ARTICLE

WILEY

Assessing glucose and oxygen diffusion in hydrogels for the rational design of 3D stem cell scaffolds in regenerative medicine

L. Figueiredo[1,2*] | R. Pace[1,2*] | C. D'Arros[1,2] | G. Réthoré[1,2] | J. Guicheux[1,2,3] | C. Le Visage[1,2*] | P. Weiss[1,2,3*]

[1] Inserm, UMR 1229, RMeS, Regenerative Medicine and Skeleton, Université de Nantes, ONIRIS, Nantes, France

[2] UFR Odontologie, Université de Nantes, Nantes, France

[3] CHU Nantes, PHU 4 OTONN, Nantes, France

Correspondence
Jérôme Guicheux, Inserm, UMR 1229, RMeS, Regenerative Medicine and Skeleton, Université de Nantes, UFR Odontologie, Place Alexis Ricordeau,44042 Nantes, France.
Email: jerome.guicheux@univ-nantes.fr

Funding information
Nanofar ERASMUS MUNDUS, Grant/Award Number: Doctorate fellowship to LF; Nanofar Erasmus Mundus Doctorate fellowship; FUI MARBiotech

Abstract

Hydrogels are attractive biomaterials for replicating cellular microenvironments, but attention needs to be given to hydrogels diffusion properties. A large body of literature shows the promise of hydrogels as 3D culture models, cell expansion systems, cell delivery vehicles, and tissue constructs. Surprisingly, literature seems to have overlooked the important effects of nutrient diffusion on the viability of hydrogel-encapsulated cells. In this paper, we present the methods and results of an investigation into glucose and oxygen diffusion into a silated-hydroxypropylmethylcellulose (Si-HPMC) hydrogel. Using both an implantable glucose sensor and implantable oxygen sensor, we continuously monitored core glucose concentration and oxygen concentration at the centre of hydrogels. We demonstrated that we could tune molecular transport in Si-HPMC hydrogel by changing the polymer concentration. Specifically, the oxygen diffusion coefficient was found to significantly decrease from 3.4×10^{-10} to 2.4×10^{-10} m^2 s^{-1} as the polymer concentration increased from 1% to 4% (*w*/*v*). Moreover, it was revealed during in vitro culture of cellularized hydrogels that oxygen depletion occurred before glucose depletion, suggesting oxygen diffusion is the major limiting factor for cell survival. Insight was also gained into the mechanism of action by which oxygen and glucose diffuse. Indeed, a direct correlation was found between the average polymer crosslinking node size and glucose parameters, and this correlation was not observed for oxygen. Overall, these experiments provide useful insights for the analysis of nutrient transport and gas exchange in hydrogels and for the development of future cellular microenvironments based on Si-HPMC or similar polysaccharide hydrogels.

KEYWORDS

biomimetic, hydrogel, molecular diffusion, nutrient transport, scaffold, stem cells

1 | INTRODUCTION

Hydrogels have the ability to maintain a vibrant cell microenvironment. The hydrophilic polymers which comprise the hydrogels absorb significant amounts of water, up to 99% of the hydrogels mass (Hoffman, 2012). Due to the highly hydrated character, hydrogels are good candidates as extracellular matrix (ECM) analogues. Replicating the cellular microenvironment including biochemical and biophysical cues that regulate cell expansion, differentiation, and cell-matrix communication is crucial to mimicking the complex nature of ECM. Using various "top-down" or "bottom-up" microfabrication techniques, hydrogels with intricate architecture have been obtained from natural and/or synthetic polymers and extensively characterized. Populating these hydrogels with mesenchymal stem cells is increasingly the objective of tissue engineers, as these cells can be easily obtained from the adult human body (adipose tissue or bone marrow, for example) and differentiated into the desired cell lineage (Han et al., 2014). However, the assembly of a functional construct depends on a fine equilibrium between numerous mechanical and biochemical factors that

*equivalent contribution

direct cells towards quiescence, proliferation, differentiation, or death (Choi, Choi, Woo, & Cho, 2014). Hydrogels have shown promise as 3D scaffolds for in vitro cell culture and delivery vehicles for cell therapy and tissue regeneration, however, they often suffer from weak mechanical properties and inability to efficiently encapsulate cells before gelation due to their rapid (seconds) formation or the toxicity of the gelation process itself (Drury & Mooney, 2003; Hoffman, 2012). Cellulose ether derivatives can be used to form hydrogels with tunable mechanical, through silanol moities which allow cell encapsulation and a myriad of in vivo applications. These cellulose ether derivative hydrogels were developed about 20 years ago by the addition of silanol Si—OH groups along the polysaccharide polymer chain. At neutral pH, silanol groups undergo condensation reactions which lead to the formation of siloxane Si—O—Si bonds (Turczyn, Weiss, Lapkowski, & Daculsi, 2000). The siloxane bonds create a polymer network with cross-linked hydrophilic polysaccharide chains over 30 min called a silated-hydroxypropylmethylcellulose (Si-HPMC) hydrogel (Fatimi, Tassin, Turczyn, Axelos, & Weiss, 2009). Hydrogels made of Si-HPMC have been used in cartilage (Merceron et al., 2011) and bone (Laïb et al., 2009; Trojani et al., 2005; Trojani et al., 2006) and have demonstrated to be biocompatible (Laïb et al., 2009; Mathieu et al., 2012; Vinatier et al., 2005).

Cell-encapsulating hydrogel tissue constructs lack a complex microvascular system important for maintaining the viability and function of specific seeded cells in thick constructs. Surprisingly, the importance of mass transport in hydrogels has been largely overlooked in the literature despite the importance of nutrients and signalling molecules on cell survival. Gradients and eventually a deficiency of nutrients, especially in core of the constructs, have been reported in hydrogels suggesting the hydrogels offer less than sufficient nutrient transport properties (Bland, Dreau, & Burg, 2013; Malda et al., 2004). Some studies have identified oxygen as the limiting nutrient to 3D stem cell culture (Martin & Vermette, 2005), whereas others have shown glucose deprivation to be the limiting factor (Farrell, Shin, Smith, & Mauck, 2015). Even before nutrient deprivation, glucose and oxygen concentrations have been shown to influence cell metabolism (Mohyeldin, Garzón-Muvdi, & Quiñones-Hinojosa, 2010) and stem cell fate (Ardakani, Cheema, Brown, & Shipley, 2014).

Oxygen permeability in hydrogels has been evaluated with diffusion cells (Demol, Lambrechts, Geris, Schrooten, & Van Oosterwyck, 2011; Malda et al., 2004) or an implanted oxygen sensor in the construct (Cheema et al., 2012) using steady state approximations. However, as pointed out by Ehsan and George (2013), a nonsteady approach is essential when planning to use such constructs in vivo due temporal change in oxygen upon implantation. To develop a nonsteady state approach that could eventually be applied to all hydrogel constructs, we set up a unique method to systematically examine glucose and oxygen diffusion characteristics of Si-HPMC hydrogels. Using glucose sensors and fluorescent oxygen microsensors, core glucose concentrations and oxygen pressures were continuously monitored in the centre of hydrogels and during in vitro culture of cellularized hydrogels.

2 | MATERIALS AND METHODS

2.1 | Hydrogel formation

Hydroxypropylmethylcellulose (HPMC) was obtained by the trade name E4M® from Colorcon (Kent, UK). HPMC was modified by the addition of silanol groups with a degree of substitution of 0.6% as determined by inductively coupled plasma atomic emission spectroscopy to form Si-HPMC. This process has been thoroughly previously described (Bourges, Weiss, Daculsi, & Legeay, 2002; Fatimi, Tassin, Quillard, Axelos, & Weiss, 2008). Si-HPMC was dissolved in a basic solution of 0.09 M NaOH and sterilized by autoclave at 121 °C for 30 min, as previously described (Fatimi et al., 2009). To initiate self-cross-linking, the alkaline polymer solution was mixed with an acidic buffer in a 2:1 base:acid ratio to reach a final pH of 7.4 and a polymer concentration of 1%, 2%, 3%, or 4% (*w*/v). The acidic buffer consisted of a sterile 0.06 M HCl solution with 1.8% NaCl (w/v) and 6.2% (w/v) HEPES (4-(2-hydroxyethyl)piperazine-1-ethanesulfonic acid), where all products were obtained from Sigma (St. Louis, MO, USA).

2.2 | Rheology

Rheological experiments were performed using a HAAKE Modular Advanced Rheometer System (HAAKE, Germany, with Rheowin software) and a 20-mm flat geometry. Hydrogels were allowed to fully crosslink at 37 °C for 5 days before analysis. Rotational shear stress analysis was performed on 2-mL hydrogel cylinders (0.5-cm height, 2.2-cm diameter) in a 12 well-plate, with 11 replicates for each polymer concentration. Hydrogels were mechanically stressed by a sweep of increasing oscillatory strain until failure where strain (τ) was increased from 0.1 to 3,000 Pa in 50 logarithmically spaced steps and rotational frequency (ω) was kept constant at 2π/s. The 4% Si-HPMC hydrogels were more rigid and required a strain from 0.1 to 10,000 Pa in 60 logarithmically spaced steps. Shear storage modulus (G') was determined by the average of the 25 highest storage modulus values reported before sample failure. The average distance between polymer nodes in the hydrogel network, called mesh size here, was determined from G' using calculations described in Section 3.1.

2.3 | Glucose permeability

Glucose permeability experiments were performed on eight Si-HPMC hydrogel cylinders (1-cm height, 1.56-cm diameter) and molded into a 24 well plate, with polymer concentrations ranging from 1% to 4% (*w*/v). Glucose sensors from World Precision Instruments (Sarasota, FL, USA) were implanted in the centre of the hydrogels at a depth of 0.5 cm as represented in Figure 1. Glucose-free hydrogels were then exposed to 5 g/L (25 mM) glucose by the addition of 1 mL of high-glucose Dulbecco's modified Eagle's medium (DMEM) supplied by Gibco (USA). Glucose was allowed to diffuse into the hydrogels, and hydrogels were incubated in a 37 °C humidified and 5% CO_2 incubator for the next several days. The core glucose concentration was recorded over time and insight into glucose diffusion parameters were found by calculations described in Section 3.2.

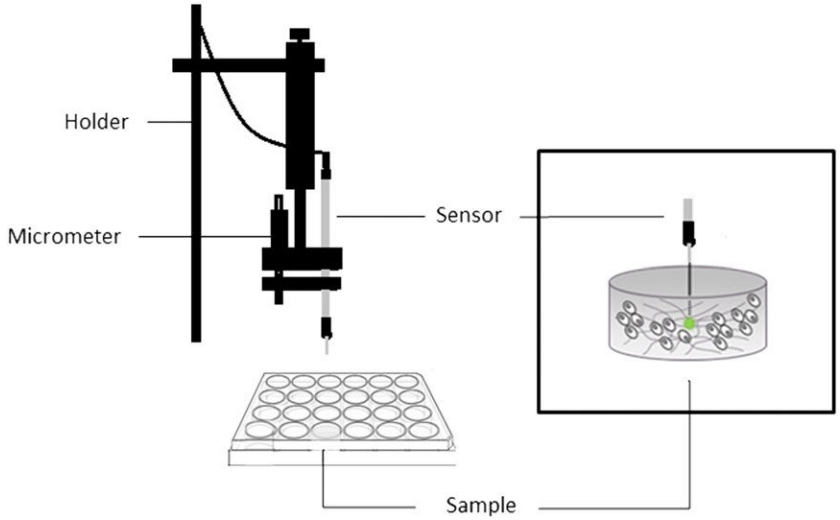

FIGURE 1 Schematic representation of the implantation of glucose and oxygen sensors into the centre of silated-hydroxypropylmethylcellulose samples [Colour figure can be viewed at wileyonlinelibrary.com]

2.4 | Oxygen permeability

Oxygen permeability experiments were performed on 16 Si-HPMC hydrogel cylinders (1-cm height, 1.56-cm diameter) and molded into a 24 well plate, with polymer concentrations ranging from 1% to 4% (*w*/*v*). Fluorescent oxygen microsensors from PreSens (Germany) were inserted in the centre of the hydrogels at a depth of 0.5 cm. Hydrogels were then topped with 1 mL of DMEM to prevent dehydration during incubation at 37 °C in a 5% O_2 incubator (hypoxic conditions) supplied by Binder (Germany). The samples were moved 48 hr later to a 20% O_2 incubator (normoxic conditions) for reoxygenation. Core oxygen pressures were recorded during incubation, and insight into oxygen permeability was obtained according to calculations in Section 3.3.

2.5 | Cell culture

Human adipose derived stem cells (hASCs) were chosen for these studies because they have previously shown sensitivity to oxygen and glucose content in 3D culture (Farrell et al., 2015). Cells were obtained from consenting liposuction patients at the Clinique Breteche in Nantes, France. They were isolated from the lipoaspirates as previously described (Merceron et al., 2010) and then cultured in 37 °C, 5% CO_2 incubators with complete culture medium (DMEM supplemented with 10% fetal bovine serum (FBS) from Hyclone, USA). The cells were expanded in CellSTACK plates (Corning, USA), detached by trypsin/EDTA at the start of each experiment, and resuspended in 100 µl of complete medium. Using 30G Luer lock syringes and a female–female Luer lock coupler, cells were mixed with not yet gelled Si-HPMC prepared as described above and then tranferred into a 24 well plate (2 ml per well). After 1 hr, 1,000 µl of culture medium was added to each well, and medium was refreshed every 2 days. Final polymer concentrations ranged from 1 to 4% (*w*/*v*), and final cell seeding density ranged from 1 to 8 million cells per millilitre.

2.6 | Cell viability

Cell viability measurements were performed at 6, 72, and 168 hr after cell seeding using a Live and Dead assay kit (Molecular Probes, USA). Hydrogels were washed twice with DMEM to remove esterase activity of the complete medium. Hydrogels were then incubated with 2-µM calcein-AM solution and 4-µM Ethidium homodimer-1 solution in DMEM for 30 min at room temperature. Samples were collected from seeded hydrogels with a 2-mm diameter biopsy punch that was positioned at the centre of the construct. Samples were imaged using a Nikon Eclipse C1 confocal microscope equipped with both 488- and 543-nm lasers. The height acquisition was at least 150 µm. Three-dimensional cell counting was performed with Volocity software (PerkinElmer, Waltham, MA, USA), and results are presented as a percentage of live cells (mean value ± SEM, $n = 6$ independent experiments).

2.7 | Mesh size calculation

The average size between the crossing linking nodes of the Si-HPMC polymer network, known as mesh size, was determined from Equation 1 (Peppas, 1986), where the average mesh size (ξ)[m] is a function of the storage modulus (G')[Pa], the Boltzman constant (K) [J/K], and temperature (T)[K].

$$\xi = \left(\frac{KT}{G'}\right)^{1/3}. \quad (1)$$

2.8 | Glucose permeability calculation

Glucose permeability (T_{50}) was defined as the time needed to reach 50% of the equilibrium glucose concentration. The equilibrium was reached when the concentration remained constant for at least 10 measurements, with the relative change between two consecutive measurements calculated to be less than 0.1%. The T_{50} value was obtained by first determining the hydrogels equilibrium concentration and then finding the time where the glucose probe first reported a value above half of the equilibrium concentration with the glucose probe reporting the concentrations every 50 s.

2.9 | Oxygen permeability calculation

There was no solution flow or reaction in our system, therefore, oxygen transport is modelled by diffusion alone governed by Fick's second law shown in Equation 2. The following Equation 3 results when following integration steps similar to those of the Fourier Field Equation for equimolar counter diffusion into an infinite plane (Crank, 1975). The equation can then be rearranged to the more useful Equation 4. The probe oxygen data (pO_2gel) are a function time (t), oxygen diffusion coefficient (Dv), surface oxygen partial pressure (pO_2air), initial oxygen partial pressure (pO_2ini), and depth of the probe (x). The material's oxygen diffusion coefficient was solved by a data regression of the probe oxygen data (pO_2gel) with respect to time (t) and finding the diffusion coefficient which yielded the least squared mean error.

$$\frac{\partial(pO_2)}{\partial t} = D_v \frac{\partial^2 \mu}{\partial x^2}, \tag{2}$$

$$\frac{pO_{2air} - pO_{2gel}}{pO_{2air} - pO_{2ini}} = \frac{8}{\pi} \sum_{n=0}^{\infty} \left((1+2n)^{-2} e^{\left(-D_v t \pi^2 (1+2n)^2 / 4 x^2\right)} \right), \tag{3}$$

$$pO_{2gel} = pO_{2air} + \frac{8}{\pi}(pO_{2ini} - pO_{2air}) \sum_{n=0}^{\infty} \left((1+2n)^{-2} e^{\left(-D_v t \pi^2 (1+2n)^2 / 4 x^2\right)} \right). \tag{4}$$

2.10 | Statistical methods

Correlations between groups were assessed with Pearson's test (two-tailed). Statistical significance was determined by one-way ANOVA with a post hoc Tukey test with GraphPad 6 (GraphPad Software Inc., La Jolla, CA) statistical analysis. Statistical significance was set at $p < 0.05$.

3 | RESULTS

3.1 | Hydrogel mechanical properties

The study revealed a correlated ($p < .05$) and significant ($p < .05$) decrease of the network mesh size from 19.0 nm ± 1.2 nm to 7.8 nm ± 0.3 nm as polymer concentration increases from 1% to 4% (w/v). A significant increase of the storage modulus, G', from 0.61 to 8.8 kPa was observed when Si-HPMC concentration increased from 1% to 4% (w/v; Figure 2a). Network mesh sizes were calculated from G' values according to this section and are shown in Figure 2b. Each tested hydrogel concentration was found to have statistically different ($p < .05$) properties from one another.

3.2 | Glucose diffusion

A relationship between polymer concentration and glucose diffusion was found using 2-ml Si-HPMC hydrogels containing 0-mM glucose covered with culture medium (1 ml) containing 25-mM glucose. A glucose sensor positioned in the centre of the hydrogels and the time needed for glucose to reach half the maximum concentration (T_{50}) were calculated from the method described in this section. Figure 3 shows a correlated ($p < .05$) significant ($p < .05$) increase of T_{50} from 0.8 h ± 0.21 h to 1.6 h ± 0.07 h when Si-HPMC concentration increases from 1% to 4% (w/v). On the other hand, a correlation ($p < .05$) was found between mesh size and T_{50}, showing a relationship between the two parameters.

3.3 | Oxygen diffusion

Fluorescent oxygen sensors monitored oxygen concentration at the centre of the hydrogels when hydrogels were transferred from 20% O_2 (normoxic conditions) to 5% O_2 (hypoxic conditions) incubators to assess oxygen diffusion parameters. Figure 4a shows the recorded de-oxygenation profiles. Control experiments were performed by using water or culture medium in the absence of

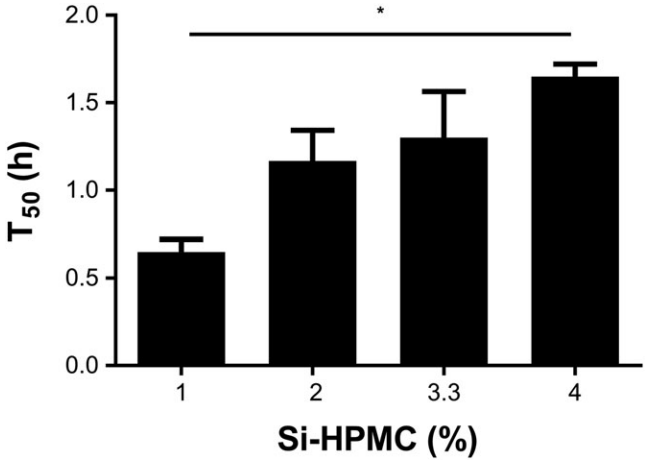

FIGURE 3 Glucose diffusion in silated-hydroxypropylmethylcellulose (Si-HPMC) hydrogels. Glucose T_{50} was defined as the time to reach half the maximum concentration of glucose at the core of Si-HPMC hydrogels covered with culture medium and is represented as a function of polymer concentration. Results are presented as mean values ± SEM ($n = 3$). One-way ANOVA * $p < .05$

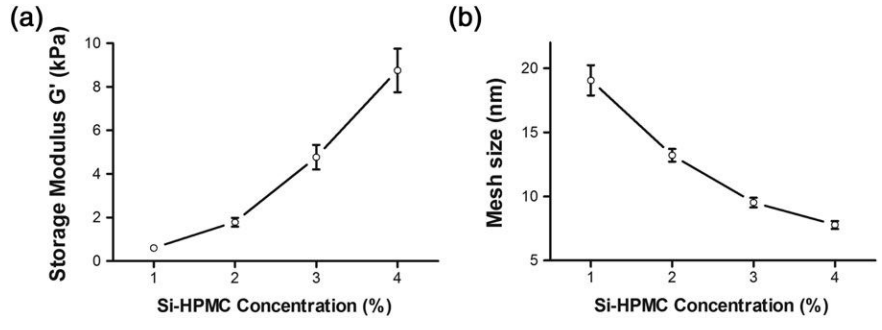

FIGURE 2 Silated-hydroxypropylmethylcellulose (Si-HPMC) hydrogel characterization. Storage modulus (a) and network mesh size (b) are represented as a function of polymer concentration. Results are presented as mean values ± SEM ($n = 3$)

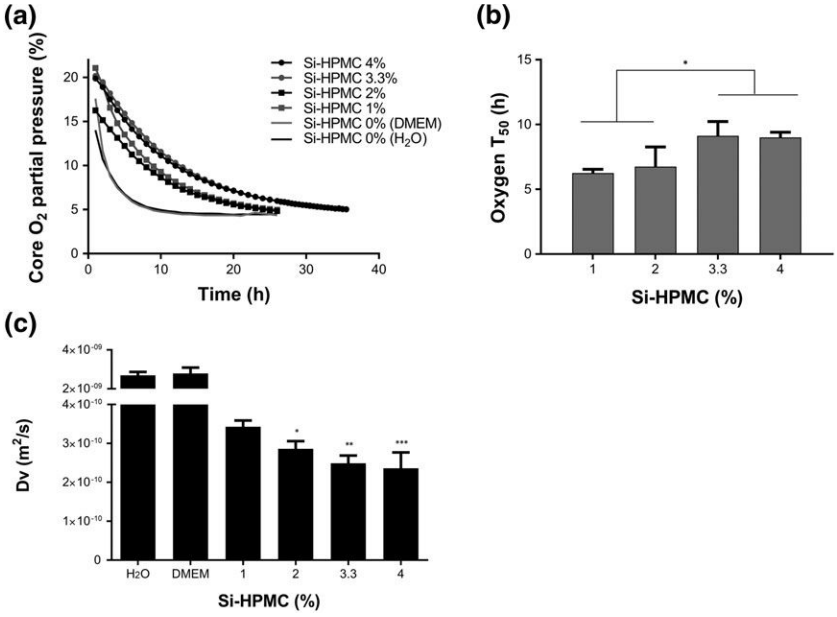

FIGURE 4 Oxygen diffusion in silated-hydroxypropylmethylcellulose (Si-HPMC) hydrogels. (a) De-oxygenation at the core of Si-HPMC hydrogels transferred from normoxic (20% O2) to hypoxic (5% O_2) conditions. Values are means with $n = 4$. (b) Oxygen T_{50} was defined as the time to reach half the equilibrium concentration of oxygen at the core of Si-HPMC hydrogels. Values are means ± SD ($n = 4$). (c) Oxygen diffusion coefficient (Dv), calculated from de-oxygenation curves, as a function of Si-HPMC concentration. Values are means ± SD ($n = 4$). One-way ANOVA $^*p < .05$, $^{**}p < .01$, $^{***}p < .001$ when comparing to 1% Si-HPMC. DMEM = Dulbecco's modified Eagle's medium

hydrogels. Equilibrium at 5% O_2 was reached within 10 hr for the control experiments. By contrast, equilibrium was not reached before 24 hr for any hydrogel, whatever the polymer concentration. Although O_2 equilibrium was reached slightly after 24 hr for 1% and 2% hydrogels, O_2 equilibrium was only reached after 35 hr for 3.3% and 4% hydrogels. The time to reach half the oxygen equilibrium concentration (T_{50}) was calculated to express oxygen diffusion. Figure 4b shows the absence of a linear relationship between oxygen T_{50} and polymer concentration.

The diffusion coefficient, Dv, was calculated according to this section and is represented in Figure 4c for control media (water and culture medium) and hydrogels. Whereas the calculated oxygen diffusion coefficient was similar in water (2.7×10^{-09} m^2/s) and culture medium (2.8×10^{-09} m^2/s), Dv was significantly ($p < .05$) decreased in hydrogels, regardless of the polymer concentration. Moreover, increasing polymer concentration from 1% to 2%, 3.3%, and 4% led to a correlated ($p < .05$) significant ($p < .05$) reduction of oxygen diffusion ability.

3.4 | Effect of polymer concentration on glucose and oxygen diffusion in 3D cell culture

In the next series of experiments, hASCs were incorporated into hydrogels by mixing a cell suspension with the self-setting Si-HPMC hydrogel to investigate the relationship between polymer network, nutrient diffusion, and 3D cell culture. First, 1 million cells/ml were seeded in 2 ml of 1%, 2%, 3.3%, and 4% hydrogels, that were then covered with culture medium (glucose 25 mM) and incubated in a normoxic environment (20% O_2). Glucose concentration and oxygen partial pressures at the core of cellularized hydrogels were recorded at different time points (6, 72, and 168 hr). Figure 5a presents glucose

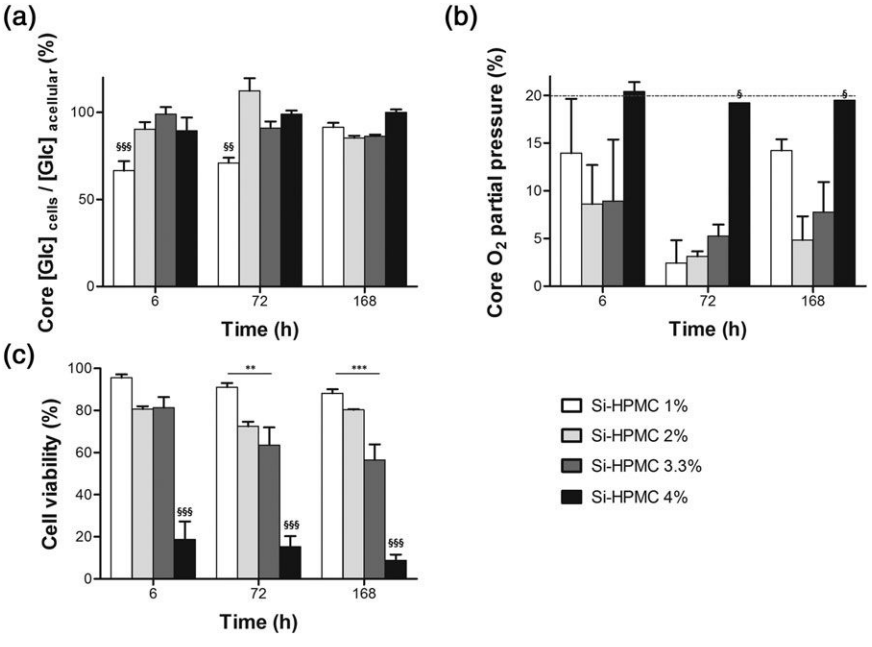

FIGURE 5 Effect of polymer concentration on core glucose concentration and oxygen content in silated-hydroxypropylmethylcellulose (Si-HPMC) hydrogels seeded with 1 million hASCs/ml. (a) Glucose content expressed as a percentage of the glucose concentration of hydrogels prepared without cells (acellular). (b) Core oxygen partial pressure. (c) Cell viability measured using a Live and Dead assay followed by confocal imaging. Values are means ± SEM ($n = 3$). §, §§, and §§§ indicate a significant difference with all other groups at the same time point ($p < .05$, $p < .01$, and $p < .001$, respectively). ** and *** indicate a significant difference ($p < .01$ and $p < .001$, respectively)

measurements in cell seeded hydrogels as a percentage of the glucose concentration on hydrogels prepared without cells (acellular).

There was no difference in glucose concentration at 6 and 72 hr, except for the 1% hydrogel. However, at 168 hr, all groups presented a similar glucose concentration close to acellular constructs. Figure 5b shows that both polymer concentration and culture duration greatly affected the oxygen pressure. Oxygen measurements (Figure 5b) show that 1%, 2%, and 3% cellularized hydrogels had a significantly lower oxygen core concentration as compared with acellular controls at all time points. Hydrogels with 2% and 3% Si-HPMC presented a lower oxygen pressure than 1% Si-HPMC. However, 4% Si-HPMC cellularized hydrogels presented a core oxygen partial pressure that remained constant at all times and equal to the one of acellular controls at all time points. This observation was mirrored in glucose concentrations that were found to be similar in 4% hydrogels and acellular controls at all time points (Figure 5a). It is worth noting that in the 4% hydrogel, both glucose and oxygen partial pressures are similar to those of acellular hydrogels, which is in accordance with the low cell viability (Figures 5c and S1). On the contrary, cell viability remained higher than 60% for 3.3% hydrogels and even higher than 80% for 1% and 2% hydrogels during the whole experiment (data not shown).

3.5 | Effect of cell density on glucose and oxygen in 3D cell culture

A 2% Si-HMPC hydrogel was seeded with 1, 2, 4, or 8 million hASCs per millilitre in order to determine if and when a nutrient would reach depletion. Figure 6a presents the results of glucose measurements in cell seeded hydrogels expressed as a percentage of the glucose concentration of hydrogels prepared without cells (acellular). A dramatic decrease in glucose concentration was observed in hydrogels seeded with a large number of cells compared with acellular hydrogels. For 8 million cells/ml, a significant reduction of glucose concentration (31% ± 13%) was obtained in 6 hr, and the glucose concentration remained at 63.5% ± 13.5% with the addition of 4 million cells/ml. After 72 and 168 hr, hydrogels seeded with 4 and 8 million cells/ml presented a glucose concentration of less than 20% of the control hydrogel. However, after 168 hr, hydrogels seeded with 1 and 2 million cells/ml presented glucose concentrations of 85.3% ± 1.3% and 61.0% ± 17.0%, respectively, indicating cell density had a great impact on glucose available to cells.

A similar trend was observed for core oxygen partial pressures (Figure 6b). Cell densities higher than 4 million/ml led to an almost complete depletion of O_2 at 72 h and 168 hr, and oxygen levels of 4.8% ± 2.4% and 4.5% ± 3.6% were found in hydrogels seeded with 1 and 2 million cells/ml, respectively. Although all cells died at the core of the 8 million cell hydrogels (Figures 6c and S2), cell viability remained quite high in all other hydrogels and even higher than 80% for 1 million cell/ml hydrogels during the whole experiment (data not shown).

4 | DISCUSSION

Understanding diffusion in biomaterials is essential for studying not only cell survival but also cell functions and differentiation in 3D culture. Diffusion limitations have been reported to be one of the primary prohibitive factors in scaling up large 3D tissue models. In particular, oxygen and nutrients such as glucose must diffuse from gas and liquid phases through a solid phase composed of either natural ECM or polymer hydrogels, in order to reach the cells. Oxygen permeability has been studied extensively in the field of soft contact lenses, where oxygen dissolves in the tear film and moves within the hydrogel by a diffusive permeability mechanism (Gavara & Compañ, 2016). With regard to hydrogels supporting 3D culture and viability of cells, few studies have shown a range of control over oxygen permeability, and most designs have focused on decreasing the number of cross-links nodes and introducing micropores to increase molecular diffusivity in the matrix.

Here, we report a correlation between Si-HPMC hydrogel mesh size and glucose diffusion characteristics and a similar trend for oxygen. However, a 50% reduction of the hydrogel mesh size yielded a 50% glucose diffusion but a 30% reduced oxygen diffusion. This could be due to the structural differences between glucose and oxygen. Glucose is quite water soluble and should move freely with the diffusing water,

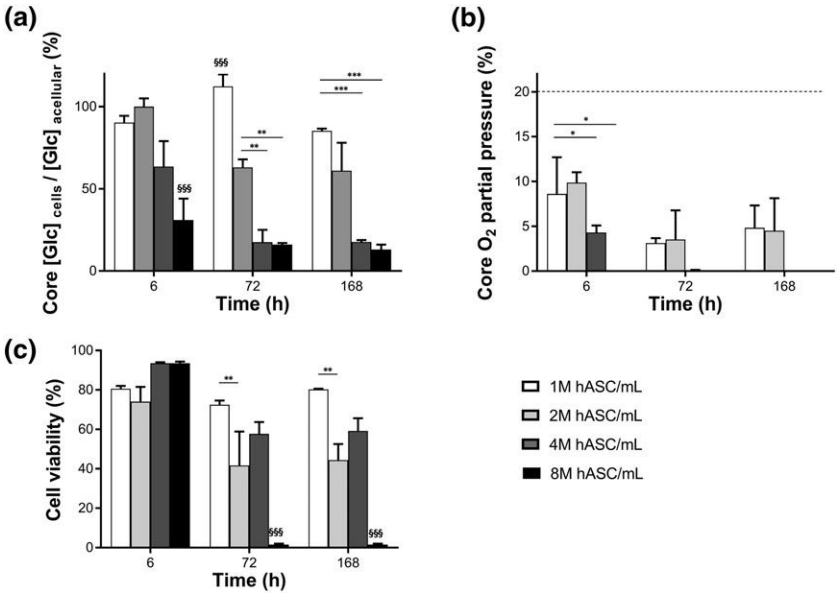

FIGURE 6 Effect of cell density on core glucose concentration and oxygen content in 2% (w/v) silated-hydroxypropylmethylcellulose (Si-HPMC) hydrogels. (a) Glucose content in hydrogels seeded with 1, 2, 4, or 8 million hASCs/ml expressed as a percentage of the glucose concentration of hydrogels prepared without cells (acellular). (b) Core oxygen partial pressure in hydrogels incubated in normoxic conditions. (c) Cell viability measured using a Live and Dead assay followed by confocal imaging. Values presented are means ± SEM (n = 3). §§§ indicates a significant difference with all other groups at the same time point (p < .001). *, **, and *** indicate a significant difference (p < .05, p < .01, and p < .001, respectively)

whereas oxygen has a weaker solubility. Tortuosity parameter is used to reflect the internal architecture of the scaffold, gathering the effects of pore size, pore size distribution, and the pore interconnections. Taking into account the glucose diffusion-mesh size relationship, these results suggest that glucose is more dependent on the tortuosity of a material than oxygen. Other studies have shown evidence in agreement that glucose diffusivity increases with pore size, however, the trend was not linear for materials of different origin, highlighting the importance of the morphology of the pore (Suhaimi, Wang, Thornton, & Das, 2015; van Stroe-Biezen, Everaerts, Janssen, & Tacken, 1993).

Multiple studies have reported approximations of the oxygen diffusivity in acellular hydrogels equal to the diffusivity in water. However, our results presented here show that these approximations do not apply for all types of hydrogels. Specifically, we report oxygen measurements which indicate a hydrogel with 99% water and 1% polysaccharide polymer exhibited 12.7% the oxygen diffusivity of 100% water (2.7×10^{-9} m^2 s^{-1}; Wise & Houghton, 1966). However, doubling the polymer concentration to 2% only lowers to 10.6% of oxygen diffusivity in water. Other variables, besides tortuosity, must be affecting oxygen diffusion, such as an interaction of the molecule with the polymer. The diffusion coefficient of small molecules has been reported to be typically around 10^{-9} to 10^{-10} m^2/s in polymer hydrogels, with small molecules such as oxygen typically closer to 10^{-9} m^2/s and slightly larger molecules such as glucose closer to 10^{-10} m^2/s (McMurtrey, 2016). Larger proteins such as albumin generally have a smaller diffusion coefficient in the range of 10^{-11} m^2/s (Johnson, Berk, Jain, & Deen, 1996).

In other hydrogel systems, oxygen diffusivity has been reported to be between 2% and 96% of that in water, a summary can be found in Table 1. Diffusion coefficient decreases with increasing concentration except for ionic-hardening gels, possibly due to the formation of different structure at different concentrations. For the studied concentrations, synthetic hydrogels also present reduced diffusivity. Although Si-HPMC oxygen diffusion ranks low in the category of hydrogels (0.24 to 0.34×10^{-9}), it is of the same order of magnitude as biologic scaffold materials composed of ECM (0.2 to 0.7×10^{-9}; Valentin et al., 2009). As suggested in Table 1, a more complex configuration is associated with lower diffusion coefficients in these biological scaffold materials.

In our study, seeding cells in different hydrogel concentrations did not affect glucose concentration in the centre of the constructs but showed the dependence of the oxygen on polymer concentration which could be expected by the difference between oxygen and glucose T_{50}. Besides being an important metabolic regulator of stem cells, low oxygen tension acts in the niche level as a cue for stem cell fate (Mohyeldin et al., 2010). This work has shown that adding high cell densities resulted in oxygen depletion of our in vitro construct and seems to be linked to concomitant repercussions on cell viability. Although low oxygen tension may be desirable for the replication of the stem cell niche, complete extinction of oxygen in an in vivo construct has been associated with compromised cell viability. We hypothesized that the presence of cells may be acting as a diffusion oxygen barrier (Sachlos & Czernuszka, 2003) with low diffusivity of oxygen through cells (3×10^{-10} m^2/s; Demol et al., 2011). Each

TABLE 1 Oxygen diffusion coefficient of biomaterials commonly used in tissue engineering at 37 °C

	Concentration (*w/v*, otherwise indicated)	Oxygen diffusion coefficient ($\times 10^{-9}$ m^2 s^{-1})	Reference
Water	n/a	2.7	(Wise & Houghton, 1966)
Agar	2% 5% 8%	2.4 2.0 1.6	
Agarose	2% 5% 8%	2.6 2.0 1.7	(Hulst, Hens, Buitelaar, & Tramper, 1989)
Alginate - Ca++	1% 2% 3%	1.8 2.0 1.8	
Biologic scaffold materials			
Small intestinal submucosa Urinary bladder matrix Urinary bladder submucosa	n/a n/a n/a	0.24–0.56 0.38–0.46 0.66	(Valentin et al., 2009)
Collagen I	1 mg/ml	2.5	(Colom et al., 2014)
Fibrin	2.5–10 mg/ml	1.7	(Ehsan & George, 2013)
	33 mg/ml	0.31	(Demol et al., 2011)
Cartilaginous constructs[a]	n/a	0.8	(Malda et al., 2004)
Poly(vinyl alcohol)[b]	1.1 mg/ml	0.6	(van Stroe-Biezen et al., 1993)
Basement membrane[c]	12 mg/ml	1.7	(Colom et al., 2014)
Si-HPMC	1% 2% 3.3% 4%	0.34 0.29 0.25 0.24	n/a

Note. n/a = not applicable; Si-HPMC = silated-hydroxypropylmethylcellulose.

[a]Based on polyethylene glycol terephthalate/polybutylene terephthalate. [b]Glutaraldehyde-cross-linked. [c]From Engelbreth-Holm-Swarm tumour (Cultrex® BME, Trevigen).

mesenchymal stem cell uses roughly 1×10^{-7} μmol oxygen per hour during proliferation (Pattappa, Heywood, de Bruijn, & Lee, 2011), which removes oxygen that has already diffused. This hypoxic condition at the centre of hydrogels can have cell fate consequences. A recent method article reported a novel analytic mass transfer model to estimate molecular dynamics and diffusion characteristics for cerebral organoids (McMurtrey, 2016). The models proposed above show glucose to initially be more of a temporary limiting factor for cell metabolism than oxygen due to its lower diffusivity, but after diffusion has approached steady state, oxygen is the limiting nutrient in all cases under the given range of parameters. Our results would suggest that to achieve a higher cell density, the issue of oxygen diffusion must be addressed. Higher ability of oxygen diffusion in the early stages of implantation could be achieved in less concentrated hydrogels, but that would mean sacrificing the mechanical proprieties of the construct. Knowing that in vivo cells are usually found within 100 μm of a capillary, prevascularization or the addition of an oxygen carrier could be the answer for more concentrated hydrogels.

5 | CONCLUSION

Si-HPMC hydrogels have heavily restricted nutrient diffusion properties despite being more than 95% water. The glucose diffusion through the polysaccharide hydrogel was directly correlated to the average node distance of the polymer network while the same cannot be said for oxygen. The diffusion of oxygen was suspected to be the limiting factor of cell viability in Si-HPMC hydrogels. The oxygen concentration inside of cellularized hydrogels was more dependent on cell density than on polymer concentration. Populating low polymer concentration constructs with cells resulted in high cell viability, but mechanical properties were sacrificed. On the other hand, high cell density resulted in a fatal deficiency of nutrients leading further studies to be directed to enhancing oxygen and nutrient diffusion in these constructs. Overall, these experiments provided us with useful insights for the development of future cellular microenvironments based on Si-HPMC hydrogels or similar polysaccharide hydrogels. Additionally, this method can be readily extended to analyzing nutrient delivery and gas exchange in a variety of material hydrogels for regenerative medicine applications.

ACKNOWLEDGEMENTS

Financial support was given by FUI MARBiotech and a Nanofar Erasmus Mundus Doctorate fellowship to L. F.

CONFLICT OF INTEREST

The authors have declared that there is no conflict of interest.

ORCID

L. Figueiredo http://orcid.org/0000-0003-2731-132X
R. Pace http://orcid.org/0000-0003-4492-0039
J. Guicheux http://orcid.org/0000-0003-2754-3024
C. Le Visage http://orcid.org/0000-0003-1816-1649
P. Weiss http://orcid.org/0000-0002-6159-8590

REFERENCES

Ardakani, A. G., Cheema, U., Brown, R. A., & Shipley, R. J. (2014). Quantifying the correlation between spatially defined oxygen gradients and cell fate in an engineered three-dimensional culture model. *J. R. Soc. Interface*, *11*, 1–11. https://doi.org/10.1098/rsif.2014.0501

Bland, E., Dreau, D., & Burg, K. J. (2013). Overcoming hypoxia to improve tissue-engineering approaches to regenerative medicine. *Journal of Tissue Engineering and Regenerative Medicine*, *4*, 505–514. https://doi.org/10.1002/term.540

Bourges, X., Weiss, P., Daculsi, G., & Legeay, G. (2002). Synthesis and general properties of silated-hydroxypropyl methylcellulose in prospect of biomedical use. *Advances in Colloid and Interface Science*, *99*, 215–228.

Cheema, U., Rong, Z., Kirresh, O., Macrobert, A. J., Vadgama, P., & Brown, R. A. (2012). Oxygen diffusion through collagen scaffolds at defined densities: Implications for cell survival in tissue models. *Journal of Tissue Engineering and Regenerative Medicine*, *6*(1), 77–84. https://doi.org/10.1002/term.402

Choi, Y. C., Choi, J. S., Woo, C. H., & Cho, Y. W. (2014). Stem cell delivery systems inspired by tissue-specific niches. *Journal of Controlled Release*, *193*, 42–50. https://doi.org/10.1016/j.jconrel.2014.06.032

Colom, A., Galgoczy, R., Almendros, I., Xaubet, A., Farré, R., & Alcaraz, J. (2014). Oxygen diffusion and consumption in extracellular matrix gels: Implications for designing three-dimensional cultures. *Journal of Biomedical Materials Research - Part A*, *102*, 2776–2784. https://doi.org/10.1002/jbm.a.34946

Crank, J. (1975). *The mathematics of diffusion*. Clarendon Press.

Demol, J., Lambrechts, D., Geris, L., Schrooten, J., & Van Oosterwyck, H. (2011). Towards a quantitative understanding of oxygen tension and cell density evolution in fibrin hydrogels. *Biomaterials*, *32*, 107–118. https://doi.org/10.1016/j.biomaterials.2010.08.093

Drury, J. L., & Mooney, D. J. (2003). Hydrogels for tissue engineering: Scaffold design variables and applications. *Biomaterials*, *24*, 4337–4351.

Ehsan, S. M., & George, S. C. (2013). Nonsteady state oxygen transport in engineered tissue: Implications for design. *Tissue Engineering. Part A*, *19*, 1433–1442. https://doi.org/10.1089/ten.TEA.2012.0587

Farrell, M. J., Shin, J. I., Smith, L. J., & Mauck, R. L. (2015). Functional consequences of glucose and oxygen deprivation on engineered mesenchymal stem cell-based cartilage constructs. *Osteoarthritis and Cartilage*, *23*(1), 134–142. https://doi.org/10.1016/j.joca.2014.09.012

Fatimi, A., Tassin, J. F., Quillard, S., Axelos, M. A., & Weiss, P. (2008). The rheological properties of silated hydroxypropylmethylcellulose tissue engineering matrices. *Biomaterials*, *29*(5), 533–543.

Fatimi, A., Tassin, J.-F., Turczyn, R., Axelos, M. A., & Weiss, P. (2009). Gelation studies of a cellulose-based biohydrogel: The influence of pH, temperature and sterilization. *Acta Biomaterialia*, *5*, 3423–3432. https://doi.org/10.1016/j.actbio.2009.05.030

Gavara, R., & Compañ, V. (2016). Oxygen, water, and sodium chloride transport in soft contact lenses materials. *Journal of Biomedical Materials Research Part B: Applied Biomaterials*, *105*, 2218–2231. https://doi.org/10.1002/jbm.b.33762

Han, Y. L., Wang, S., Zhang, X., Li, Y., Huang, G., Qi, H., … Xu, F. (2014). Engineering physical microenvironment for stem cell based regenerative medicine. *Drug Discovery Today*, *19*, 763–773. https://doi.org/10.1016/j.drudis.2014.01.015

Hoffman, A. S. (2012). Hydrogels for biomedical applications. *Advanced Drug Delivery Reviews*, *64*, 18–23. https://doi.org/10.1016/j.addr.2012.09.010

Hulst, A. C., Hens, H. J. H., Buitelaar, R. M., & Tramper, J. (1989). Determination of the effective diffusion coefficient of oxygen in gel materials in relation to gel concentration. *Biotechnology Techniques*, *3*, 199–204.

Johnson, E. M., Berk, D. A., Jain, R. K., & Deen, W. M. (1996). Hindered diffusion in agarose gels: Test of effective medium model. *Biophysical Journal*, *70*, 1017–1023.

Laïb, S., Fellah, B. H., Fatimi, A., Quillard, S., Vinatier, C., Gauthier, O., … Weiss, P. (2009). The in vivo degradation of a ruthenium labelled

polysaccharide-based hydrogel for bone tissue engineering. *Biomaterials*, *30*, 1568–1577. https://doi.org/10.1016/j.biomaterials.2008.11.031

Malda, J., Rouwkema, J., Martens, D. E., Le Compte, E. P., Kooy, F. K., Tramper, J., … Riesle, J. (2004). Oxygen gradients in tissue-engineered PEGT/PBT cartilaginous constructs: Measurement and modeling. *Biotechnology and Bioengineering*, *86*(1), 9–18.

Martin, Y., & Vermette, P. (2005). Bioreactors for tissue mass culture: Design, characterization, and recent advances. *Biomaterials*, *26*, 7481–7503.

Mathieu, E., Lamirault, G., Toquet, C., Lhommet, P., Rederstorff, E., Sourice, S., … Lemarchand, P. (2012). Intramyocardial delivery of mesenchymal stem cell-seeded hydrogel preserves cardiac function and attenuates ventricular remodeling after myocardial infarction. *PLoS One*, *7*, e51991. https://doi.org/10.1371/journal.pone.0051991

McMurtrey, R. J. (2016). Analytic models of oxygen and nutrient diffusion, metabolism dynamics, and architecture optimization in three-dimensional tissue constructs with applications and insights in cerebral organoids. *Tissue Engineering Part C: Methods*, *22*, 221–249. https://doi.org/10.1089/ten.TEC.2015.0375

Merceron, C., Portron, S., Masson, M., Lesoeur, J., Fellah, B. H., Gauthier, O., … Vinatier, C. (2011). The effect of two- and three-dimensional cell culture on the chondrogenic potential of human adipose-derived mesenchymal stem cells after subcutaneous transplantation with an injectable hydrogel. *Cell Transplantation*, *20*, 1575–1588. https://doi.org/10.3727/096368910X557191

Merceron, C., Vinatier, C., Sophie, P., Martial, M., Amiaud, J., Guigand, L., … Guicheux, J. (2010). Differential effects of hypoxia on osteochondrogenic potential of human adipose-derived stem cells. *American Journal of Physiology. Cell Physiology*, *298*, 355–364. https://doi.org/10.1152/ajpcell.00398.2009

Mohyeldin, A., Garzón-Muvdi, T., & Quiñones-Hinojosa, A. (2010). Oxygen in stem cell biology: A critical component of the stem cell niche. *Cell Stem Cell*, *7*, 150–161. org/https://doi.org/10.1016/j.stem.2010.07.007

Pattappa, G., Heywood, H. K., de Bruijn, J. D., & Lee, D. A. (2011). The metabolism of human mesenchymal stem cells during proliferation and differentiation. *Journal of Cellular Physiology*, *226*, 2562–2570. https://doi.org/10.1002/jcp.22605

Peppas, N. A. (1986). *Hydrogels in medicine and pharmacy*. CRC Press.

Sachlos, E., & Czernuszka, J. T. (2003). Making tissue engineering scaffolds work. Review: The application of solid freeform fabrication technology to the production of tissue engineering scaffolds. *European Cells & Materials*, *5*, 29–40. https://doi.org/10.22203/eCM.v005a03

van Stroe-Biezen, S. A. M., Everaerts, F. M., Janssen, L. J. J., & Tacken, R. A. (1993). Diffusion coefficients of oxygen, hydrogen peroxide and glucose in a hydrogel. *Analytica Chimica Acta*, *273*, 553–560.

Suhaimi, H., Wang, S., Thornton, T., & Das, D. B. (2015). On glucose diffusivity of tissue engineering membranes and scaffolds. *Chemical Engineering Science*, *126*, 244–256. org/https://doi.org/10.1016/j.ces.2014.12.029

Trojani, C., Boukhechba, F., Scimeca, J.-C., Vandenbos, F., Michiels, J.-F., Daculsi, G., … Rochet, N. (2006). Ectopic bone formation using an injectable biphasic calcium phosphate/Si-HPMC hydrogel composite loaded with undifferentiated bone marrow stromal cells. *Biomaterials*, *27*, 3256–3264.

Trojani, C., Weiss, P., Michiels, J.-F., Vinatier, C., Guicheux, J., Daculsi, G., … Rochet, N. (2005). Three-dimensional culture and differentiation of human osteogenic cells in an injectable hydroxypropylmethylcellulose hydrogel. *Biomaterials*, *26*, 5509–5517.

Turczyn, R., Weiss, P., Lapkowski, M., & Daculsi, G. (2000). In situ self hardening bioactive composite for bone and dental surgery. *Journal of Biomaterials Science. Polymer Edition*, *11*, 217–223.

Valentin, J. E., Freytes, D. O., Grasman, J. M., Pesyna, C., Freund, J., Gilbert, T. W., & Badylak, S. F. (2009). Oxygen diffusivity of biologic and synthetic scaffold materials for tissue engineering. *Journal of Biomedical Materials Research - Part A*, *91*, 1010–1017. https://doi.org/10.1002/jbm.a.32328

Vinatier, C., Magne, D., Weiss, P., Trojani, C., Rochet, N., Carle, G. F., … Guicheux, J. (2005). A silanized hydroxypropyl methylcellulose hydrogel for the three-dimensional culture of chondrocytes. *Biomaterials*, *26*, 6643–6651.

Wise, D. L., & Houghton, G. (1966). The diffusion coefficients of ten slightly soluble gases in water at 10–60°C. *Chemical Engineering Science*, *21*, 999–1010.

SUPPORTING INFORMATION

Additional Supporting Information may be found online in the supporting information tab for this article.

Figure S1. 3D viability of 1 million hASCs/mL cultured in hydrogel of increasing Si-HPMC concentration. Scale bar: 100 μm.

Figure S2. 3D viability of increasing hASC densities cultured in 2% Si-HPMC hydrogel. Scale bar: 100 μm.

How to cite this article: Figueiredo L, Pace R, D'Arros C, et al. Assessing glucose and oxygen diffusion in hydrogels for the rational design of 3D stem cell scaffolds in regenerative medicine. *J Tissue Eng Regen Med*. 2018;1–9. https://doi.org/10.1002/term.2656

Discussion and conclusions

In vivo, stem cells are subject to a nutrient and oxygen gradient that is connected to their fate. [71] The same phenomena is to be expect in engineered constructs subject to static culture conditions, however depending on the cell density and dimensions of the construct, these gradients can be fatal [101].

Although Si-HPMC hydrogels are mainly constituted of water, which could favour solute diffusion, it was evidenced that high polymer concentrations impair oxygen diffusion. The glucose diffusion through the polysaccharide hydrogel was directly correlated to the average node distance of the polymer network while the same cannot be said for oxygen.

The insight given here into the oxygen diffusion properties of Si-HPMC can be used to tune a material to a specific niche. For example, if one is trying to encourage angiogenesis, a higher Si-HPMC percentage could be used to limit native oxygen diffusion. However, if one wishes to implant Si-HPMC *in vivo*, the maximum radius of the injected material can be determined before anoxia is reached.

The seeding of high cell densities resulted in oxygen depletion of the *in vitro* construct and seems to be linked to concomitant repercussions on cell viability. Although low oxygen tension may be desirable for the replication of the stem cell niche, complete extinction of oxygen in an *in vivo* construct has been associated with compromised cell viability. We hypothesized that the presence of cells may be acting as a diffusion oxygen barrier with low diffusivity of oxygen through cells.

These results suggest that in order to achieve a higher cell density, the issue of oxygen diffusion must be addressed. Higher ability of oxygen diffusion in the early stages of implantation could be achieved in less concentrated hydrogels, but that would mean sacrificing the mechanical proprieties of the construct. Knowing that in

vivo cells are usually found within 100 μm of a capillary, prevascularization or the addition of an oxygen carrier could be the answer for more concentrated hydrogels.

Chapter 4 – Quantification of the impact on oxygen diffusion and cell viability after the creation of a microchannel network inside stem cell constructs through bioprinting technique

Introduction

Thick constructs of hydrogel heavily seeded with stem cells have been shown to suffer from poor cell viability as described in Chapter 3 of this thesis. Large dimensions tissue engineered constructs are necessary for repairing large defects, or even replacing organs of the human body. In fact, tissue engineering represents a vast range of resources for the future of regenerative medicine through the re-creation of functional tissue units fit to replace or restore damaged tissue. However, limitations in the fabrication of complex and functional constructs still represent a big challenge in today's efforts. Nutrient diffusion and permeability has placed a barrier in the development of complex and clinical relevant dimensions constructs, making vascularization a strategic challenge for tissue engineering [102]. *In vivo* cells lie within a 200 μm radius from a capillary due to the diffusion limit of oxygen. In thick

constructs, cells located in the interior will to face hypoxia when implanted *in vivo* [103]. Besides being the natural answer to the diffusion limit, the vascularization of thick constructs, has also been associated with a pivotal role in governing tissue formation [104].

Various approaches were developed to address this challenge, from vasculogenesis and angiogenesis induction[105] to pre-vascularization [106] or vascular tissue microfabrication [107]. The incorporation of biomolecular cues or seeding of vascular-inducing cells in the scaffold requires a long time to establish a full functional vasculature. A different approach consists of 3D bioprinting multiple materials to build thick constructs with vascular-like networks through layer-by-layer deposition of bioink and a template sacrificial material. An important advantage of pre-vascularization over *in vivo* vascularization induction is the immediate perfusion of oxygen and nutrients bypassing the lag time to vascular-like networks to be formed.

In this chapter, a simple method to bioprint a complex thick structure is presented, using gelatin as a sacrificial ink and Si-HPMC as the bioink, where interconnected microchannels can be found within 300 µm of every cell present in the construct. The vascular-like constructs were perfused with a peristaltic pump, connected to the microchannels, creating flow of oxygen, nutrients and waste materials. A quantification of the oxygen levels in bioprinted constructs with perfusable microchannel networks is reported along with the consequences on cell viability. The work presented in this chapter is an approach to validate prevascularizarion as a means of increasing oxygen diffusion into large dimension hydrogels, seeded with high cell density. This approach has now been submitted for publication and can be found on the following pages under the title:

Article 3 - Quantifying oxygen levels in 3D bioprinted cell-laden thick constructs with perfusable microchannel networks

Quantifying oxygen levels in 3D bioprinted cell-laden thick constructs with perfusable microchannel networks

Lara Figueiredo[1,2,3], Catherine Le Visage[2,3], Pierre Weiss[2,3] and Jing Yang[1]

[1] Regenerative Medicine and Cellular Therapies Group, School of Pharmacy, University of Nottingham NG7 2RD, UK

[2] Inserm, UMR 1229, RMeS, Regenerative Medicine and Skeleton, Université de Nantes, ONIRIS, Nantes, F-44042, France

[3] Université de Nantes, UFR Odontologie, Nantes, 44042, France

Abstract

The survival and function of thick tissue engineered implanted constructs depends on pre-existing, embedded functional vascular-like structures, that are able to integrate with the host vasculature. Bioprinting has been employed to build perfusable vascular-like networks within thick constructs. However, the improvement of oxygen transportation facilitated by these vascular-like networks has not been directly quantified. Using an optical fiber oxygen sensor, we have measured the oxygen content at different positions within 3D bioprinted constructs with and without perfusable microchannel networks. Perfusion has been found to play an essential role in maintaining relatively high oxygen content in cell-laden constructs and consequently high cell viability. The concentration of oxygen changes following switching on and off the perfusion. Oxygen concentration depletes quickly after pausing perfusion, but recovers rapidly after resuming the perfusion. The quantification of oxygen levels within cell-laden hydrogel constructs could provide insight into channel network design and cellular responses.

Keywords: 3D bioprinting, microfluidics; microchannels; oxygen; hydrogel;

1. Introduction

Tissue engineering holds promise for the production of replacement tissues and organs to address the current shortage in donated organs [1][2]. However, the fabrication of complex and functional tissues/organs is still very challenging. One of the challenges is to fabricate a functional blood vessel network, that can integrate with the host to facilitate nutrient and oxygen transport [3][4]. Diffusion limit of oxygen *in vivo* is approximately 200 μm and cells have to reside within this distance from a capillary to survive [5][6]. Furthermore, the interactions between vascular promoting factors, endothelial cells and nerve cells have demonstrated that a microvascularization system helps innervation and tissue formation [7].

Various approaches including angiogenesis induction by growth factors [8] and engineered vascular-like perfusable networks [9] [10][11] have been developed to address the challenge of vascularisation. Growth factors such as vascular endothelial growth factor (VEGF) and basic fibroblast growth factor (bFGF) stimulate the recruitment of endothelial cells[12] and have been shown to improve vascularization after implantation of tissue engineered constructs [8]. However, this strategy requires a relatively long time to establish a fully functional vasculature. During this period the cells in the constructs rely on the diffusion of oxygen and nutrients from the host, which can comprise cell survival in thick constructs. The mass transportation before the establishment of a vasculature is limited, which suggests the requirement of prevascularisation [13]. An important advantage of pre-vascularization, over *in vivo* vascularization induction, is the immediate perfusion of oxygen and nutrients, bypassing the time-lag for vasculature to be formed [14]. 3D bioprinting has been employed to fabricate pre-vascularised tissue constructs, in which typically a bioink and a sacrificial material are co-printed to form construct. The sacrificial material is removed afterwards to make perfusable channel networks [10][15] .

Several elegant methods for 3D printing perfusable constructs with vascular-like microchannels have been reported. Miller et al. have produced a 3D carbohydrate lattice that was dissolved in media after matrix bulk embedding. For hepatocytes seeded constructs it was shown that the perfused construct with channels had sustained cellular metabolism when compared with gel slabs [9]. Thick constructs (>1 cm), integrating human mesenchymal stem cells (hMSCs), human neonatal dermal fibroblasts (hNDFs) and human umbilical vein endothelial cells (HUVECs), that were perfused for long durations (>6 weeks), have been assembled by coprinting multiple inks at ambient conditions. When actively perfused with osteogenic media, these vascularised cell-laden constructs showed significant higher level of calcium phosphate formation deep within the core, compared to avascular constructs [16].

The improvement of cell survival and function has been attributed to the increased transport of nutrients, oxygen and waste products. However, to our knowledge, the oxygen level in bioprinted cell seeded prevascularised constructs is yet to be quantified. Local oxygen quantification will serve as a measurement of the efficacy of the bioprinted channels. In this study, we selected silated-hydroxypropylmethylcellulose (Si-HPMC) hydrogel, a cellulose ether derivative, that has been used in cartilage [17], bone [18] tissue engineering and was demonstrated to be biocompatible [18] [19] [20]. Si-HPMC hydrogel crosslinking is promoted by pH neutralization, which makes it a good candidate for bioprinting as it is a cytocompatible process and has a printing time window of about 30 minutes during which the gel viscosity increases [21]. In modelling studies some reports found approximations of the oxygen diffusivity in acellular hydrogels equal to the diffusivity in water. However, previous characterization of the Si-HPMC has shown that these approximations do not apply for all types of hydrogels. Specifically, oxygen diffusivity in a hydrogel with 99% water and 1% Si-HPMC was 12.7% of that in water (2.7×10^{-9} m^2s-^1) [22], suggesting the importance of vascularization for constructs of large dimensions.

Herein, a thick structure with perfusable channels and cell-laden Si-HPMC was bioprinted. The oxygen levels within the 3D bioprinted constructs with perfusable channels was quantified, in the presence of cells, using an optical fiber oxygen

sensor. This is the first time, to the best of our knowledge, that oxygen concentrations in 3D bioprinted cell seeded constructs with an organized 3D channel architecture were quantified. Our findings show that microchannels alone are not sufficient to maintain sufficient oxygen levels and that perfusion is key for sustaining a high oxygen concentration and cell viability within the constructs.

2. Materials and methods

2.1. Solutions preparation

Hydroxypropylmethylcellulose (HPMC) E4M®, obtained from Colorcon (Kent, UK) was silanized in a process previously described to form Si-HPMC [23]. Si-HPMC polymer was dissolved in 0.2 M NaOH aqueous solution then dialyzed against a 0.09 M NaOH solution with a molecular weight cut off of 6-8 kDa. The viscous solution was autoclaved at 121℃ and kept at room temperature until usage. For the preparation of the hydrogel, one volume of 3 wt % Si-HPMC was mixed with half volume of acidic buffer to achieve a final concentration of 2% Si-HPMC and pH of 7.4. The acidic buffer consisted of a sterile 0.06M HCl solution with 1.8% NaCl (w/v) and 6.2% (w/v) HEPES (4-(2-hydroxyethyl) piperazine-1-ethanesulfonic acid). All products were obtained from Sigma (St. Louis, MO, USA).

A 6% (w/v) gelatin solution was prepared by dissolving gelatin (porcine skin, gel strength ~300 g Bloom (Sigma)) powder in PBS at 60℃ under agitation. After complete dissolution the solution was autoclaved at 121℃ and stored at 4℃ in aliquots.

2.2. Sheep primary cells culture

Sheep primary bone marrow stromal cells (sMSC) were expanded in complete medium which consists of αMEM,10% foetal bovine serum 1% antibiotic/antimycotic, 1% L-glutamine and 50 µg/mL ascorbic acid. Cells were cultured until 80% confluence and used between passages 2 and 5.

2.3. 3D bioprinting of constructs

Si-HPMC was mixed with the acidic buffer as described in 2.1 using two syringes connected by a Luer Lock. sMSC were trypsinized, centrifuged and the resulting pellet was resuspended in 100 µl of complete medium. 25 minutes after Si-HPMC neutralization 24 million sMSC were added to 3 mL of hydrogel with a micropipette without creating air bubbles. Cells were homogenized in the hydrogel through mixing in two syringes connected by a Luer Lock. The bioink (sMSC/Si-HPMC) was then transferred to a syringe barrel and printed with a 27 gauge needle at room temperature. For the bioprinting of constructs with microchannels gelatin 6% was co-printed through a 30 gauge needle at 10°C using a cooling system installed on the 3D printer (3DDiscovery, RegenHU, Switzerland). The two materials were printed in a glass round coverslip using the same extrusion 3D printer. The BioCAD software on the printer was used to design the 3D constructs with and without microchannels. For the bioprinting of the construct without microchannels only Si-HPMC was bioprinted in a total of 10 layers. For the bioprinting of the construct with microchannels the two bottom layers and the two top layers were composed of Si-HPMC only. Six intermediary layers combined Si-HPMC and gelatin materials. Si-HPMC strands were 0.6 mm wide and gelatine strands were 0.3 mm wide. For each intermediary layer, one layer of Si-HPMC and two superimposing layers of gelatin were printed with a total height of 0.4 mm per layer. Total dimensions of the constructs were 9x9x4 mm (length×width×height).

Constructs on top of coverslips were transferred to a Petri dish enclosed in a second adapted Petri dish that allowed the attachment of the adaptors of the perfusion tubbing into the channels when necessary.

2.4. Observation of printed micro-channels

Constructs with microchannels and without cells were embedded in OCT compound immediately after printing and frozen at 80 °C overnight. The frozen samples were cryosectioned at a thickness of 200 µm using a cryo-microtome (Leica CM1900). Cryosections were incubated at 37°C in PBS for total removal of gelatin.

Trypan blue was added to provide contrast and samples were observed with a Leica DM IRB microscope and photographs were taken with a QImaging QICAM camera.

2.5. Oxygen concentration measurements

Oxygen partial pressure in the 3D printed constructs was monitored at 24 hours, at different depths using a micromanipulator (Eppendorf TransferMan NK2, Germany), with a needle type oxygen microsensor (PreSens, Germany). The microsensor, a retractable 230 µm diameter optic fiber, allows real-time oxygen measurements, without oxygen consumption, through dynamic fluorescence quenching, with data reported to an Oxy-4 transmitter. Since oxygen diffusion is a temperature dependent phenomenon, all measurements were performed at 37°C.

2.6. Cell viability

Cell viability measurements were performed at day 0, 1, 7 and 14 using a Live & Dead assay kit (Invitrogen, USA). Briefly, hydrogels were washed twice with αMEM to remove esterase activity of the serum-supplemented growth medium, then incubated with 2µM calcein-AM solution and 4 µM Ethidium homodimer-1 in αMEM for 30 min at room temperature. Samples 500µm×500µm×200µm were then collected from the centre of the constructs and imaged at 3 different locations with a fluorescence microscope (Leica, GmbH, Germany). Images were analysed with ImageJ to count green and red cells. Results are presented as a percentage of live cells (mean value ± SEM, n=3 independent experiments).

2.7. Perfusion of the printed constructs

Gelatin was first removed by incubating the constructs at 37 °C for one hour in complete αMEM. Silicone tubing was connected through a 22 gauge needle to the inlet of the channel network guided through an in-house printed PCL adaptor. Constructs were immersed in culture medium that was pumped into the constructs using a peristaltic pump at a 500 µl/min rate (Watson-Marlow, UK). For the perfusion

cycles, the pump was stopped and the tubbing was kept attached, while performing oxygen continuous measurements, until oxygen levels reached stable readouts. The pump was reinitiated until initial oxygen levels were recovered.

3. Results

3.1. 3D printing and characterization of the perfusable constructs

Previous results showed that Si-HPMC hydrogel starts crosslinking after pH neutralisation, gel point occurs at 30 minutes [24] and crosslinking continues at room temperature during several hours. In this study, cells were mixed with the polymer solution 5 minutes before gel point to minimise mechanical shear stress. 3D printing was carried out using the bioink (sMSC/Si-HPMC) after the gelling point to form a stable construct with designed dimensions of 9×9×4 mm^3 (length×width×height).

Better printability was achieved by autoclaving gelatin at 120°C to reduce its molecular weight, turning it less brittle and thinner strands of gelatin could be printed at 10°C. The thermally reversible gelation of gelatin allowed for the removal of this material at 37°C which is convenient when working with cell seeded constructs [25].

The schematic representation in Figure 1A-C shows the design of microchannels embedded in cell-laden hydrogels. The construct was bioprinted layer-by-layer, with gelatin strands in subsequent layers being printed on top of the bioink strands, in order to avoid superimposing and conserve the integrity of the thick construct. Gelatin strands superimposed at a single point at the centre of the constructs to allow the connection of channels in all the layers.

After 3D printing, constructs were immersed in PBS for one hour at 37°C to remove the gelatin. The structure of the construct was not affected by the removal of gelatin, or by the large proportion of microchannels, as shown in Figure 1 D-E (before and after gelatin removal respectively). A construct cross section shows the distribution of microchannels within the 10-layer construct with six layers of microchannels (Figure 1G-H). It appears that some microchannels may have fused

together (Figure 1G and 1H). However, this could be due to deformation caused by the cryo-sectioning process and the thinness of the sectioned hydrogel slice.

In order to show that microchannels at all layers were interconnected, the construct was perfused with a dye solution. It was observed that the dye solution occupied all the volume of the hollow microchannels (MOVIE 1 can be found at https://tinyurl.com/ybtwmpsw), suggesting that there was no obstruction of microchannels and all channels were in fact interconnected.

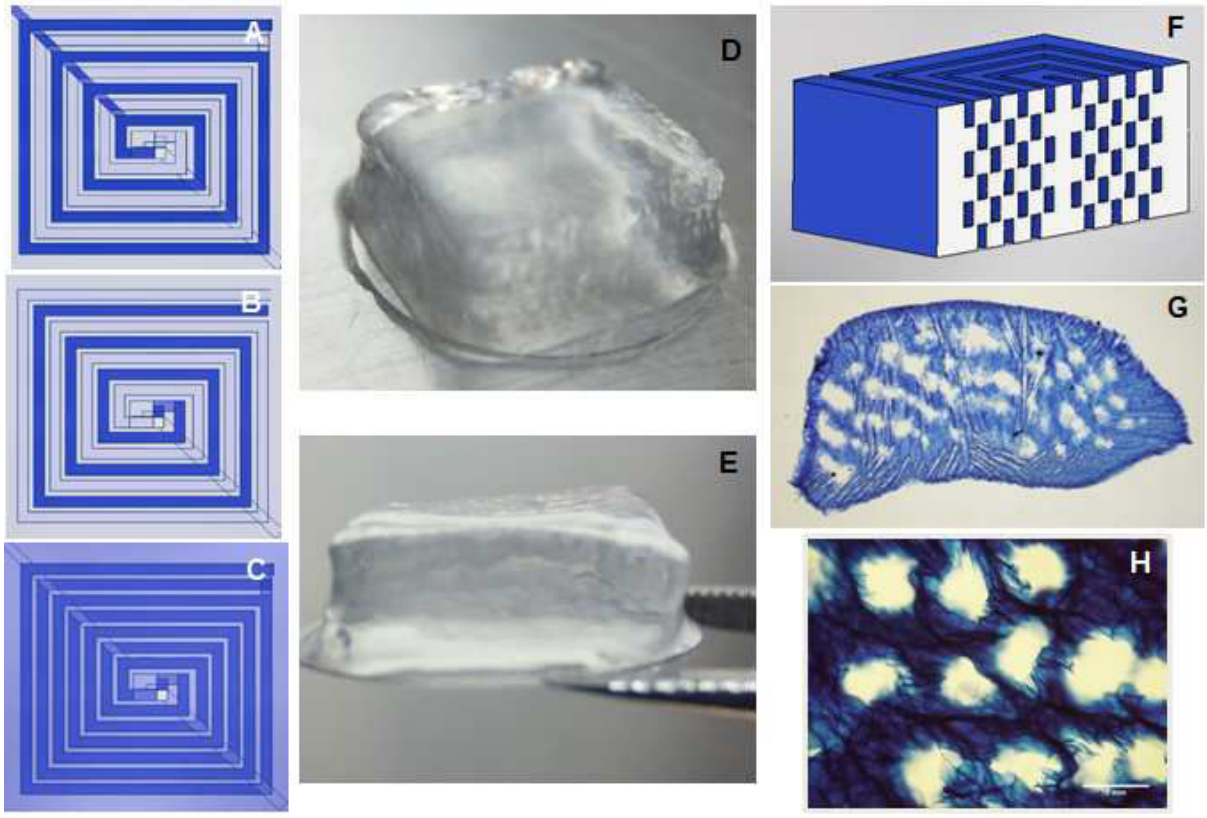

Figure 1 – 3D printed Si-HPMC constructs with microchannels. A) Design of the first of the odd layers of the construct, darker line represents gelatin printed strands, lighter lines represent Si-HPMC strands. B) Design of even layers of the construct. C) Representation of the top view of the construct morphology of the 3D bioprinted construct of cell-laden Si-HPMC. Printed constructs with microchannels D) before and E) after gelatin removal (9×9×4mm). F) Representation of a cross section of the channelled construct (without bottom and top Si-HPMC-only layers). G) Optical image of the transversal slice of the stained construct exhibiting microchannels after

gelatin removal. H) a zoomed-in part of the transversal slice. Si-HPMC: silanized hydroxypropylmethycellulose.

3.2. Oxygen diffusion in the different constructs

According to previous results, oxygen concentration at the centre of similar constructs without microchannels was shown to be reduced after 6 hours of incubation [22], at 24 hours differences were expected for the different types of constructs. After one day of incubation, oxygen concentration was measured at the top, middle and bottom levels of three types of constructs: bulk constructs without microchannels, channelled constructs with and without perfusion. Due to the loss in mass after gelatin microchannels evacuation, different constructs did not conserve the same measurements after incubation. In order to establish reference points for the comparison between constructs top, middle and bottom points were defined. Top was defined at the height were the oxygen sensor first touched the construct with the guidance of a micromanipulator. Bottom was defined as the point where oxygen sensor reached the surface where the construct was placed. The difference between top and bottom height was established as height of the construct. The middle was then calculated for each construct as the half the height. Replicated measurements were done in three central and independent points and always restarted from top to bottom, in order to exclude interference by oxygen consumption by the cells while measurements took place. All constructs were seeded at a cell density of 8 million cells/mL and all constructs were completely immersed in culture media except for the bottom side that was not directly exposed to the media. With a calculated 20% density of microchannels, it is not possible to distinguish between readings done with the oxygen sensor at the interior of the microchannels or at the interstitial space between the microchannels. In the absence of perfusion, oxygen concentration decreases from the top to the bottom of the constructs, independently of the presence of microchannels (Figure2). Without perfusion, bulk constructs showed similar oxygen concentrations at the three different positions compared to constructs with microchannels. With perfusion, the three positions at different heights showed similar high oxygen concentrations, suggesting the importance of perfusion for

effective mass transport. Oxygen concentrations in constructs with microchannels and perfusion were similar to that in stagnant pure media (18%±0.35).

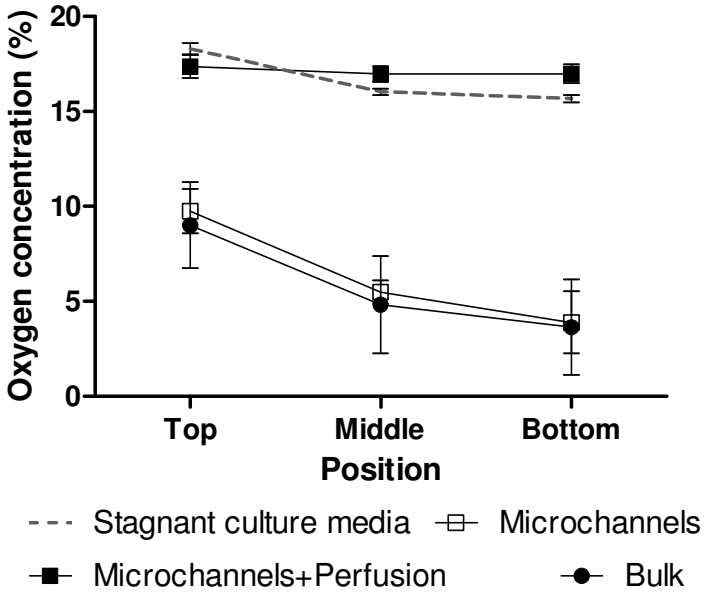

Figure 2: Oxygen levels at different heights of the constructs with and without perfusion, 24h after bioprinting of the constructs. "Microchannels" refers to the constructs with microchannels and without perfusion; "Microchannels+Perfusion" refers to the constructs with microchannels and perfusion; "Bulk" refers to the constructions without channels. All constructs were seeded with a cell density of 8 million cells/mL (n=3± SEM).

When perfusion was turned off an exponential drop in oxygen concentration took place. The oxygen concentration in the middle of the construct dropped approximately 5%, from 17% to 12% in less than 20 minutes (Figure 3). After perfusion resumed, the oxygen concentration recovered to 17% in 13 minutes on the first recovery and 16 minutes on the second recovery. The initial recovery was rapidly followed by a more graduate increase, as can be seen in the last part of the curve of the grey areas in Figure 3.

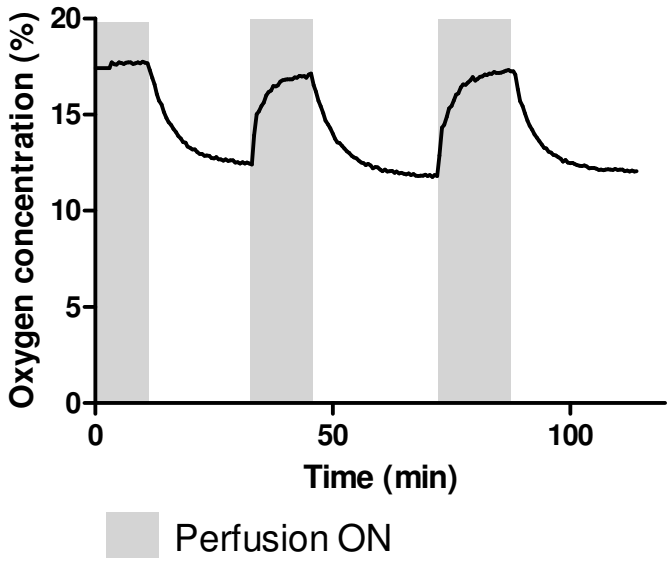

Figure 3: Oxygen concentration in the centre of a Si-HPMC 2% construct with microchannels seeded with a cell density of 8 million cells/mL and subject to perfusion cycles till recovery of oxygen concentration.

3.3. Cell viability

Cell viability was assessed at four different time points in samples recovered from the geometric centre of each cellular construct 9×9×4 mm^3 (length×width×height). Figure 4A shows that cell viability was between 76% and 71% immediately after bioprinting for the bulk constructs and constructs with microchannels, respectively. At day 1, cell viability at the centre of the bulk constructs was significantly lower than those in the construct with micro-channels and perfusion. However, there was no statistical difference between channelled constructs with and without perfusion. At day 7 and 14 the viabilities in constructs without perfusion dropped significantly compared to day 1. In contrast, the viability in perfused constructs steadily increased from day 1 to day 14, and was significantly higher than non-perfused constructs at day 7 and day 14.

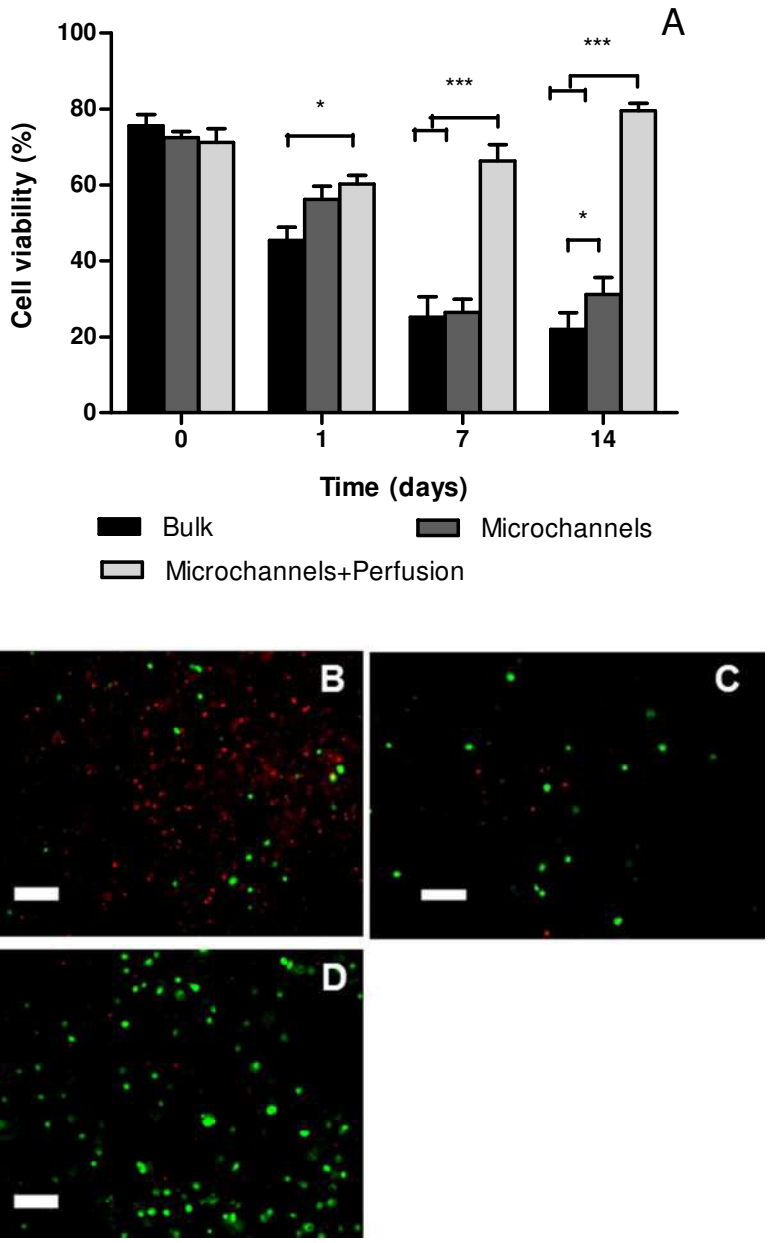

Figure 4 - Cell viability at the geometric centre of Si-HPMC 2% constructs 9×9×4 mm^3 (length×width×height) seeded with 8 million cells/mL was assessed with Live and Dead assay using confocal microscopy. A) Cell viability at 0, 1, 7 and 14 days after bioprinting. Values are means ± SEM (n=3). B-D: Confocal microscopy images of Live (green) and dead (red) cells in the centre of the constructs 14 days after bioprinting (B: Bulk construct; C: with microchannels; D: with microchannels and perfusion) (scale bar=100µm).

4. Discussion

The incorporation of vascular-like channels is expected to facilitate the transport of oxygen and nutrients in thick constructs. Although various approaches have been developed to prevascularize thick cell-laden constructs, as far as the authors know, the oxygen levels with these constructs have not been quantified before. One of the hydrogels used in our bioprinted perfusable constructs was Si-HPMC which is cyto and biocompatible as shown in previous works [18][20]. Being a self-setting hydrogel, Si-HPMC does not require UV curing, eliminating the low cell viability after repeated UV exposure required for 3D printing large-size constructs [26]. 2% Si-HPMC shows a gelling point 30 minutes after pH neutralization at room temperature, which allows a convenient time window for cell encapsulation under cytocompatible conditions before the gel becomes too viscosity for homogenous cell mixing. Previous work [22] has established that with a cell density 8M cells/mL in 2% Si-HPMC constructs, cell viability is reduced to less than 1% at 72 hours after seeding concomitantly with a complete depletion of oxygen in the centre of the constructs (10 mm high). Therefore, we selected this cell density in this study for comparison. The perfusion of micro-channels in the bioprinted thick constructs supported the survival of cells within the central region with an approximate cell viability of 80% after 14 days of culture, which demonstrated the importance of perfusion for maintaining cell viability in thick constructs.

The addition of layers of hydrogel+gelatin with no gaps to subsequent layers, provides a plane surface for the next layer, granting stability to the construct and no deformation was observed as in previous cases [27]. The high density of channels allows cells to be in close contact with perfused oxygen, not further than 300 µm.

Bulk constructs and constructs with microchannels without perfusion showed similar levels of oxygen. This shows that perfusion is necessary for the maintenance of oxygen levels in the cell-laden constructs. Simple diffusion of oxygen into thick constructs is not sufficient to compensate for the oxygen consumed by the cells at

high density. That the oxygen levels were not influenced by the presence of micro-channels in the absence of perfusion suggests the importance of connecting bioprinted perfusable constructs with the host's vasculature when grafting *in vivo*.

Conclusions:

Cellular constructs with embedded 3D interconnected micro-channel networks were successfully bioprinted using bone marrow stromal cell-laden Si-HPMC and sacrificial gelatin that can easily be removed at 37℃. Oxygen concentrations at different positions were measured in the cell-laden constructs with and without perfusable channels. We have shown that perfusion is key for maintaining a high oxygen concentration within the constructs. Without perfusion the oxygen concentration within channelled constructs was similar to that in solid constructs. When perfusion was turned off, the oxygen dropped 6% in less than 20 minutes and recovered 17% in 14 minutes after perfusion was turned on. The quantification of oxygen content in bioprinted perfusable constructs can help offer insight into the channel design and explain cellular responses.

ACKNOWLEDGEMENTS: L. Figueiredo is a recipient of an Erasmus Mundus Doctorate fellowship (Nanofar).

Bibliography

[1] R. Langer, J. Vacanti, Advances in tissue engineering, J. Pediatr. Surg. 51 (2016) 8–12. doi:10.1016/j.jpedsurg.2015.10.022.

[2] G. Orlando, K.J. Wood, R.J. Stratta, J.J. Yoo, A. Atala, S. Soker, Regenerative Medicine and Organ Transplantation: Past, Present, and Future, Transplantation. 91 (2011) 1310–1317. doi:10.1097/TP.0B013E318219EBB5.

[3] E.C. Novosel, C. Kleinhans, P.J. Kluger, Vascularization is the key challenge in tissue engineering, Adv. Drug Deliv. Rev. 63 (2011) 300–311. doi:10.1016/j.addr.2011.03.004.

[4] A. a Pezzulo, X.X. Tang, M.J. Hoegger, M.H.A. Alaiwa, S. Ramachandran, T.O. Moninger, P.H. Karp, C.L. Wohlford-, H.P. Haagsman, M. Van Eijk, B. Bánfi, A.R. Horswill, H. Hughes, J. Roy, L. a C. College, Building Vascular Networks, 487 (2013) 109–113. doi:10.1038/nature11130.Reduced.

[5] J. Rouwkema, N.C. Rivron, C.A. van Blitterswijk, Vascularization in tissue engineering, Trends Biotechnol. 26 (2008) 434–441. doi:10.1016/j.tibtech.2008.04.009.

[6] C. Maes, T. Kobayashi, M.K. Selig, S. Torrekens, S.I. Roth, S. Mackem, G. Carmeliet, H.M. Kronenberg, Osteoblast Precursors, but Not Mature Osteoblasts, Move into Developing and Fractured Bones along with Invading Blood Vessels, Dev. Cell. 19 (2010) 329–344. doi:10.1016/j.devcel.2010.07.010.

[7] T.L. Criswell, B.T. Corona, Z. Wang, Y. Zhou, G. Niu, Y. Xu, G.J. Christ, S. Soker, The role of endothelial cells in myofiber differentiation and the vascularization and innervation of bioengineered muscle tissue in vivo., Biomaterials. 34 (2013) 140–9. doi:10.1016/j.biomaterials.2012.09.045.

[8] S. Minardi, L. Pandolfi, F. Taraballi, X. Wang, E. De Rosa, Z.D. Mills, X. Liu, M. Ferrari, E. Tasciotti, Enhancing Vascularization through the Controlled Release of Platelet-Derived Growth Factor-BB, ACS Appl. Mater. Interfaces. 9 (2017) 14566–14575. doi:10.1021/acsami.6b13760.

[9] J.S. Miller, K.R. Stevens, M.T. Yang, B.M. Baker, D.-H.T. Nguyen, D.M. Cohen, E. Toro, A. a. Chen, P. a. Galie, X. Yu, R. Chaturvedi, S.N. Bhatia, C.S. Chen, Rapid casting of patterned vascular networks for perfusable engineered three-dimensional tissues, Nat. Mater. 11 (2012) 768–774. doi:10.1038/nmat3357.

[10] D.B. Kolesky, R.L. Truby, a. S. Gladman, T. a. Busbee, K. a. Homan, J. a. Lewis, 3D bioprinting of vascularized, heterogeneous cell-laden tissue constructs, Adv. Mater. 26 (2014) 3124–3130. doi:10.1002/adma.201305506.

[11] P. Datta, B. Ayan, I.T. Ozbolat, Bioprinting for vascular and vascularized tissue biofabrication, Acta Biomater. 51 (2017) 1–20. doi:10.1016/j.actbio.2017.01.035.

[12] H. Chu, Y. Wang, Therapeutic angiogenesis: controlled delivery of angiogenic factors, Ther. Deliv. 3 (2012) 693–714. doi:10.4155/tde.12.50.

[13] M.W. Laschke, M.D. Menger, Vascularization in tissue engineering: Angiogenesis versus inosculation, Eur. Surg. Res. 48 (2012) 85–92. doi:10.1159/000336876.

[14] J. Huling, I.K. Ko, A. Atala, J.J. Yoo, Fabrication of biomimetic vascular scaffolds for 3D tissue constructs using vascular corrosion casts, Acta Biomater. 32 (2016) 190–197. doi:10.1016/j.actbio.2016.01.005.

[15] S. Wust, R. Muller, S. Hofmann, 3D Bioprinting of complex channels-Effects of material, orientation, geometry, and cell embedding, J. Biomed. Mater. Res. - Part A. (2015) 2558–2570. doi:10.1002/jbm.a.35393.

[16] D.B. Kolesky, K.A. Homan, M.A. Skylar-Scott, J.A. Lewis, Three-dimensional bioprinting of thick vascularized tissues., Proc. Natl. Acad. Sci. U. S. A. 113 (2016) 3179–84. doi:10.1073/pnas.1521342113.

[17] C. Merceron, S. Portron, M. Masson, J. Lesoeur, B.H. Fellah, O. Gauthier, O. Geffroy, P. Weiss, J. Guicheux, C. Vinatier, The effect of two- and three-dimensional cell culture on the chondrogenic potential of human adipose-derived mesenchymal stem cells after subcutaneous transplantation with an injectable hydrogel., Cell Transplant. 20 (2011) 1575–88. doi:10.3727/096368910X557191.

[18] S. Laïb, B.H. Fellah, A. Fatimi, S. Quillard, C. Vinatier, O. Gauthier, P. Janvier, M. Petit, B. Bujoli, S. Bohic, P. Weiss, The in vivo degradation of a ruthenium labelled polysaccharide-based hydrogel for bone tissue engineering., Biomaterials. 30 (2009) 1568–77. doi:10.1016/j.biomaterials.2008.11.031.

[19] C. Vinatier, D. Magne, P. Weiss, C. Trojani, N. Rochet, G.F. Carle, C. Vignes-Colombeix, C. Chadjichristos, P. Galera, G. Daculsi, J. Guicheux, A silanized hydroxypropyl methylcellulose hydrogel for the three-dimensional culture of

chondrocytes., Biomaterials. 26 (2005) 6643–51. doi:10.1016/j.biomaterials.2005.04.057.

[20] E. Mathieu, G. Lamirault, C. Toquet, P. Lhommet, E. Rederstorff, S. Sourice, K. Biteau, P. Hulin, V. Forest, P. Weiss, J. Guicheux, P. Lemarchand, Intramyocardial delivery of mesenchymal stem cell-seeded hydrogel preserves cardiac function and attenuates ventricular remodeling after myocardial infarction., PLoS One. 7 (2012) e51991. doi:10.1371/journal.pone.0051991.

[21] A. Fatimi, J.-F. Tassin, R. Turczyn, M. a V Axelos, P. Weiss, Gelation studies of a cellulose-based biohydrogel: the influence of pH, temperature and sterilization., Acta Biomater. 5 (2009) 3423–32. doi:10.1016/j.actbio.2009.05.030.

[22] L. Figueiredo, R. Pace, C. D'Arros, G. Réthoré, J. Guicheux, C. Le Visage, P. Weiss, Assessing glucose and oxygen diffusion in hydrogels for the rational design of 3D stem cell scaffolds in regenerative medicine, J Tissue Eng Regen Med. 12 (2018) 1238–1246. doi:10.1002/term.2656.

[23] X. Bourges, P. Weiss, G. Daculsi, G. Legeay, Synthesis and general properties of silated-hydroxypropyl methylcellulose in prospect of biomedical use., Adv. Colloid Interface Sci. 99 (2002) 215–28. http://www.ncbi.nlm.nih.gov/pubmed/12509115.

[24] A. Fatimi, J.-F. Tassin, R. Turczyn, M. a V Axelos, P. Weiss, Gelation studies of a cellulose-based biohydrogel: the influence of pH, temperature and sterilization., Acta Biomater. 5 (2009) 3423–32. doi:10.1016/j.actbio.2009.05.030.

[25] W. Lee, V. Lee, S. Polio, P. Keegan, J.H. Lee, K. Fischer, J.K. Park, S.S. Yoo, On-demand three-dimensional freeform fabrication of multi-layered hydrogel scaffold with fluidic channels, Biotechnol. Bioeng. 105 (2010) 1178–1186. doi:10.1002/bit.22613.

[26] P. Mistry, A. Aied, M. Alexander, K. Shakesheff, A. Bennett, J. Yang, Bioprinting Using Mechanically Robust Core-Shell Cell-Laden Hydrogel Strands, Macromol. Biosci. 201600472 (2017) 1–8.

doi:10.1002/mabi.201600472.

[27] W. Jia, P.S. Gungor-Ozkerim, Y.S. Zhang, K. Yue, K. Zhu, W. Liu, Q. Pi, B. Byambaa, M.R. Dokmeci, S.R. Shin, A. Khademhosseini, Direct 3D bioprinting of perfusable vascular constructs using a blend bioink, Biomaterials. 106 (2016). doi:10.1016/j.biomaterials.2016.07.038.

Discussion and conclusions

The constitution of channels is expected to facilitate the diffusion of oxygen and nutrients in thick constructs but up to the moment of this work, the impact on oxygen levels had not been measured. Perfusable constructs were printed with Si-HPMC, a biocompatible hydrogel suitable for cell encapsulation as shown in previous work [14][108]. As a self-setting hydrogel, Si-HPMC does not require UV curing, eliminating size restrictions posed by the low permeation depth in tissue. Si-HPMC also offers tunable mechanical properties by variation of the polymer concentration as shown in Chapter 3. In the same Chapter, the limiting cell density in thick constructs (10 mm height) was established to be 8M cells/mL, resulting in cell death and complete depletion of oxygen in the centre of the constructs. With perfusion through microchannels in thick constructs an impact in the viability of cells was achieved, at 8M cells/mL the viability was around 80% after 14 days of culture.

To our knowledge this is the first data representing the oxygen levels in constructs with different types of oxygenations. The oxygen levels were not indeed influenced by the presence of microchannels in the absence of perfusion, highlighting the importance of a connection with the host's vasculature when grafting *in vivo*. Both constructs without perfusion have similar levels of oxygen even when the inner construct is transversed with microchannels. This means that perfusion is necessary for the maintenance of oxygen levels in the construct seeded with cells and that

simple diffusion of oxygen in the media is not sufficient to compensate for the oxygen consumption by the cells.

General discussion

Oxygen and nutrient diffusion is a major concern in tissue engineering and large dimension scaffolds. Hydrogel composites are desirable in tissue engineering to maintain the high water content provided by the hydrogel while enhancing its mechanical properties with other biocompatible and biodegradable materials.

The work described in Chapter 2 allowed to establish that the oxygen diffusion is not impaired by the reinforcement of Si-HPMC hydrogel with laponites. These findings are important especially for future work being done on the mimicking cartilage since the described constructs had similar mechanical properties.

How increasing polymer concentration of Si-HPMC would affect oxygen diffusion and cell viability was the next chosen subject in an effort to characterize diffusion in biomaterials with different mechanical properties to be used as stem cell niches. Although Si-HPMC hydrogels are mainly constituted of water, which could favour solute diffusion, it was evidenced that high polymer concentrations impair oxygen diffusion. The glucose diffusion through the polysaccharide hydrogel was directly correlated to the average node distance of the polymer network while the same cannot be said for oxygen.

The insight given in Chapter 3 into the oxygen diffusion properties of Si-HPMC can be used to tune a material to a specific niche. For example, if one is trying to encourage angiogenesis, a higher Si-HPMC percentage could be used to limit native oxygen diffusion. However, if one wishes to implant Si-HPMC *in vivo*, the maximum radius of the injected material can be determined before anoxia is reached.

The seeding of high cell densities resulted in oxygen depletion of the *in vitro* construct and seems to be linked to concomitant repercussions on cell viability. Although low oxygen tension may be desirable for the replication of the stem cell niche, complete extinction of oxygen in an *in vivo* construct has been associated with compromised cell viability. We hypothesized that the presence of cells may be acting as a diffusion oxygen barrier with low diffusivity of oxygen through cells.

Results in Chapter 3 suggested that in order to achieve a higher cell density, the issue of oxygen diffusion must be addressed. Higher ability of oxygen diffusion in the early stages of implantation could be achieved in less concentrated hydrogels, but that would mean sacrificing the mechanical proprieties of the construct. Knowing that in vivo cells are usually found within 100 μm of a capillary, prevascularization or the addition of an oxygen carrier could be the answer for more concentrated hydrogels

The constitution of channels was expected to facilitate the diffusion of oxygen and nutrients in thick constructs and the impact on oxygen levels was revealed in Chapter 4. Perfusable constructs were printed with Si-HPMC, an hydrogel suitable for cell encapsulation and biocompatible as shown in previous work [14][108]. As a self-setting hydrogel, Si-HPMC does not require UV curing, eliminating size restrictions posed by the low permeation depth in tissue. Si-HPMC also offers tunable mechanical properties by variation of the polymer concentration as shown in Chapter 3. In the same Chapter, the limiting cell density in thick constructs (10 mm in height) was established to be 8M cells/mL, resulting in cell death and complete depletion of oxygen in the centre of the constructs. With perfusion of microchannels in thick constructs an impact in the viability of cells was achieved, the viability of a cell density of 8M cells/mL was around 80% after 14 days of culture.

To our knowledge this is the first data representing the oxygen levels in constructs with different types of oxygenations. The oxygen levels were not indeed influenced by the presence of microchannels in the absence of perfusion, highlighting the importance of a connection with the host's vasculature when grafting *in vivo*. Both constructs without perfusion have similar levels of oxygen even when the inner construct is transversed with microchannels. This means that perfusion is necessary for the maintenance of oxygen levels in the construct seeded with cells and that simple diffusion of oxygen in the media is not sufficient to compensate for the oxygen consumption by the cells.

Conclusions and perspectives

The three main objectives of this thesis were achieved in three corresponding chapters. In Chapter 2, it was demonstrated that the addition of XLG laponite to Si-HPMC hydrogels increases the mechanical properties without interfering with the O_2 diffusion and cell viability. Laponites self-assembling capacity allows the formation of a hybrid interpenetrated network that enhances the stiffness of the hydrogel. In the future, the faster gelling composite hydrogel should be evaluated in large animal models. This experiment will allow the evaluation of the preservation of the material inside a cartilage defect as well as the clinical relevance of these composites.

Despite being more than 95% water, in Chapter 3 it was demonstrated that Si-HPMC hydrogels have heavily restricted nutrient diffusion properties. The glucose diffusion through the polysaccharide hydrogel was directly correlated to the average node distance of the polymer network while the same cannot be said for oxygen. The diffusion of oxygen was suspected to be the limiting factor of cell viability in Si-HPMC hydrogels. The oxygen concentration inside of cellularized hydrogels was more dependent on cell density than on polymer concentration. Populating low polymer concentration constructs with cells resulted in high cell viability, but mechanical properties were sacrificed. On the other hand, high cell density resulted in a fatal

deficiency of nutrients leading further studies to be directed to enhancing oxygen and nutrient diffusion in these constructs. Overall, these experiments provided us with useful insights for the development of future cellular microenvironments based on Si-HPMC hydrogels or similar polysaccharide hydrogels. Additionally, this method can be readily extended to analyzing nutrient delivery and gas exchange in a variety of material hydrogels for regenerative medicine applications.

Chapter 4 was dedicated to the quantification of the impact on oxygen diffusion and cell viability after the creation of a microchannels network inside stem cell constructs through bioprinting technique. Cellular constructs with embedded 3D interconnected micro-channel networks were successfully bioprinted using bone marrow stromal cell-laden Si-HPMC and a sacrificial gelatin that can easily be removed at 37℃. Oxygen concentrations at different positions were measured in the cell-laden constructs with and without perfusable channels. In this chapter it was shown that perfusion is key for maintaining a high oxygen concentration within the constructs. Without perfusion the oxygen concentration within channelled constructs was similar to that in solid constructs. When perfusion was turned off, the oxygen dropped by 6% in less than 20 minutes and recovered by 17% in 14 minutes after perfusion was turned on again. The quantification of oxygen content in bioprinted perfusable constructs can help offer insight into the channel design and explain cellular responses.

Bibliography

[1] R. Langer and J. P. Vacanti, “Tissue Engineering,” *Science (80-.).*, vol. 260, no. May, pp. 920–926, 1993.

[2] R. Katari, A. Peloso, and G. Orlando, “Tissue Engineering and Regenerative Medicine: Semantic Considerations for an Evolving Paradigm,” *Front. Bioeng. Biotechnol.*, vol. 2, no. January, pp. 1–6, 2015.

[3] M. N. Collins and C. Birkinshaw, “Hyaluronic acid based scaffolds for tissue engineering--a review,” *Carbohydr. Polym.*, vol. 92, no. 2, pp. 1262–79, Feb. 2013.

[4] J. A. Matthews, G. E. Wnek, A. David G. Simpson, and G. L. Bowlin, “Electrospinning of Collagen Nanofibers,” 2002.

[5] L. P. Yan, Y. J. Wang, L. Ren, G. Wu, S. G. Caridade, J. B. Fan, L. Y. Wang, P. H. Ji, J. M. Oliveira, J. T. Oliveira, J. F. Mano, and R. L. Reis, “Genipin-cross-linked collagen/chitosan biomimetic scaffolds for articular cartilage tissue engineering applications,” *J. Biomed. Mater. Res. - Part A*, vol. 95 A, no. 2, pp. 465–475, 2010.

[6] M. Xu, X., Jha, A, Harrington, DA., Farach-Carson, “Hyaluronic Acid - Based Hydrogel: from a Natural Polysaccharide to Complex Networks,” *Soft Matter*,

vol. 8, no. 12, pp. 3280–3294, 2012.

[7] L. Ouyang, C. B. Highley, C. B. Rodell, W. Sun, and J. A. Burdick, “3D Printing of Shear-Thinning Hyaluronic Acid Hydrogels with Secondary Cross-Linking,” *ACS Biomater. Sci. Eng.*, vol. 2, no. 10, pp. 1743–1751, Oct. 2016.

[8] Z. Li, H. R. Ramay, K. D. Hauch, D. Xiao, and M. Zhang, “Chitosan–alginate hybrid scaffolds for bone tissue engineering,” *Biomaterials*, vol. 26, no. 18, pp. 3919–3928, Jun. 2005.

[9] J. Venkatesan, I. Bhatnagar, P. Manivasagan, K.-H. Kang, and S.-K. Kim, “Alginate composites for bone tissue engineering: A review,” *Int. J. Biol. Macromol.*, vol. 72, pp. 269–281, Jan. 2015.

[10] F. Croisier and C. Jérôme, “Chitosan-based biomaterials for tissue engineering,” *Eur. Polym. J.*, vol. 49, no. 4, pp. 780–792, 2013.

[11] V. K. Lee and G. Dai, “Printing of Three-Dimensional Tissue Analogs for Regenerative Medicine,” *Ann. Biomed. Eng.*, no. 45, pp. 115–131, 2016.

[12] R. Turczyn, P. Weiss, M. Lapkowski, and G. Daculsi, “In situ self hardening bioactive composite for bone and dental surgery.,” *J. Biomater. Sci. Polym. Ed.*, vol. 11, no. 2, pp. 217–23, 2000.

[13] C. Merceron, S. Portron, M. Masson, J. Lesoeur, B. H. Fellah, O. Gauthier, O. Geffroy, P. Weiss, J. Guicheux, and C. Vinatier, “The effect of two- and three-dimensional cell culture on the chondrogenic potential of human adipose-derived mesenchymal stem cells after subcutaneous transplantation with an injectable hydrogel.,” *Cell Transplant.*, vol. 20, no. 10, pp. 1575–88, 2011.

[14] S. Laïb, B. H. Fellah, A. Fatimi, S. Quillard, C. Vinatier, O. Gauthier, P. Janvier, M. Petit, B. Bujoli, S. Bohic, and P. Weiss, “The in vivo degradation of a ruthenium labelled polysaccharide-based hydrogel for bone tissue engineering.,” *Biomaterials*, vol. 30, no. 8, pp. 1568–77, Mar. 2009.

[15] A. Alajati, A. M. Laib, H. Weber, A. M. Boos, A. Bartol, K. Ikenberg, T. Korff, H. Zentgraf, C. Obodozie, R. Graeser, S. Christian, G. Finkenzeller, G. B. Stark, M. Héroult, and H. G. Augustin, “Spheroid-based engineering of a human

vasculature in mice.," *Nat. Methods*, vol. 5, no. 5, pp. 439–445, 2008.

[16] M. Mousa, N. D. Evans, R. O. C. Oreffo, and J. I. Dawson, "Clay nanoparticles for regenerative medicine and biomaterial design: A review of clay bioactivity," *Biomaterials*, vol. 159, pp. 204–214, 2018.

[17] C. Boyer, L. Figueiredo, R. Pace, J. Lesoeur, T. Rouillon, C. Le Visage, J. F. Tassin, P. Weiss, J. Guicheux, and G. Rethore, "Laponite nanoparticle-associated silated hydroxypropylmethyl cellulose as an injectable reinforced interpenetrating network hydrogel for cartilage tissue engineering," *Acta Biomater.*, vol. 65, pp. 112–122, 2017.

[18] P. Gentile, V. Chiono, I. Carmagnola, and P. V Hatton, "An Overview of Poly (lactic- co -glycolic) Acid (PLGA) -Based Biomaterials for Bone Tissue Engineering," pp. 3640–3659, 2014.

[19] J. K. Park, J.-H. Shim, K. S. Kang, J. Yeom, H. S. Jung, J. Y. Kim, K. H. Lee, T.-H. Kim, S.-Y. Kim, D.-W. Cho, and S. K. Hahn, "Solid Free-Form Fabrication of Tissue-Engineering Scaffolds with a Poly(lactic-co-glycolic acid) Grafted Hyaluronic Acid Conjugate Encapsulating an Intact Bone Morphogenetic Protein-2/Poly(ethylene glycol) Complex," *Adv. Funct. Mater.*, vol. 21, no. 15, pp. 2906–2912, Aug. 2011.

[20] J. Y. Kim and D. W. Cho, "Blended PCL/PLGA scaffold fabrication using multi-head deposition system," *Microelectron. Eng.*, vol. 86, no. 4–6, pp. 1447–1450, 2009.

[21] L. Ruiz-Cantu, A. Gleadall, C. Faris, J. Segal, K. Shakesheff, and J. Yang, "Characterisation of the surface structure of 3D printed scaffolds for cell infiltration and surgical suturing," *Biofabrication*, vol. 8, no. 1, p. 015016, 2016.

[22] J. Huling, I. K. Ko, A. Atala, and J. J. Yoo, "Fabrication of biomimetic vascular scaffolds for 3D tissue constructs using vascular corrosion casts," *Acta Biomater.*, vol. 32, pp. 190–197, 2016.

[23] S. J. Morrison and A. C. Spradling, "Stem Cells and Niches: Mechanisms That Promote Stem Cell Maintenance throughout Life," *Cell*, vol. 132, no. 4, pp. 598–611, 2008.

[24] F. M. Watt and R. R. Driskell, “The therapeutic potential of stem cells,” *Philos. Trans. R. Soc. London. Ser. B Biol. Sci.*, vol. 365, no. 1537, pp. 155–163, 2010.

[25] A. E. Omole and A. O. J. Fakoya, “Ten years of progress and promise of induced pluripotent stem cells: historical origins, characteristics, mechanisms, limitations, and potential applications.,” *PeerJ*, vol. 6, p. e4370, 2018.

[26] F. H. Bach, R. J. Albertini, P. Joo, J. L. Anderson, and M. M. Bortin, “Bone-marrow transplantation in a patient with the Wiskott-Aldrich syndrome.,” *Lancet (London, England)*, vol. 2, no. 7583, pp. 1364–6, Dec. 1968.

[27] Y. L. Han, S. Wang, X. Zhang, Y. Li, G. Huang, H. Qi, B. Pingguan-Murphy, Y. Li, T. J. Lu, and F. Xu, “Engineering physical microenvironment for stem cell based regenerative medicine,” *Drug Discovery Today*, vol. 19, no. 6. pp. 763–73, 2014.

[28] N. Kim and S.-G. Cho, “Clinical applications of mesenchymal stem cells.,” *Korean J. Intern. Med.*, vol. 28, no. 4, pp. 387–402, 2013.

[29] A. J. Engler, S. Sen, H. L. Sweeney, and D. E. Discher, “Matrix elasticity directs stem cell lineage specification.,” *Cell*, vol. 126, no. 4, pp. 677–89, Aug. 2006.

[30] R. Schofield, “The relationship between the spleen colony-forming cell and the haemopoietic stem cell.,” *Blood Cells*, vol. 4, no. 1–2, pp. 7–25, 1978.

[31] E. Fuchs, T. Tumbar, and G. Guasch, “Socializing with the Neighbors : Stem Cells and Their Niche,” vol. 116, pp. 769–778, 2004.

[32] P. Davy and R. Allsopp, “Adult Stem Cells,” *DNA Repair (Amst).*, pp. 203–223, 2011.

[33] S. W. Lane, D. T. Scadden, and D. G. Gilliland, “The leukemic stem cell niche: current concepts and therapeutic opportunities.,” *Blood*, vol. 114, no. 6, pp. 1150–7, Aug. 2009.

[34] J. L. Wilson and T. C. McDevitt, *Chapter 22 – Biofunctional Hydrogels for Three-Dimensional Stem Cell Culture*. Elsevier Inc., 2017.

[35] R. Peerani, B. M. Rao, C. Bauwens, T. Yin, G. A. Wood, A. Nagy, E.

Kumacheva, and P. W. Zandstra, “Niche-mediated control of human embryonic stem cell self-renewal and differentiation,” *EMBO J.*, vol. 26, no. 22, pp. 4744–4755, 2007.

[36] N. Brandenberg and M. P. Lutolf, *Chapter 27 - Employing Microfluidic Devices to Induce Concentration Gradients A2 - Vishwakarma, Ajaykumar*. Elsevier Inc., 2017.

[37] D. A Brafman, “Bioengineering of Stem Cell Microenvironments Using High-Throughput Technologies,” *J. Bioeng. Biomed. Sci.*, vol. s5, p. , Feb. 2011.

[38] X. Yin, B. E. Mead, H. Safaee, R. Langer, J. M. Karp, and O. Levy, “Engineering Stem Cell Organoids,” *Cell Stem Cell*, vol. 18, no. 1, pp. 25–38, 2016.

[39] S. M. Dellatore, A. S. Garcia, and W. M. Miller, “Mimicking Stem Cell Niches to Increase Stem Cell Expansion,” *October*, vol. 19, no. 5, pp. 534–540, 2009.

[40] R. Peerani and P. W Zandstra, “Review series Enabling stem cell therapies through synthetic stem cell – niche engineering,” *Strategies*, vol. 120, no. 1, pp. 60–70, 2010.

[41] S. W. Crowder, V. Leonardo, T. Whittaker, P. Papathanasiou, and M. M. Stevens, “Material Cues as Potent Regulators of Epigenetics and Stem Cell Function,” *Cell Stem Cell*, vol. 18, no. 1, pp. 39–52, 2016.

[42] M. P. Lutolf, P. M. Gilbert, and H. M. Blau, “Designing materials to direct stem-cell fate.,” *Nature*, vol. 462, no. 7272, pp. 433–41, Nov. 2009.

[43] F. Gattazzo, A. Urciuolo, and P. Bonaldo, “Extracellular matrix: A dynamic microenvironment for stem cell niche,” *Biochim. Biophys. Acta - Gen. Subj.*, vol. 1840, no. 8, pp. 2506–2519, 2014.

[44] J. Barthes, H. Özçelik, M. Hindié, A. Ndreu-Halili, A. Hasan, and N. E. Vrana, “Cell microenvironment engineering and monitoring for tissue engineering and regenerative medicine: the recent advances.,” *Biomed Res. Int.*, vol. 2014, p. 921905, 2014.

[45] F. M. Watt and W. T. S. Huck, “Role of the extracellular matrix in regulating

stem cell fate," *Nat. Publ. Gr.*, vol. 14, no. 8, pp. 467–473, 2013.

[46] J. D. Humphrey, E. R. Dufresne, M. A. Schwartz, N. Haven, N. Haven, N. Haven, and N. Haven, "Mechanotransduction and extracellular matrix homeostasis Jay," *Nat Rev Mol Cell Biol.*, vol. 15, no. 12, pp. 802–812, 2015.

[47] P. M. Gilbert, K. L. Havenstrite, K. E. G. Magnusson, A. Sacco, N. A. Leonardi, P. Kraft, N. K. Nguyen, S. Thrun, M. P. Lutolf, and H. M. Blau, "Substrate elasticity regulates skeletal muscle stem cell self-renewal in culture.," *Science*, vol. 329, no. 5995, pp. 1078–81, Aug. 2010.

[48] J. R. Tse and A. J. Engler, "Stiffness gradients mimicking in vivo tissue variation regulate mesenchymal stem cell fate," *PLoS One*, vol. 6, no. 1, 2011.

[49] N. Huebsch, P. R. Arany, A. S. Mao, D. Shvartsman, O. a Ali, S. a Bencherif, J. Rivera-feliciano, and D. J. Mooney, "NIH Public Access," vol. 9, no. 6, pp. 518–526, 2010.

[50] O. Jeon, D. S. Alt, S. W. Linderman, and E. Alsberg, "Biochemical and Physical Signal Gradients in Hydrogels to Control Stem Cell Behavior," *Adv. Mater.*, vol. 25, no. 44, pp. 6366–6372, Nov. 2013.

[51] F. R. Maia, K. B. Fonseca, G. Rodrigues, P. L. Granja, and C. C. Barrias, "Matrix-driven formation of mesenchymal stem cell-extracellular matrix microtissues on soft alginate hydrogels," *Acta Biomater.*, vol. 10, no. 7, pp. 3197–3208, 2014.

[52] O. Chaudhuri, L. Gu, D. Klumpers, M. Darnell, A. Sidi, J. C. Weaver, N. Huebsch, H. Lee, E. Lippens, G. N. Duda, and D. J. Mooney, "and Activity," vol. 15, no. 3, pp. 326–334, 2016.

[53] K. M. Mabry, S. Z. Payne, and K. S. Anseth, "Microarray analyses to quantify advantages of 2D and 3D hydrogel culture systems in maintaining the native valvular interstitial cell phenotype," *Biomaterials*, vol. 74, pp. 31–41, Jan. 2016.

[54] B. M. Baker and C. S. Chen, "Deconstructing the third dimension - how 3D culture microenvironments alter cellular cues," *J. Cell Sci.*, vol. 125, no. 13, pp. 3015–3024, 2012.

[55] H. Tanaka, C. L. Murphy, C. Murphy, M. Kimura, S. Kawai, and J. M. Polak, “Chondrogenic differentiation of murine embryonic stem cells: Effects of culture conditions and dexamethasone,” *J. Cell. Biochem.*, vol. 93, no. 3, pp. 454–462, Oct. 2004.

[56] A. W. Lund, B. Yener, J. P. Stegemann, and G. E. Plopper, “The natural and engineered 3D microenvironment as a regulatory cue during stem cell fate determination.,” *Tissue Eng. Part B. Rev.*, vol. 15, no. 3, pp. 371–80, Sep. 2009.

[57] M. J. Dalby, N. Gadegaard, and R. O. C. Oreffo, “Harnessing nanotopography and integrin–matrix interactions to influence stem cell fate,” *Nat. Mater.*, vol. 13, no. 6, pp. 558–569, May 2014.

[58] R. Keller, “Cell migration during gastrulation.,” *Curr. Opin. Cell Biol.*, vol. 17, no. 5, pp. 533–41, Oct. 2005.

[59] S. D. Subramony, B. R. Dargis, M. Castillo, E. U. Azeloglu, M. S. Tracey, A. Su, and H. H. Lu, “The guidance of stem cell differentiation by substrate alignment and mechanical stimulation,” *Biomaterials*, vol. 34, no. 8, pp. 1942–1953, Mar. 2013.

[60] D. F. Ward Jr., R. M. Salasznyk, R. F. Klees, J. Backiel, P. Agius, K. Bennett, A. Boskey, and G. E. Plopper, “Mechanical Strain Enhances Extracellular Matrix-Induced Gene Focusing and Promotes Osteogenic Differentiation of Human Mesenchymal Stem Cells Through an Extracellular-Related Kinase-Dependent Pathway,” *Stem Cells Dev.*, vol. 16, no. 3, pp. 467–480, Jun. 2007.

[61] S. Oh, K. S. Brammer, Y. S. J. Li, D. Teng, A. J. Engler, S. Chien, and S. Jin, “Stem cell fate dictated solely by altered nanotube dimension.,” *Proc. Natl. Acad. Sci. U. S. A.*, vol. 106, no. 7, pp. 2130–5, Feb. 2009.

[62] F. Zamani, M. Amani-Tehran, M. Latifi, M. A. Shokrgozar, and A. Zaminy, “Promotion of spinal cord axon regeneration by 3D nanofibrous core-sheath scaffolds,” *J. Biomed. Mater. Res. Part A*, vol. 102, no. 2, pp. 506–513, Feb. 2014.

[63] M. a Schwartz and C. S. Chen, “Deconstructing Dimensionality,” *Science (80-.*

)., vol. 339, no. 6118, pp. 402–404, 2013.

[64] D. M. Brunette, “The effects of implant surface topography on the behavior of cells.,” *Int. J. Oral Maxillofac. Implants*, vol. 3, no. 4, pp. 231–46, 1988.

[65] E. T. den Braber, J. E. de Ruijter, L. A. Ginsel, A. F. von Recum, and J. A. Jansen, “Orientation of ECM protein deposition, fibroblast cytoskeleton, and attachment complex components on silicone microgrooved surfaces.,” *J. Biomed. Mater. Res.*, vol. 40, no. 2, pp. 291–300, May 1998.

[66] P. Viswanathan, M. Guvendiren, W. Chua, S. B. Telerman, K. Liakath-Ali, J. A. Burdick, and F. M. Watt, “Mimicking the topography of the epidermal–dermal interface with elastomer substrates,” *Integr. Biol.*, vol. 8, no. 1, pp. 21–29, 2016.

[67] J. T. Connelly, J. E. Gautrot, B. Trappmann, D. W.-M. Tan, G. Donati, W. T. S. Huck, and F. M. Watt, “Actin and serum response factor transduce physical cues from the microenvironment to regulate epidermal stem cell fate decisions.,” *Nat. Cell Biol.*, vol. 12, no. 7, pp. 711–718, 2010.

[68] D. D. and K. J. L. B. Erik Bland, “Overcoming hypoxia to improve tissue-engineering approaches to regenerative medicine,” *J. Tissue Eng. Regen. Med.*, vol. 4, no. 7, pp. 505–514, 2013.

[69] S. Tan and N. Barker, “Engineering the niche for stem cells.,” *Growth Factors*, vol. 31, no. 6, pp. 175–84, 2013.

[70] M. V. Gómez-Gaviro, R. Lovell-Badge, F. Fernández-Avilés, and E. Lara-Pezzi, “The vascular stem cell niche,” *J. Cardiovasc. Transl. Res.*, vol. 5, no. 5, pp. 618–630, 2012.

[71] A. Mohyeldin, T. Garzón-Muvdi, and A. Quiñones-Hinojosa, “Oxygen in stem cell biology: a critical component of the stem cell niche,” *Cell Stem Cell*, vol. 7, no. 2, pp. 150–61, Aug. 2010.

[72] J. Malda, J. Rouwkema, D. E. Martens, E. P. Le Compte, F. K. Kooy, J. Tramper, C. A. van Blitterswijk, and J. Riesle, “Oxygen gradients in tissue-engineered PEGT/PBT cartilaginous constructs: Measurement and modeling,”

Biotechnol. Bioeng., vol. 86, no. 1, pp. 9–18, 2004.

[73] A. L. Farris, A. N. Rindone, and W. L. Grayson, “Oxygen Delivering Biomaterials for Tissue Engineering,” pp. 1–22, 2016.

[74] D. B. Kolesky, K. A. Homan, M. A. Skylar-Scott, and J. A. Lewis, “Three-dimensional bioprinting of thick vascularized tissues.,” *Proc. Natl. Acad. Sci. U. S. A.*, vol. 113, no. 12, pp. 3179–84, 2016.

[75] K. C. Rustad, V. W. Wong, M. Sorkin, J. P. Glotzbach, M. R. Major, J. Rajadas, M. T. Longaker, and G. C. Gurtner, “Enhancement of mesenchymal stem cell angiogenic capacity and stemness by a biomimetic hydrogel scaffold.,” *Biomaterials*, vol. 33, no. 1, pp. 80–90, Jan. 2012.

[76] M. Lutolf and H. Blau, “Artificial stem cell niches,” *Adv. Mater.*, vol. 21, pp. 3255–3268, 2009.

[77] C.-C. Lin and K. S. Anseth, “PEG Hydrogels for the Controlled Release of Biomolecules in Regenerative Medicine,” *Pharm. Res.*, vol. 26, no. 3, pp. 631–643, Mar. 2009.

[78] A. Ranga, S. Gobaa, Y. Okawa, K. Mosiewicz, A. Negro, and M. P. Lutolf, “3D niche microarrays for systems-level analyses of cell fate.,” *Nat. Commun.*, vol. 5, p. 4324, Jul. 2014.

[79] K. A. Kilian, B. Bugarija, B. T. Lahn, and M. Mrksich, “Geometric cues for directing the differentiation of mesenchymal stem cells.,” *Proc. Natl. Acad. Sci. U. S. A.*, vol. 107, no. 11, pp. 4872–7, Mar. 2010.

[80] J. Oh, J. B. Recknor, J. C. Recknor, S. K. Mallapragada, and D. S. Sakaguchi, “Soluble factors from neocortical astrocytes enhance neuronal differentiation of neural progenitor cells from adult rat hippocampus on micropatterned polymer substrates,” *J. Biomed. Mater. Res. A*, vol. 91, no. 2, pp. 575–585, 2010.

[81] M. Mattotti, Z. Alvarez, J. A. Ortega, J. A. Planell, E. Engel, and S. Alcántara, “Inducing functional radial glia-like progenitors from cortical astrocyte cultures using micropatterned PMMA,” *Biomaterials*, vol. 33, no. 6, pp. 1759–1770, Feb. 2012.

[82] M. J. Sawkins, K. M. Shakesheff, L. J. Bonassar, and G. R. Kirkham, “3D Cell and Scaffold Patterning Strategies in Tissue Engineering,” *Recent Pat. Biomed. Eng.*, vol. 6, pp. 3–21, 2013.

[83] A. Khademhosseini and R. Langer, “A decade of progress in tissue engineering,” *Nat. Protoc.*, vol. 11, no. 10, pp. 1775–1781, 2016.

[84] S. V Murphy and A. Atala, “3D bioprinting of tissues and organs.,” *Nat. Biotechnol.*, vol. 32, no. 8, pp. 773–785, 2014.

[85] U. De Nantes and L. Visage, “Assessing glucose and oxygen diffusion in hydrogels for the rational design of 3D stem cell scaffolds in regenerative medicine,” 2017.

[86] S. S.-J. J. Y. H. J. J. YongdooPark, “Cellular behavior in micropatterned hydrogels by bioprinting system depended on the cell types and cellular interaction,” *J. Biosci. Bioeng.*, vol. 116, no. 2, pp. 224–230, Aug. 2013.

[87] U. Tritschler, I. Zlotnikov, P. Fratzl, H. Schlaad, S. Grüner, and H. Cölfen, “Gas barrier properties of bio-inspired Laponite–LC polymer hybrid films,” *Bioinspir. Biomim.*, vol. 11, no. 3, p. 035005, May 2016.

[88] J. L. Drury and D. J. Mooney, “Hydrogels for tissue engineering: scaffold design variables and applications,” *Biomaterials*, vol. 24, no. 24, pp. 4337–4351, Nov. 2003.

[89] I. El-Sherbiny and M. Yacoub, “Hydrogel scaffolds for tissue engineering: Progress and challenges,” *Glob. Cardiol. Sci. Pract.*, vol. 2013, no. 3, pp. 316–42, 2013.

[90] Y. Martin and P. Vermette, “Bioreactors for tissue mass culture: Design, characterization, and recent advances,” *Biomaterials*, vol. 26, no. 35, pp. 7481–7503, 2005.

[91] M. J. Farrell, J. I. Shin, L. J. Smith, and R. L. Mauck, “Functional consequences of glucose and oxygen deprivation onengineered mesenchymal stem cell-based cartilage constructs,” *Osteoarthr. Cartil.*, vol. 23, no. 1, pp. 134–142, 2015.

[92] M. Deschepper, M. Manassero, K. Oudina, J. Paquet, L. Monfoulet, M. Bensidhoum, D. Logeart-Avramoglou, and H. Petite, “Proangiogenic and Prosurvival Functions of Glucose in Human Mesenchymal Stem Cells Upon Transplantation,” *Stem Cells*, vol. 31, no. 3, pp. 526–535, 2013.

[93] A. G. Ardakani, U. Cheema, R. A. Brown, and R. J. Shipley, “Quantifying the correlation between spatially defined oxygen gradients and cell fate in an engineered three-dimensional culture model,” *J. R. Soc. Interface*, vol. 11, no. 98, pp. 1–11, 2014.

[94] S. a. M. van Stroe-Biezen, F. M. Everaerts, L. J. J. Janssen, and R. a. Tacken, “Diffusion coefficients of oxygen, hydrogen peroxide and glucose in a hydrogel,” *Anal. Chim. Acta*, vol. 273, no. 1–2, pp. 553–560, Feb. 1993.

[95] Z. Rong, U. Cheema, and P. Vadgama, “Needle enzyme electrode based glucose diffusive transport measurement in a collagen gel and validation of a simulation model.,” *Analyst*, vol. 131, no. 7, pp. 816–21, Jul. 2006.

[96] H. Suhaimi, S. Wang, T. Thornton, and D. B. Das, “On glucose diffusivity of tissue engineering membranes and scaffolds,” *Chem. Eng. Sci.*, vol. 126, pp. 244–256, Apr. 2015.

[97] J. Demol, D. Lambrechts, L. Geris, J. Schrooten, and H. Van Oosterwyck, “Towards a quantitative understanding of oxygen tension and cell density evolution in fibrin hydrogels.,” *Biomaterials*, vol. 32, no. 1, pp. 107–18, Jan. 2011.

[98] U. Cheema, Z. Rong, O. Kirresh, A. J. Macrobert, P. Vadgama, and R. A. Brown, “Oxygen diffusion through collagen scaffolds at defined densities : implications for cell survival in tissue models,” *J. Tissue Eng. Regen. Med.*, vol. 6, no. 1, pp. 77–84, 2012.

[99] X. Bourges, P. Weiss, G. Daculsi, and G. Legeay, “Synthesis and general properties of silated-hydroxypropyl methylcellulose in prospect of biomedical use.,” *Adv. Colloid Interface Sci.*, vol. 99, no. 3, pp. 215–28, Dec. 2002.

[100] C. Vinatier, D. Magne, P. Weiss, C. Trojani, N. Rochet, G. F. Carle, C. Vignes-Colombeix, C. Chadjichristos, P. Galera, G. Daculsi, and J. Guicheux, “A

silanized hydroxypropyl methylcellulose hydrogel for the three-dimensional culture of chondrocytes.," *Biomaterials*, vol. 26, no. 33, pp. 6643–51, Nov. 2005.

[101] J. Malda, T. B. F. Woodfield, F. Van Der Vloodt, F. K. Kooy, and D. E. Martens, "The effect of PEGT / PBT scaffold architecture on oxygen gradients in tissue engineered cartilaginous constructs," vol. 25, pp. 5773–5780, 2004.

[102] E. C. Novosel, C. Kleinhans, and P. J. Kluger, "Vascularization is the key challenge in tissue engineering," *Adv. Drug Deliv. Rev.*, vol. 63, no. 4, pp. 300–311, 2011.

[103] J. Rouwkema, N. C. Rivron, and C. A. van Blitterswijk, "Vascularization in tissue engineering," *Trends Biotechnol.*, vol. 26, no. 8, pp. 434–441, 2008.

[104] C. Maes, T. Kobayashi, M. K. Selig, S. Torrekens, S. I. Roth, S. Mackem, G. Carmeliet, and H. M. Kronenberg, "Osteoblast Precursors, but Not Mature Osteoblasts, Move into Developing and Fractured Bones along with Invading Blood Vessels," *Dev. Cell*, vol. 19, no. 2, pp. 329–344, Aug. 2010.

[105] A. Hasan, A. Paul, N. E. Vrana, X. Zhao, A. Memic, Y. S. Hwang, M. R. Dokmeci, and A. Khademhosseini, "Microfluidic techniques for development of 3D vascularized tissue," *Biomaterials*, vol. 35, no. 26, pp. 7308–7325, 2014.

[106] D. Richards, J. Jia, M. Yost, R. Markwald, and Y. Mei, "3D Bioprinting for Vascularized Tissue Fabrication," *Ann. Biomed. Eng.*, pp. 1–16, 2016.

[107] P. Datta, B. Ayan, and I. T. Ozbolat, "Bioprinting for vascular and vascularized tissue biofabrication," *Acta Biomater.*, vol. 51, pp. 1–20, 2017.

[108] E. Mathieu, G. Lamirault, C. Toquet, P. Lhommet, E. Rederstorff, S. Sourice, K. Biteau, P. Hulin, V. Forest, P. Weiss, J. Guicheux, and P. Lemarchand, "Intramyocardial delivery of mesenchymal stem cell-seeded hydrogel preserves cardiac function and attenuates ventricular remodeling after myocardial infarction.," *PLoS One*, vol. 7, no. 12, p. e51991, 2012.

Titre : Matrices biomimétiques 3D pour concevoir des niches de cellules souches *in vitro*

Mots clés : Ingénierie tissulaire, échafaudage, cellules souches, oxygène

Résumé : L'ingénierie tissulaire (IT) est un domaine interdisciplinaire de la médecine régénératrice en évolution rapide qui réunit la science des matériaux, le génie biomédical et la biologie cellulaire, dans le but de reconstruire les tissus vivants lors d'une lésion ou d'une perte. Pour cette raison, l' IT présente un impact important en régénérations cliniques, en augmentant l'offre potentielle de tissus pour les thérapies de transplantation. Le biomatériau support jouant un rôle d'échafaudage est une pièce maîtresse de l'IT, puisqu'il vise à imiter la matrice extracellulaire (ECM) que l'on trouve dans les tissus naturels. Néanmoins, une limitation majeure dans la réalisation de construction associant des biomatériaux à des cellules est le faible transport de l'oxygène et des nutriments et des déchets produits par les cellules.
Cette thèse présente les résultats d'une étude sur la diffusion de l'oxygène sur la viabilité cellulaire dans les constructions avec des cellules souches dans un hydrogel renforcé avec des Laponites (argile). L'impact de la diffusion de l'oxygène et des nutriments sur la viabilité cellulaire dans des constructions avec des hydrogels et des cellules souches à plusieurs concentrations est également présenté et discuté. Enfin l'impact sur la diffusion de l'oxygène et la viabilité cellulaire après la création d'un réseau de micro canaux à l'intérieur des constructions d'hydrogels et de cellules souches, par une technique de bioprinting, a été quantifié et constitue la dernière partie du présent travail. Pour conclure, ce travail a montré l'importance de la diffusion de l'oxygène et des nutriments pour la réalisation de constructions complexes pour l'ingénierie tissulaire ou afin de simuler en 3 dimensions la niche cellulaire pour des besoins de modélisation.

Title : 3D biomimetic matrices to design in vitro stem cell niches

Keywords : Tissue engineering, scaffold, stem cells, oxygen

Abstract : Tissue engineering (TE) is a rapidly evolving interdisciplinary field that joins together materials science, biomedical engineering and cellular biology, in a quest to reconstruct living tissues upon injury or loss. For this reason TE has the potential to have a large impact in clinical implantations, expanding tissue supply for transplantation therapies.
The scaffold is a centrepiece in TE, since it aims to mimic the extracellular matrix (ECM) that is found in natural tissue. Nonetheless, a major constraint in achieving larger constructs has been the lack of means to transport oxygen and waste produced by the cells. The construction of complex structures with an integrated vasculature, with high spatial resolution, is now a reality that opens the door for more complex and larger engineered tissues and organs.
This thesis presents the results of a study on the impact on oxygen diffusion and cell viability in stem cell seeded constructs, after biomaterial (hydrogel) mechanical reinforcement with a laponite clay, considered to be of great potential for regenerative medicine.
The impact on oxygen and nutrient diffusion and cell viability in stem cell seeded constructs after hydrogel mechanical reinforcement through polymer concentration is also presented and discussed.
The impact on oxygen diffusion and cell viability after the creation of a microchannel network inside stem cell constructs, through a bioprinting technique, was quantified and constitutes the last part of the present work.